UNIVERSITA' DEGLI STUDI DI PARMA
Dipartimento di Bioscienze

Dottorato di ricerca in Ecologia

XXVI Ciclo

THE ROLE OF ARCHAEA IN THE NITROGEN CYCLE OF COASTAL LAGOON SEDIMENTS

Claudia Pala

Tutor: Prof. Pierluigi Viaroli **Co-Tutor: Dott.ssa Elena Manini**

CONTENTS

I.GENERAL INTRODUCTION

I.1.Ecological role of prokaryotes

Prokaryotes are an essential component of the earth's biota. They catalyze unique and indispensable transformation in the biogeochemical cycles of the biosphere, produce important components of the earth's atmosphere, and represent a large portion of life's genetic diversity. The prokaryotes inhabit all habitats explored on the earth and the their cellular carbon, nitrogen and phosphorus are estimated to be 350-550 Pg of C, 85-130 Pg of N and 9-14 Pg of P, representing the half Carbon pool and largest pool of these nutrient in living organisms (Whitman et al., 1998).

Prokaryotes have a key role within the food webs both as primary producers and as secondary producers. Autotrophic CO_2 fixation represents the most important biosynthetic process in biology. For along time it has been thought that photoautotrophy was the sole life-strategy capable to sustain local and worldwide food webs. However after the historic discovery of deep-sea hydrothermal vents at the Galapagos Rift in 1977 (Corliss et al., 1979) and the subsequent investigations (Jannasch and Wirsen, 1979; Jannasch and Mottl, 1985), it has became clear that chemolithoautotrophic microbes can supply most, if not all, of the primary biomass input to the local ecosystems. Furthermore, recently, it has been pointed out that chemolithoautotrophs can have an important ecological role to sustain biological communities in large environments such as soil (i.e. Yuan et al., 2012) and "dark" ecosystems (i.e. Reinthaler et al., 2010; Molari et al., 2013; Santoro et al., 2013).

The role that bacteria play in the aquatic carbon cycle was unveiled after the postulation of the so-called "microbial loop" hypothesis (Pomeroy 1974, Williams 1981, Azam et al. 1983; Fig. 1). Our knowledge of the role of bacteria in the oceanic carbon flux and the trophic interactions involving microorganisms has considerably advanced in the last 25 years (Azam 1998, Fenchel, 2008),

leading to the discovery of new players (i.e. Archaea) and life strategies (i.e. photoheterotrophy, mixotrophy) acting in the microbial loop.

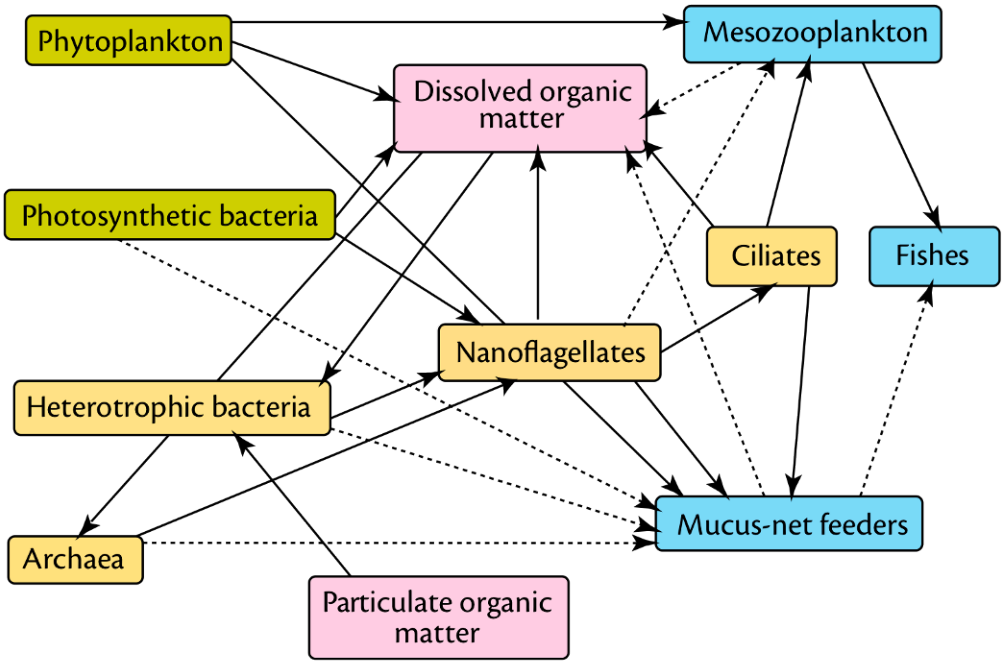

Fig.1 Microbial loop in aquatic Carbon cycle

Despite the ecological importance of prokaryotes, our comprehension how they influence ecosystem functioning is constrained by a poor knowledge on the controlling factors that affect prokaryotic distribution, diversity, community composition and metabolism.

The idea to break open the "black box" of marine prokaryotic biodiversity, by the application of different molecular tools (cloning and sequencing, *in situ* hybridization, DNA fingerprinting and metagenomic methods), has been the basis of the ecological studies on ocean ecosystems in the last 20 years. Very often these studies were focused on bacterioplankton to describe phylogenetic diversity, global distribution (Giovannoni and Stingl, 2005; Ciccarelli et al., 2006; Baldwin et al., 2005; Pommier et al., 2007; Fuhrman et al., in press), community structure and its patterns of distribution (Karner at al., 2001; Church et al., 2003; Herndl et al., 2005; Teira et al., 2006; Varela et al., 2007; Kirchman

et al., 2007; Tamburini et al., 2008). In this regard, available studies on aquatic benthic prokaryotic assemblages have mainly addressed phylogenetic rather than ecological issues. Moreover, data on diversity of aquatic benthic prokaryotes are spatially and temporally scattered and mostly reported from peculiar environments such as deep hydrothermal vents (Moyer et al. 1995, 1998; Takai and Horikoshi, 1999; Teske et al. 2002; Lopez-Garcia et al. 2003), abyssal trenches (Kato et al. 1997) and sub-surface marine sediments (Parkes et al., 1994; Coolen et al., 2002; Inagaki et al., 2003; Inagaki et al., 2006; Biddle et al., 2006). Even less information is available for the aquatic benthic Archaea diversity (Vetriani et al. 1999; Gillan and Danis, 2007; Auguet et al., 2010). On the other hand though, there is a huge lack of works describing the aquatic benthic prokaryotic community structure, especially to compare the relative contribution of the two prokaryotic domains (Bacteria and Archaea). Various quantitative molecular techniques have been used to directly compare the quantities of *Bacteria* and *Archaea* in aquatic sediments. These techniques have included indirect methods, such as Q-PCR, rRNA slot-blot hybridisation, and intact polar lipids (IPLs), and direct methods, such as whole-cell fluorescence *in-situ* hybridisation (FISH) and catalysed reporter deposition (CARD)-FISH. However, to date, only few studies have been carried out describing prokaryotic communities in marine sediments (Llobet-Brossa et al., 1998; Ravenschlag et al., 2001; Ishii et al., 2004; Biddle et al., 2006; Schippers et al., 2005; Molari and Manini, 2012; Molari et al., 2012).

I.2.Archaea

Archaea are the third domain of life, and they have been placed between those of Bacteria and Eukarya. Since the early 1990s, numerous studies have documented that these microorganisms are a widespread and important component of marine microbial communities (Fuhrman et al., 1992; DeLong, 1992; Karner et al., 2001; Lipp et al., 2008). The broad distribution and abundance of Archaea in soils and oceans implies that they contribute to global

biogeochemical cycles and to biomass/energy transfer through the food webs.

Although the application of culture-independent molecular 16S-rRNA-based tools (e.g. rRNA hybridisation), cloning and sequencing has considerably enhanced the study of these prokaryotes, their abundance and biogeochemical roles in aquatic ecosystems have been little understood until more recently (Karner et al., 2001; Ingalls et al., 2006).

Archaea were first recognised, in marine coastal water, by Fuhrman and colleagues (1992) and DeLong (1992), based on 16S rRNA gene surveys. They were initially grouped into three previously undetected lineages that were termed Group I, affiliated to the kingdom of Crenarchaeota, and Groups II and III within the kingdom Euryarchaeota (DeLong, 1992) (Fig. 2a). In particular, organisms within Group I (a lineage distinct from, but specifically associated with, cultured hyperthermophilic organisms) were found in many moderate habitats including soils (Bintrim et al., 1997; Buckley et al., 1998; Sandaa et al., 1999; Jurgens et al., 2000; Simon et al., 2000; Ochsenreiter et al., 2003), the ocean's plankton (DeLong, 1992; Fuhrman et al., 1992), estuaries (Crump and Baross, 2000), marine and freshwater sediments (MacGregor et al., 1997; Schleper et al., 1997; Vetriani et al., 1998; Keough et al., 2003), but also in the deep subsurface (Takai et al., 2001). Extensive surveys of 16S rRNA gene sequences from marine and soil samples revealed that Group I Crenarchaeota can be separated into a number of distinct clades, with the majority of soil and marine sequences placed within two of these, referred to as Group 1.1a and 1.1b lineages, respectively (Fig. 2b). While aspects of the physiology and energy metabolism of these organisms remained unknown for a long time, some initial indirect insights into the carbon metabolism of marine Archaea were obtained using stable isotope, microautoradiography or natural radiocarbon analyses. They indicated that both modes of carbon assimilation occurred within marine Archaea, that is autotrophy (using inorganic carbon as a nutrient source) (e.g. Kuypers et al., 2001; Pearson et al., 2001; Wuchter et al., 2003) and

heterotrophy (using organic carbon compounds as nutrients) (Ouverney and Fuhrman, 2000; Herndl et al., 2005; Ingalls et al., 2006; Teira et al., 2006).

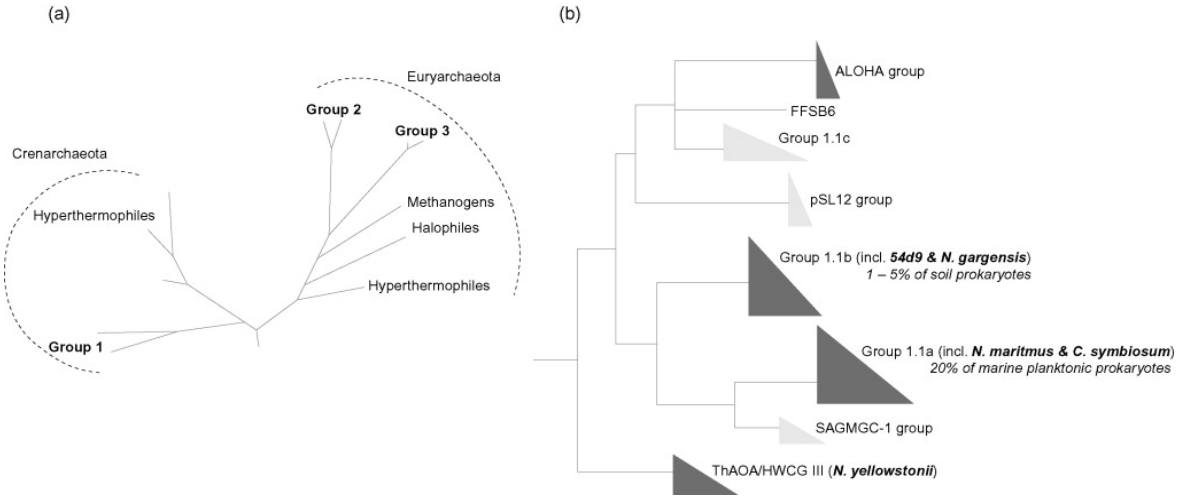

Figure 2 (a) Phylogenetic relationship between various archaeal 16S rRNA gene-defined lineages, including sequences from cultivated organisms and environmental samples. Groups 1, 2 and 3 represent lineages which were originally discovered in planktonic marine habitats, with Group 1 sequences now recovered in nearly all terrestrial and aquatic habitats. **(b)** Phylogenetic relationships of Group I archaea. Black triangles represent groups in which amoA genes have been discovered (adapted from Prosser and Nicol, 2008).

I.3.Nitrogen Cycle

The global nitrogen cycle describes the transformation of nitrogen gases and nitrogen-containing compounds on the earth. It consists of mainly microbial-driven processes, including assimilation, ammonification, nitrification, denitrification, nitrogen fixation, and anaerobic ammonia oxidation.

Nitrification involves ammonia oxidation to convert ammonia (NH_3) to nitrite (NO_2) by ammonia-oxidizing organisms and nitrite oxidation to convert nitrite to nitrate (NO_3) by nitrite-oxidizing organisms (Fig. 3). Ammonia oxidation is often the rate-limiting step of nitrification in a wide variety of environments, and therefore critical to wastewater nitrogen removal and global N cycling (Kowalchuk and Stephen, 2001; Hu et al., 2003; Choi and Hu, 2008).

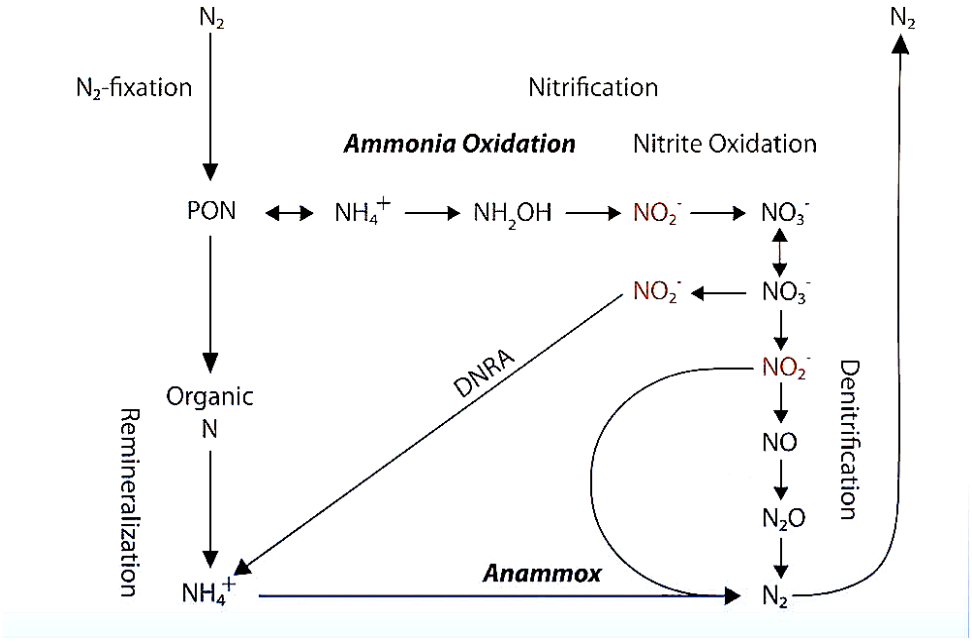

Fig.3 Microbial nitrogen transformations above, below and across an oxic/anoxic interface in the marine environment (based in part on Arrigo, 2005). Nitrite is highlighted in red to emphasize the central role of this metabolic intermediate/product within and between N- cycling pathways. Key functional genes discussed in the text are shown in yellow: amo, ammonia mono-oxygenase; hao, bacterial hydroxylamine oxidoreductase (? 1⁄4 unknown gene/enzyme in AOA); nir, nitrite reductase; and nor, nitric oxide reductase. For clarity, other functional genes and the process of nitrate/nitrite assimilation are not shown.

I.4.Ammonia-oxidizing organisms

There are two major microbial groups involved in ammonia oxidation: ammonia-oxidizing bacteria and ammonia-oxidizing archaea. While there are heterotrophic ammonia oxidizers (Otte et al., 1999), chemolithotrophic AOB were long thought to be responsible for ammonia oxidization. The recent discovery of AOA in natural and engineered systems demonstrates the role of AOA in nutrient removal and global N cycling.

I.4.1.Ammonia-oxidizing bacteria (AOB)

Ammonia-oxidizing bacteria utilize reduced nitrogen (e.g., ammonia) as an energy source, carbon dioxide as a carbon source, and molecular oxygen as an electron acceptor. These chemolithotrophic AOB commonly belong to the Beta- and Gammaproteobacteria, including Nitrosomonas (Beta), Nitrosospira (Beta),

and Nitrosococcus (Gamma) (Madigan et al., 2000).

Nitrosomonas/Nitrosospira species appear to dominate the natural and engineered systems through the survey of 16S rRNA and amoA gene sequences from both cultures and environ- mental clones (Whitby et al., 1999; Nold et al., 2000; Park et al., 2002). Therefore, AOB of the beta-subclass Proteobacteria have been used as model organisms in microbial ecological studies (Kowalchuk and Stephen, 2001). Caution should be made, however, that it is unlikely to discover the entire group of AOB by molecular probes (Purkhold et al., 2000), as the whole AOB community composition has yet to be established.

In addition, some AOB have an anaerobic metabolism (Bock et al., 1995; Mulder et al., 1995). Organisms related to Planctomycetales use nitrite (rather than O_2) as the electron acceptor, which results in N_2 production (Mulder et al., 1995; Strous et al., 1999). The anammox process in the environment appears to be highly active in any N-containing ecosystem with a pronounced anoxic zone (Francis et al., 2007).

I.4.2.Ammonia-oxidizing archaea (AOA)

While ammonia-oxidizing bacteria (AOB) are considered critical in nitrification, recently molecular biological studies demonstrate that members of the kingdom Crenarchaeota, within the Archaeal domain, play an important role in nitrification in soils and aquatic systems (Koenneke et al., 2005; Hansel et al., 2008; Tourna et al., 2008). Koenneke and colleagues isolated a new strain of marine ammonia-oxidizing archaea (AOA), Candidatus ‘‘N. maritimus’’, which contains putative genes for all three subunits (amoA, amoB, and amoC) of ammonia monooxygenase, the enzyme responsible for ammonia oxidation (Koenneke et al., 2005). Candidatus ‘‘Cenarchaeum symbiosum’’ is also shown to harbour the genes for ammonia oxidation, although a pure culture is currently not available (Hallam et al., 2006a,b). These archaeal species may contribute substantially to ammonia oxidation in marine and terrestrial environments

(Horner-Devine and Martiny, 2008).

I.4.3.Growth rate and activity

Candidatus ‘‘N. maritimus’’ is capable of using ammonia as the sole energy source and presents a similar growth rate and cell production of AOB (Koenneke et al., 2005). The maximum growth rate of the pure culture is 0.78 day-1, which is similar to that of AOB in wastewater systems (Grady et al., 1999), and at a higher range of rates estimated for natural bacterioplankton communities (0.05 and 0.3 day-1) (Koenneke et al., 2005). In soils, the cell-specific rates for AOA are around 0.5 fmol NH3 h-1 cell-1, which is in the lower range reported for AOB (Okano et al., 2004) but is three to six times higher than that estimated for marine AOA (Koenneke et al., 2005; Herrmann et al., 2008). In seawater batch cultures Crenarchaeota can grow faster than bacteria (0.23 and 0.47 day^{-1} for Crenarchaeota versus 0.13 and 0.29 day^{-1} for bacteria) (Herndl et al., 2005). However, analysis of field samples in the dark ocean indicates that planktonic archaea generally grow slower than bacteria (Herndl et al., 2005).

I.4.4.Metabolism and metabolic pathway

Currently little is known about the ammonia oxidation pathways in Archaea (Hallam et al., 2006a, b). Crenarchaeota often utilize a 3-hydroxypropionate pathway or the Krebs cycle for autotrophic carbon fixation, as opposed to the Calvin cycle for the AOB (Ward et al., 2007). One important factor to distinguish Archaea from Bacteria is the adaptation to chronic energy stress. Low-permeability membranes and specific catabolic pathways are the main biochemical mechanisms to help Archaea deal with chronic energy stress (Valentine, 2007).

Like heterotrophs, Crenarchaeota are capable of using dissolved organic carbon, such as aminoacids, as a carbon source (Herndl et al., 2005; Wuchter et al., 2006). Genomic analysis of Candidatus ‘‘C. symbiosum’’ indicates that it has

the potential to function as a mixotroph, utilizing both carbon dioxide and organic material as carbon sources (Hallam et al., 2006a,b) Candidatus ‘‘N. maritimus’’ tends to have autotrophic characteristics because recent cultivation studies support an ammonia-based chemolithoautotrophic energy metabolism, while the organic materials excreted by phototrophic organisms inhibit its growth (Koenneke et al., 2005). Radiocarbon data suggest either that the marine Archaea include both autotrophs and heterotrophs or are a single population with a uniformly mixotrophic metabolism (Ingalls et al., 2006). Whether the AOA are predominantly autotrophic or have a facultative/mixotrophic metabolism to utilize alternative energy sources warrants further exploration.

I.4.5.Ecological niches of ammonia- oxidizing Archaea

The wide distribution of AOA in the environment is currently well established. Their abundance over AOB is striking in many ecosystems. The recent information definitely indicates the contribution of AOA to ammonia oxidation in the upper water columns of the Gulf of California, in the Black Sea and in thermophilic springs (Lam et al., 2007; Beman et al., 2008; Reigstad et al., 2008). However, information on the link between the occurrence of AOA and the environmental parameters is limited. Being retrieved by cultivation-independent phylogenetic surveys, the majority of the AOA studies reflect the site properties, which are clearly affected by hydrological and biogeochemical factors. Thus, it is hard to pinpoint one parameter as responsible for the AOA occurrence in these highly complex environments. However, the properties of the sites, where the AOA abundance was reported, were taken into consideration. AOA, being ubiquitous, seem to have a wide range of growth conditions, and some ecotypes might be unique to the specific environments as well. The questions of why AOA are dominant compared with AOB in the majority of the studied environments and what parameters are effective in their occurrence and abundance remain unclear. Many research questions need to be resolved: (1) the presence and activity of AOA in sulfide-containing

environments; (2) the relationship between low ammonium-containing environments and the substrate affinity of the AOA; (3) their responses to the changes in the organic carbon or nutrient content in soils; (4) their affinity for phosphate compared with their bacterial counterparts; (5) their existence and, in some cases, abundance over AOB in low-pH, sulfidic, low-ammonium and/or low-phosphate-containing environments. This speculation integrates the higher abundance of AOA in the low-pH environments and in the majority of the sulfide-containing sites, where the soluble phosphate will be more available despite the very phosphate-poor conditions. The schematic representation of the proposed speculation in terms of dominant/active ammonia-oxidizing community type with respect to phosphate, DO, ammonia and pH levels and the resultant possible sulfide exposures are shown in Fig. 3. The question of whether there are environmental factors shaping the specific niches of AOA or some ecotypes and their contribution to the nitrogen cycle will be the areas of active research.

It is, therefore, worthwhile to further investigate the low-nutrient environments and the niche of low pH as well as sulfide-containing natural and engineered systems for AOA. The examination of environments such as freshwater sediments, cold seeps sediments, acidic or alkaline lakes and soils, eutrophic to oligotrophic waters, biological nutrient removal systems, and also the sites involving anammox reaction will be essential for our understanding of these archaeal ammonia oxidizers and their role in the N and C cycles. Investigating the effect of environmental parameters (such as phosphate, pH, DO, ammonium and sulfide) and their concentration levels on the expression of archaeal *amoA* genes will help to identify their tolerance levels and further use, and even their management in natural and engineered systems.

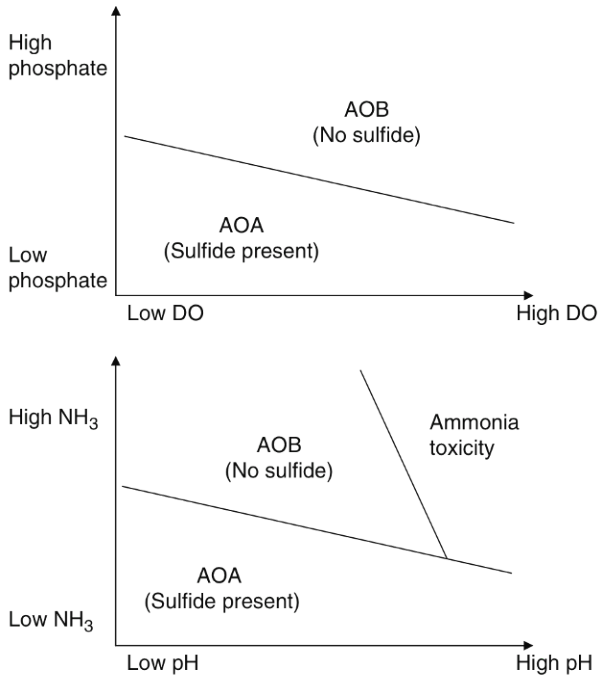

Fig. 4 The proposed dominant/active ammonia-oxidizing community type in response to the varying phosphate, pH, ammonia and DO values under the resultant possible sulfide exposures, (Erguder et al., 2009)

I.5.Lagoon ecosystems

Lagoons are transition areas characterized by shallow waters, reduced hydrodynamics, high productivity and high sedimentation rates (Viaroli et al., 1996). Coastal lagoons are therefore sensitive to the phenomena of evaporation and precipitation, which together with tidal currents cause rapid changes in the chemical and physical properties (i.e. temperature, salinity, pH) and wide fluctuations in oxygen concentrations and sulphide (Pusceddu and Danovaro, 2007; Viaroli et al., 2008). The lagoons are also areas subject to high anthropogenic pressure, they receive inputs of fresh water, nutrients derived from organic and inorganic effluents of urban, agricultural, industrial and domestic sewage. Furthermore many lagoons are intensive aquafarming sites. All these factors alter the normal functioning of ecosystem causing eutrophic, dystrophy and during the summer (with temperatures between 25 and 30° C) algal blooms and consequent anoxic crises (Pugnetti et al., 1992; Cioffi et al., 1995; Harzallah and Chapelle, 2002). However, although the lagoon sediments

are sites of intense nitrification (Ottosen et al. 1999; Nizzoli et al., 2002), the community structure, distribution and activity of AOB and AOA are largely unknown. At the same time, such knowledge would be vital for the prediction of nitrogen turnover under increasing pressures in the near future and its impact on aquaculture. Furthermore the strong spatial and temporal variability of biological and chemical-physical parameters of this transitional aquatic environment make the lagoon sediments a natural laboratory to investigate the ecological niches of AOB vs AOA.

I.5.1. Sacca di Goro

The Sacca di Goro (44.78–44.83°N, 2.25–12.33°E), enclosed between the Po di Goro, the Bosco della Mesola, and a series of sandy sediments in continuous evolution due to sediment transport from the river, known as "scanni", has a surface of 25.6 km^2 and a volume of 40x106 m^3. It is characterized by shallow waters which rarely exceed the depth of 2 m (Colombo et al., 1990). The good penetration of the solar irradiation in the shallow waters coupled with the high load of nutrients of the tributaries and the high rate of recycling of the organic matter, leads to very high values of photo-synthetic productivity (Colombo et al., 1990), making the Sacca di Goro of special economical interest. The annual yields of bivalves are 300-600 $t \cdot y^{-1}$and 150-200 $t \cdot y^{-1}$ for common mussels (*Mytilus galloprovincialis)* and clams (*Tapes decussatus),* respectively (Colombo et al., 1990). A large part of the Sacca di Goro (Valle di Gorino) is considered as wetland and was introduced in the "Ramsar List of Wetlands of International Importance" in July 1981 (Bencivelli, 1998). The Convention of Ramsar signed in 1971 in Ramsar (Iran), provides the framework for international cooperation for the conservation and wise use of wetlands and their resources (The Ramsar Convention Bureau, 1998, http://www.ramsar.org).

The environmental parameters of the waters in the lagoon vary substantially both in time and in space. They are affected on one side by tidal effects through a single wide mouth, and on the other sides by the inflow of fresh water. The

input of fresh water is due mainly to the imports from Po di Volano and Canale Bianco and, as diffused inflow, from the Po di Goro branch (O'Kane et al., 1992). The quality of the waters is influenced mainly by hydrodynamics controlling the zoning of the lagoon and the redistribution of the nutrients. According to their results, the Sacca di Goro can be subdivided into two macro areas: an eastern area (Valle di Gorino) and a western area (Goro-Volano) (O'Kane et al., 1992). The eastern area is characterized by minor movements of the water mass and by relatively low salinity, owing mainly to the inflow of fresh water distributed along the Sacca di Goro-Po di Goro boundary. Due to its morphological features (low sea bottom and numerous cropping areas), the water flow is scarce with a horizontal velocity smaller than 5 to 6 $cm \cdot s^{-1}$. In addition, the combined effect of the tide entering the mouth, along with the lower density of the water in the Valle di Gorino, gives rise to stagnation of the water resulting in long permanence periods (O'Kane et al., 1992).

In the north-western area there is major water movement and the water exchange takes place within short periods of time, the horizontal velocity reaching fairly high values of 19-31 $cm \cdot s^{-1}$. Owing to the tidal flow, the fresh waters derived from the tributaries between Po di Volano and the Canal Bianco are deviated towards the northern border of the lagoon, thus originating a circulation which conveys them to the eastern central area (O'Kane et al., 1992). This zoning is substantially identical with other zonings, based on the morphology of the lagoon (Pambianchi et al., 1994) and the water chemistry (Colombo et al., 1994), identifying 3 zones:

1. The eastern area (Valle di Gorino), characterized by a depth of 0.4 to 0.7 m (Ferrari et al., 1992).
2. The western area (Foce del Po di Volano) with water depths between 0.5 m and 1.5 m.

3. The central area with the deepest waters (1-2 m). Colombo and co-workers (1994) divided this area into two subareas, (a) the southern area (Goro) and (b) and the area close to the mouth and that connects the Sacca di Goro with the open sea.

III.5.1.1. The catchment of the Sacca di Goro

The whole drainage basin of the lagoon has a surface of ca. 2956 km^2. It is an area with in- tensive agriculture which is also highly industrialized (Pambianchi et al., 1994). Main tributary of the Sacca di Goro is the Po di Volano. The outflow from this channel is regulated at the "Sluice of Tieni". Since June 1987 the sluice gate at Tieni is kept closed so that the actual catchment of the Po di Volano, and hence the Sacca di Goro, can be considered as the area downstream of Tieni with a total of 676 km^2 (Spinelli et al., 1996). The water management in this region induces a seasonal variation in the outflow of the Po di Volano, the arable land being drained during wintertime and irrigated during summertime. The annual flow in 1997 was 300·106 m^3. In the eastern part of the Sacca di Goro fresh water from the Po di Goro branch is entering the lagoon, the volume of this water being variable with time and not yet quantified (Bencivelli, 1999).

Input of nitrogen to the lagoon originates mainly from the Po di Volano, which transports from 95% to 98% of the total nitrogen load (Bencivelli, 1990). The highest nitrate concentrations in the Po di Volano are found during the months of March and April, indicating that nitrate enters the river mainly by leaching from the arable soils after fertilization. The positive correlation which is found between the concentration of nitrate in the water of the Po di Volano and the flow rate of the river is an additional indication that nitrate is coming from the drained agricultural areas (Spinelli et al., 1996). The concentrations of ammonium are highest in autumn and winter, when organic matter is decomposed (Spinelli et al., 1996).

I.5.1.2. The macroalga ulva rigida

A massive growth of the alga *Ulva rigida* was observed in the Sacca di Goro since 1987, particularly in the eastern part, the Valle di Gorino (Viaroli et al., 1994). The nitrophilic macroalga *Ulva rigida* is certainly most important for the Sacca di Goro (Christian et al., 1998; Viaroli et al., 1995). It if found in floating beds, and its effect on the ecosystem of the lagoon is multiple (Ceccherelli et al., 1994):

- ⇒ it impedes benthonic larves to sink down to the sediment
- ⇒ it changes the micro-circulation of the water in the bottom layers
- ⇒ the food chain shifts from grazing to detrital
- ⇒ it changes the water chemistry by consuming oxygen during decomposition thus creating hypoxic or even anoxic conditions.

The macroalga starts growing at the end of the winter and finishes its growing cycle at the end of spring. Limiting factor for the growth of *Ulva rigida* is, as in many other eutrophic marine environments, the concentration of dissolved inorganic nitrogen (Colombo et al., 1994). The alga is able to accum ulate large quantities of nitrogen. In April, when the biomass of *Ulva rigida* reaches 4 kg $\cdot m^{-2}$, the content of total nitrogen in the shoots of the alga can be as high as 4%. (Viaroli et al., 1994).

II.AIMS AND HYPOTHESIS OF THE THESIS

The overall aim of my PhD project is to study the ecology of ammonia oxidizing prokaryotes in coastal aquatic transition ecosystems in order to understand their role in the nitrogen cycle in response to higher dynamics and heterogeneity, both spatial and temporal, of the lagoon environmental settings. Furthermore, I hypothesize that in lagoon sediments ammonia oxidizing *Archaea* are dominant, and thus primarily responsible for nitrification, under low values of dissolved oxygen and pH. Specifically, the research is organized and directed to answer the following ecological questions:

i) how do different chemical and physical characteristics, especially variation of pH and dissolved oxygen, affect abundance of Archaea vs. Bacteria?
ii) what is the actual relevance and contribution of AOA and AOB to net nitrification?

III.SEDIMENT MICROBIAL COMMUNITIES COMPOSITION IN AN ESTUARINE TRANSITION ECOSYSTEM

III.1. Abstract

Coastal aquatic transition ecosystems are hot-spots of organic matter and nutrient fluxes between terrestrial and marine aquatic ecosystems. However, the microbial and biogeochemical controls of many of these processes are still poorly understood. In particular, microbial activities in transitional area are important for aquatic nitrogen cycling. In recent years our understanding of the processes involved in the nitrogen cycle and microorganisms that mediate them has been drastically changed. We have analysed the abundance and community structure of prokaryotes in sediments from three distinct sites of Sacca of Goro of the Po estuary (Italy) with specific chemical, physical and biological characteristics. This research significantly advances our understanding of the role of Bacteria and Archaea in coastal transition systems subject to high inputs of nitrogen and under strong anthropogenic pressure.

First results suggest that Archaea are an important component of microbial community (20%) overlooked until now. They are also constant along the layers investigated, while *Bacteria* tend to decrease in the subsurface.

In conclusion the abiotic parameters (temperature, dissolved oxygen, pH and salinity) explain the variations in the composition of prokaryotic communities.

III.2. Introduction

Site of study and Sampling Strategy

The sampling area was carried out in the Sacca of Goro (Fig. 1), a shallow-water embayment of the Po River Delta (44.78–44.83°N, 2.25–12.33°E) approximately triangular in shape with a surface area of 26 km^2, an average depth of 1.5 m, and it is connected to the sea by two mouths about 0.9 km wide each. Main inputs of freshwater are from the Po di Volano, the Canal Bianco and Giralda. The tidal amplitude is ca. 80 cm. This ecosystem is one the most important aquaculture systems in Italy, and is subject to anthropogenic eutrophication type that cause the growth of macroalgae (*Chlorophyceae*) in the east, where growth is responsible for anoxia and dystrophy in the summer, and phytoplankton in the central part (Viaroli et al., 2001). The Sacca di Goro is also a site of intense nitrification (Ottosen et al., 1999; Nizzoli et al., 2002). Sampling sites will be chosen, following the pattern of Erguder et al. (2009), based on the concentration of nutrients (phosphate, ammonia), dissolved oxygen and values of pH. Sampling was done in two distinct periods, summer and winter (2011/12), for which are reported temperature, dissolved oxygen, pH and salinity data (Viaroli et al 2008; Azzoni et al 2005; Viaroli and Christian 2003). For each sampling period and within individual sampling sites were sampled three stations. In each station the top cm (first 5cm) of sediments were collected, in three replicates.

The stations sampled in summer 2011 are: **Giralda**, which is characterized by silt-clay sediment, low salinity and low hydrodynamics; **Gorino**, characterized by muddy sediment, presence of macroalgae that was often followed by summer anoxia and dystrophic crises; **Scanno di Piallazza (Mare)**, characterized by sandy sediment, high salinity with the average depth is 1.5 meters. At each site, sediment cores were collected identifying three horizons (oxic, suboxic and anoxic layers). Within each layer the structure of the prokaryotic community was investigated by means of in situ hybridization (FISH). Specific probes were

used for the domain of Bacteria and Archaea. Finally, the following physical-chemical and biological variables were measured at all sampling sites: nutrients (nitrate and ammonia), dissolved oxygen, pH, salinity, temperature, chlorophyll-a, organic matter characterization. The same sampling scheme was carried out in late winter 2012.

Fig.1 The sampling site: Sacca di Goro Lagoon.

III.3.Material and Methods

III.3.1. Sampling and Environmental Parameters

Two sampling campaigns were conducted: one in summer 2011 and the other one in winter 2012. The sampling activities were carried out using a small boat of Ferrara's Province. The sediment was collected using transparent Plexiglas carrots of 8 cm diameter, chemical-physical parameters of water and water/sediments interface (salinity, temperature, pH, dissolved oxygen) were measured *in situ* using a multiparametric probe (ISI Instruments, mod. 556).

III.3.1.1. Ammonia

The determination of NH_4^+ in the microcosm experiment samples is based on a series of reactions, catalyzed photochemically, leading to the formation of the indophenol blue. The concentration was determined spectrophotometrically using salicylate and hypochlorite in the presence of sodium nitroprussiate (Bower and Holm-Hansen, 1980).

Before to start with the procedure for the determination of NH_4^+, samples from Gorino and Mare were diluted 1:5, for Giralda was not necessary the dilution.

Procedure:

Reagent A: -Trisodium citrate
-Sodium hydroxide

Reagent B: -Sodium nitroprusside
-Sodium salicylate

Reagent D: -Sodium dichloroisocyanurate

Add 0.2 ml of reagent B and 0.2 ml of reagent D, leave the samples capped for 1hour in the dark.

Prepare 5 blank and the calibration curve using a stock of ammonium solution and water in a range appropriate for the concentrations of the samples.

After 1hour starting reading 2 blank only with distilled water and after, start with the reading of the samples using spectrophotometer λ= 690nm, finish reading analyzing at least 5 blank.

Prepare a standard curve by plotting absorbance readings of standards against ammonia concentrations of standards. Compute sample concentration by comparing sample absorbance with the standard curve, (Fig. 2).

The concentration was calculated according to the following equation:

μgN – NH_4 / L= (ABS x f) f = slope of the calibration curve

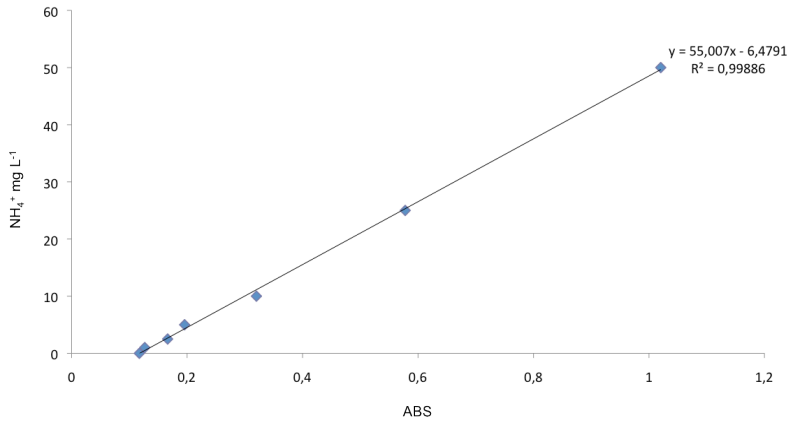

Fig. 2. Calibration curve for determination of NH_4^+ concentration.

III.3.1.2. Nitrate

NO_3^- is reduced almost quantitatively to nitrite (NO_2^-) in the presence of cadmium (Cd). This method uses commercially available Cd granules treated with copper sulfate ($CuSO_4$) and packed in a glass column.

The NO_2^- produced thus is determined by diazotizing with sulfanilamide and coupling with N-(1-naphthyl)-ethylenediamine dihydrochloride to form a highly colored azo dye that is measured colorimetrically. A correction may be made for

any NO_2^- present in the sample by analyzing without the reduction step. The applicable range of this method is 0.01 to 1.0 mg NO_3^- N l^{-1}. The method is recommended especially for NO_3^- levels below 0.1 mg N l^{-1} where other methods lack adequate sensitivity.

$$NO_3^- + H_2O + 2\ e^- \rightarrow NO_2^- + 2\ OH^-$$

$$NO_2^- + 3\ OH^- + 6\ e^- \rightarrow NH_3^+ + 7\ OH^-$$

Purchase or construct the reduction column (Fig. 3) from a 100 ml volumetric pipet by removing the top portion. The column also can be constructed from two pieces of tubing joined end to end: join a 10 cm length of 3 cm ID tubing to a 25 cm length of 3.5 mm-ID tubing. Add a TFE stopcock with metering valve1 to control flow rate.

Use a spectrophotometer at λ=543 nm.

Reagents:

- Nitrate-free water, as a blank;
- Copper cadmium granules, wash 25 g new or used to 100 mesh Cd granules with HCl 6N and rinse with water. Swirl Cd with 100 ml 2% $CuSO_4$ solution for 5 min or until blue color partially fades. Decant and repeat with fresh $CuSO_4$ until a brown colloidal precipitate begins to develop. Gently flush with water to remove all precipitated Cu.
- Ammonium chloride solution (NH_4Cl), dissolve 97.5 g NH_4Cl in 500 ml of distilled water. Adjust to pH 8.5 with NH4OH. Diluted 1:10 Ammonium chloride solution.
- Hydrochloric acid, HCl, 6N;
- Copper sulfate solution, 2%: Dissolve 20g $CuSO_4 \cdot 5H_2O$ in 500 ml of distilled water.

Reagents for calibration curve:

- Dissolve 155 g of NaCl in distilled water;
- Dissolve 50 g of $MgSO_4 \cdot 7H_2O$ in distilled water;
- Dissolve 0.25 g of $NaHCO_3$ in distilled water;

NOTE: these reagents are used for sea water.

Solution A:

Stock Nitrate solution, potassium nitrate (KNO_3) as colour reagent, dissolve 0.7218 g in distilled water and dilute to 1000 mL (10 mg $N\text{-}NO_3\ l^{-1}$).

Solution B:

Diluite 100 ml of the stock Nitrate solution in 1000 ml of distilled water (10 mg $N\text{-}NO_3\ l^{-1}$).

Preparation of reduction column:

Insert a glass wool plug into bottom of reduction column and fill with water. Add sufficient Cu-Cd granules to produce a column 18 cm long. Maintain water level above Cu-Cd granules to prevent entrapment of air. Wash column with 200 ml dilute NH_4Cl solution. Activate column by passing through it, at 7 to 10 ml min^{-1}, at least 100 ml of a solution composed of 25% 1.0 mg NO_3^--N l^{-1} standard and 75% NH_4Cl solution.

Sample reduction:

To 25 ml sample or a portion diluted to 25 ml, add 75 ml NH_4Cl solution and mix. Pour mixed sample into column and collect at a rate of 7 to 10 ml min^{-1}. Discard first 25 ml. Collect the rest in original sample flask. There is no need to wash columns between samples, but if columns are not to be reused for several hours or longer, pour 50 ml dilute NH_4Cl solution on to the top and let it pass through the system. Store Cu-Cd column in this solution and never let it dry.

Colour development and measurement:

As soon as possible, and not more than 15 min after reduction, add 2 ml color reagent to 50 ml sample and mix. Between 10 min and 2 h afterward, measure absorbance at 543 nm against a distilled water-reagent blank.

NOTE: If NO_3^- concentration exceeds the standard curve range (about 1 mg N l^{-1}), use remainder of reduced sample to make an appropriate dilution and analyze again.

Standards preparation:

Using the intermediate NO_3^--N solution, prepare standards in the range 0.05 to 1.0 mg NO_3^--N l^{-1} by diluting the following volumes to 100 ml in volumetric flasks: 0.5, 1, 2, 5, and 10 ml. Carry out reduction of standards exactly as described for samples.

Obtain a standard curve by plotting absorbance of standards against NO_3^--N concentration. Compute sample concentrations directly from standard curve.

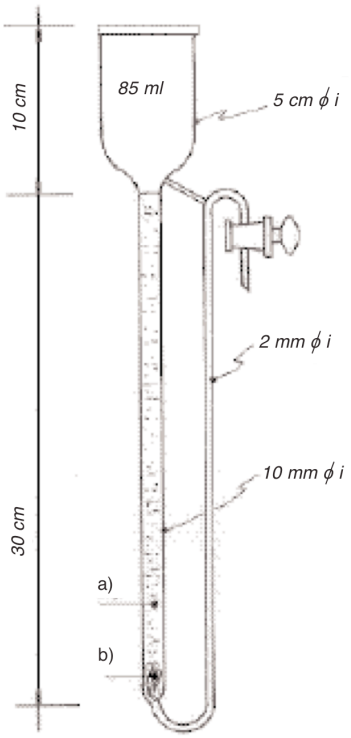

Fig. 3. Glass column for Nitrate reduction; a) Cadmium copper; b) copper wires or glass wool.

Once the sediment core is extruded from the liner, whenever studies of the total organic matter or community structure composition are required, the core can be sliced into the layers needed using a plastic (inert) knife. The top 5 cm of the corer are sliced into 0.1–1.0 cm thick layers, whereas, deeper in the core, layer thickness can be extended to 2–5 cm. Sediment layers for the subsequent analysis of total organic matter contents are then immediately homogenized and stored frozen at −20°C until analysis. For the prokaryotic community structure studied by FISH, three different layers of sediment oxic, suboxic and anoxic were determined using a multiparameter probe, through Redox potential (Eh).

III.3.2. Organic Matter Composition

The biochemical composition of sediment organic matter is generally used to gather information on the origin, quality and availability of the deposited organic material (Danovaro et al., 1993), and it is important both in a biogeochemical perspective (as organic matter degradation rates affect its burial in the sediments; Hartnett et al., 1998) and from a trophodynamic point of view (as organic matter quality influences metabolism and distribution of benthic assemblages; Graf, 1992; Dell' Anno et al., 2002).

III.3.2.1. Chlorophyll-a and phaeopigments

The extraction of chlorophyll-a and phaeopigments from the sediment was performed according to the procedure proposed by Lorenzen & Jeffrey (1980). In short, an aliquot of wet sediment (about 0.5 grams) is placed in a test tube where it was added a few mg of magnesium carbonate (MgCO3) to avoid the rapid degradation of chlorophyll-a. Subsequently it was added, to perform the extraction, 5 ml of 90% acetone. The samples are then sonicated in an ultrasonic bath for 3 minutes, and then left in the dark for 12 hours at 4°C. The tube with the sediment is centrifuged at 2500 rpm for 15 minutes, the acetone extract is aspirated and then read to spectrofluorimeter at a wavelength of 665 nm and 750 nm. The phaeopigments are read at same wavelengths after acidification of the chlorophyll-a extract with 100 μl of HCl 0.1 N. Once removed the supernatant, the sediment was dried in stove at 60°C and weighed. The concentrations were obtained using the formulas of Plante-Cuny (1974) and expressed as micrograms of pigment per gram of dry sediment.

III.3.2.2. Proteins

The determination of total protein was performed following the procedure of Hartree (1972) , obtained by the modification of the method of Lowry et al., (1951). This methodology exploits the colorimetric properties of proteins to react first with the cupric tartarate and later with the Foling Ciocalteu reagent in a basic environment (pH 10). The addition of the solution of phenol and

phosphomolybdate allows to obtain a blue color stable and proportional to the protein content. In 1990, the Hartree method has been adapted to the analysis of aquatic sediments. The colored samples are then read, within 2 hours of treatment, with the spectrophotometer at a wavelength of 650 nm. Readings relative to those obtained samples are subtracted from the white sediment (sediment calcined in a furnace at 450°C for 4 hours). For the calculation of the concentrations we used a calibration curve obtained with standard solutions of bovine serum albumin at increasing concentrations. The concentrations are then expressed in mg equivalent of bovine albumin per gram of dry sediment.

III.3.2.3. Carbohydrates

The determination of total carbohydrates was conducted following the method of Dubois et al., (1956), adapted to the aquatic sediments from Gerchacov & Hatcher (1972). The method is based on the ability of the sugars to react with phenol in the presence of concentrated sulfuric acid. The exothermic reaction that develops after the addition of the acid acts as a catalyst for the final coloration of the sample. The sample is subjected to ultrasonic treatment for 3 minutes to facilitate the extraction of carbohydrates, thus enabling the detachment of the organic particles from the mineral substrate to which they are adherent (Danovaro & Fabiano 1990) . The absorbance is measured in a spectrophotometer at a wavelength of 485 nm and reading at a wavelength of 600 nm is used to correct the interference value of the sedimentary matrix. Readings relative to those obtained samples are subtracted from the white sediment (sediment calcined in a furnace at 450°C for 4 hours). The concentrations of the carbohydrates are derived from a calibration curve obtained by reacting increasing concentrations of D (+) - Glucose and are expressed in mg of glucose equivalents per gram of dry sediment.

III.3.2.4. Lipids

The determination of total lipids was carried out with the method proposed by

Bligh & Dyer (1959), which exploits the lipid solubility in organic solvents, in this case methyl alcohol and chloroform. This method has been adapted to the sediments from Danovaro & Fabiano (1990). The absorbance of the samples is read in a spectrophotometer at a wavelength of 375 nm. Readings relative to those obtained samples are subtracted from the white sediment (sediment calcined in a furnace at 450°C for 4 hours). For the calculation of the concentrations is used a standard curve obtained by reacting increasing concentrations of tripalmitin. The concentrations were expressed in mg of tripalmitin equivalents per gram of dry sediment.

III.3.2.5. Biopolymeric carbon

The biopolymeric carbon (BPC) is expressed as a measure of organic carbon in sediments and potentially available to heterotrophic benthic organisms. The sum of the three major classes of biochemical compounds of organic matter (carbohydrates, proteins and lipids) gives us the estimate of the carbon biopolymer. The values obtained are then converted into carbon equivalents assuming as conversion factors, respectively, 0:49, 0:40 and 0.75 (Fabiano et al., 1995).

III.3.3. Fluorescence In Situ Hybridization (FISH) and Total Prokaryotic number

This technique allows the visualization, identification, and localization of individual prokaryotic cells. Is used for many applications in all fields of microbiology and not only allows the identification of culturable microorganisms, but also so-called non-cultivable organisms, allowing a study on the analysis of the community structure of prokaryotic, such as Bacteria and Archaea (Llobet - Brossa et al., 1998; Murray et al., 1998) .

Through the hybridization procedure, each ribosome within a bacterial cell (containing the 5S rRNA, 16S and 23S) is colored by a fluorescent oligonucleotide probe specific for the rRNA of different phylogenetic groups.

The high number of ribosomes per cell provides for a natural amplification of the signal which allows the display to microscope optical epifluorescence (Amann et al., 1995; Giovannoni et al., 1988; DeLong et al., 1999).

The procedure involves the following steps: (i) sample fixation, (ii) sample preparation, (iii) sample filtration, (iv) permeabilization, (v) hybridization, (vi) washing to remove the excess of probe, (vii) mounting on slides for viewing under the microscope epifluorescence and documentation.

The samples were fixed using formalin to 2%, for the preparation the samples is centrifuged (2500 rpm for 5 minutes), washed once in PBS (145mm NaCl, 1.4 mM NaH2PO4, Na2HPO4 8mm (pH 7.4), then re-centrifuged to remove the supernatant and resuspended in an appropriate volume of PBS and 96% ethanol (1:1). The next step involves the sonication for 3 minutes with 30 seconds intervals with shaking.

For the filtration of the sample it was used the polycarbonate filters of porosity 0.2 microns. The filters were immersed in 0.2 % (w / v) of the Low-Gelling-Point Agarose in reagent grade water (filtered 0.2 mM) at 35°C in a non-humid environment for 20 minutes, then dehydrated in 96% ethanol for a minutes at room temperature . This first step allows a greater adhesion of microbial cells on the filter.

Before proceeding to the step of hybridization, the filter is sectioned, by a cutter sterile, in various parts depending on the probes used .

The step of hybridization of the samples is achieved by adding to each filter section a 10:1 mixture of hybridization buffer (900mm NaCl , 20mM Tris-HCl pH 7.4 , 0:01 % SDS , 35 % formamide) for probe (50ng/µl). The hybridization is carried out in the dark in a room thermostated at a temperature of 46°C for 1.5-3h .

Probes have been used for universal Eubacteria (EUB338: 5'-GCT GCC TCC CGT AGG AGT-3'; EUB338II: 5’-GCA-GCC-ACC-CGT-AGG-TGT-3’;

EUBIII: 5’-GTC-GCC-ACC-CGT-AGG-TGT-3’) for the Archaea (915 Archaea: 5'- GTG CTC CCC CGC CAA TTC CT-3') and to control non-specific binding of EUB338 probe NON EUB (5’-ACT-CCT-ACG-GGA-GGC-AGC-3’) was used, labeled in both 5 ' with a fluorescent molecule (Cy3).

The samples are washed in a washing buffer (20 mM Tris -HCl pH 7.4, 900 mm NaCl, 0:01 % SDS, 5 mM EDTA) to remove excess probe. This operation is performed in the dark in a room thermostated at a temperature of 48°C for 15-30 min. The filters are then rinsed in water and left to dry reagent able to air.

After the washing, the filter sections are stained with 30 µL of 4',6-Diamidino-2-phenylindole hydrochloride (DAPI; 1:1000 dilution), for the detection of total prokaryotic cells and incubated in the dark for 3-5 minutes. Subsequently the sections of the filter are washed in 96% ethanol for a few seconds and then rinsed with reagent grade water and let air dry.

The sample is finally mounted on a slide with 20 L of a solution of PBS-glycerol-ascorbic acid (an anti-whitener). The count is made at the epifluorescence microscope (prokaryotes Total: Ex 359nm and Em 441nm; Eubacteria and Archaea: Ex 546/12nm and Em 590nm).

They were observed from 10 to 20 fields distributed with criterion of randomness over the entire area of the filter for a total of cells equal to 300. For the calculation was applied to the following formula:

N° cells/g dry sediment = [N x filter area (mm^2) x 1.44] / field area (mm^2) x weight of sediment (g)

where:

N = average number of cells in the fields explored;

1:44 = correction factor for sediment samples (coefficient of extraction);

filter area = is the area in which the sample is deposited and not the total;

field area = area of a grid inserted into the eyepiece.

III.3.4. Statistical Analysis

Normality and homoscedasticity of data was examined and, when required, data was transformed and newly tested. The spatial variability of the bacterial and archaeal abundance and relative abundances, expressed as a percentage of total prokaryotes, were investigated using univariates analysis of variance (ANOVA). A Student-Newman-Keuls (SNK) post hoc comparison test (at a = 0.05) was also carried out when significant differences were encountered to identify any clear sediments profile patterns. All ANOVA and SNK tests were conducted using StatSoft 5.0. software. Distance-based permutational multivariate analyses of variance (PERMANOVA; Anderson, 2001) were used to test for difference in bacterial and archaeal abundances in sediments of different stations and sampling periods (including in the analysis only the top and bottom layers, in order to have a balance design). To assess whether and how much physiological parameters (i.e. temperature, salinity, DO, pH), nitrogen nutrients and sedimentary organic matter explained changes in the abundances of Archaea and Bacteria, non-parametric multivariate multiple regression analyses were carried out using the routine DISTLM forward (McArdle and Anderson, 2001).

III.4.Results

III.4.1.Environmental Parameters and Organic Matter Composition

The water parameters measured *in situ* at Giralda, Gorino and Mare stations are reported in Tab. 1.

Table.1 Environmental parameters of Giralda, Gorino and Mare, in Summer 2011 and Winter 2012

	Station	Depth (m)	Environmental Parameters	Water/sediment interface	First layer 0-0.5 cm	Second layer 0.5-2	Third layer 5 cm		Water/sediment interface	First layer 0-0.5 cm	Second layer 0.5-2 cm	Third layer 5 cm
ummer								**Winter**				
	Mare	1.5	T (°C)	23.3	-	-	-		13	-	-	-
			Salinity (‰)	25	-	-	-		29	-	-	-
			pH	7.8	7.8	-	-		-	-	-	-
			OD (%)	82	-	-	-		-	-	-	-
			Eh (mV)	-	205.3	-	-		-	-	-	-
			Ammonia (µM)	12	-	-	-		-	7.5	-	-
			Nitrite (µM)	3	-	-	-		-	2.9	-	-
			Nitrate (µM)	7	-	-	-		-	192	-	-
	Gorino	0.9	T (°C)	27.3	-	-	-		8.1	-	-	-
			Salinity (‰)	18.6	-	-	-		24	-	-	-
			pH	8.1	8.2	7.5	7.6		-	8.2	8	7.9
			OD (%)	80	-	-	-		-	89		
			Eh (mV)	-	106.4	-80.1	-172.8		-	85.5	22	-248
			Ammonia (µM)	9	-	-	-		-	15	-	-
			Nitrite (µM)	0.6	-	-	-		-	1	-	-
			Nitrate (µM)	2.2	-	-	-		-	30	-	-
	Giralda	0.5	T (°C)	27.8	-	-	-		-	-	-	-
			Salinity (‰)	5	-	-	-		-	-	-	-
			pH	7.5	7.5	7.3	7.2		-	7.8	7.7	7.7
			OD (%)	70	62.6	-	-		-	94		
			Eh (mV)	-	94.3	-172	-179.9		-	198	182	121
			Ammonia (µM)	48	-	-	-		-	80	-	-
			Nitrite (µM)	3	-	-	-		-	5	-	-
			Nitrate (µM)	48	-	-	-		-	125	-	-

III.4.1.1. Clorophyll-a and pheopigments

Gorino is the station that had the highest chlorophyll-a and pheopigments content both in summer, 300 µg g^{-1} (June 2011), and in winter, 170 µg g^{-1} (February 2012) (Fig. 4A-4B). The oxic layer of Gorino had the higher concentration of chlorophyll-a and pheopigments, 120 µg g^{-1} (Fig. 4A). In Giralda station did not notice much difference of chlorophyll-a and pheopigments content in the three different layers of sediment between summer and winter (Fig. 4A-4B). Mare station had lower content of chlorophyll and pheopigments. The oxic layer of Mare during the summer period had the highest concentration of chlorophyll and pheopigments 50 µg g^{-1} (Fig. 4A)

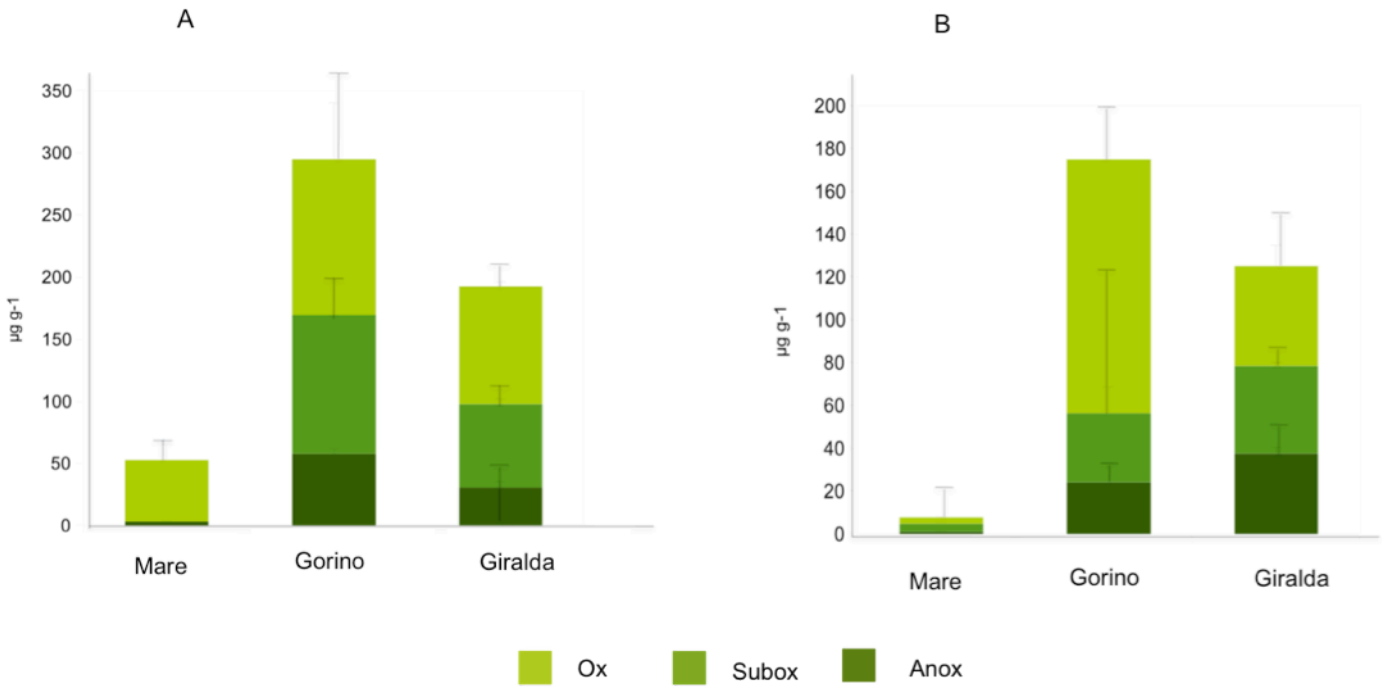

Fig.4 A) Chlorophyll-a and pheopigments content in the three stations during the summer; **B)** Chlorophyll-a and pheopigments content in winter

III.4.1.2. Proteins

Gorino is the station that had the highest proteins content 27 mg g^{-1} during winter (Fig. 5B). In winter the anoxic layer had proteins concentration of 15 mg g^{-1} maximum in all the layers considered (Fig. 5B). Giralda had higher proteins content in the oxic layer during summer, 13 mg g^{-1} (Fig. 5A). During winter the proteins content was similar in the three layers, 5 mg g^{-1} (Fig. 5B).

Mare station had the lowest presence of proteins, especially in summer 0.5 mg g^{1} (Fig. 5A).

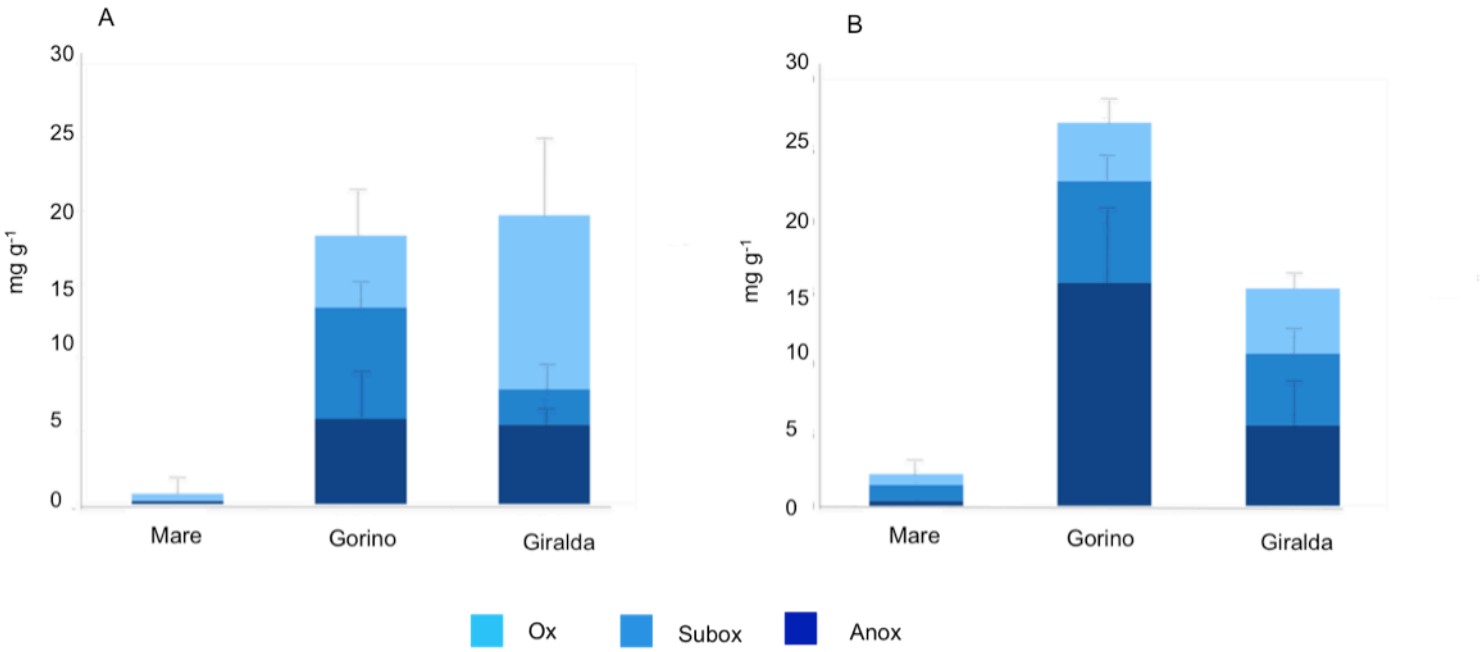

Fig.7 A) Proteins content in the three stations during the summer; **B)** Proteins content in winter

III.4.1.3.Lipids

During the summer Giralda had the highest content of lipids, 9.5 mg g^{-1}. In particular, we note that the oxic layer was characterized by the highest amount of lipids, 7 mg g^{-1} (Fig. 6A).

The suboxic layer of Gorino in summer had the highest lipids content, 3 mg g^{-1} (Fig. 6A).

During the winter Gorino and Giralda sediments had the same amount of lipids, 10 mg g^{-1}, (Fig. 6B). In Giralda station the oxic layer had the highest lipids content, about to 5.5 mg g^{-1}, (Fig. 6B). Gorino suboxic and anoxic layers had similar lipids values, 3.5 mg g^{-1}, which were higher than those observed in the oxic layer for the same station, 3 mg g^{-1} (Fig. 6B).

Mare station both in summer and in winter had the lowest lipids content with values ranging from a minimum of 1 mg g^{-1} during the summer (Fig. 6A) at 2 mg g^{-1} during the winter (6B).

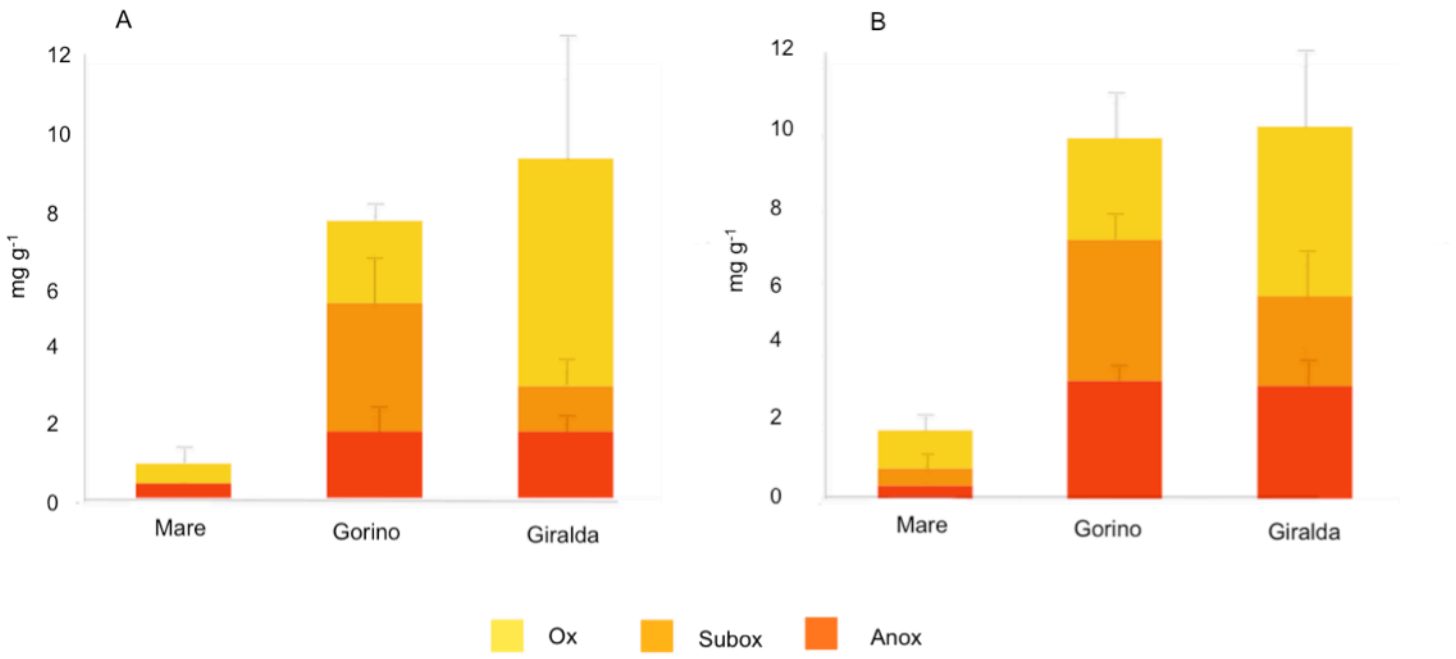

Fig.6 A) Lipids content in the three stations during the summer; **B)** Lipids content in winter

III.4.1.4. Carbohydrates

Both in summer and in winter Giralda had the highest content of carbohydrates, 6 mg g^{-1} and 11 mg g^{-1}, respectively (Fig. 7A-7B). During the summer the suboxic layer presented values of carbohydrates, equal to 3.5 mg g^{-1}, which decreased to 1 mg g^{-1} in the anoxic layer (Fig. 7A).

During the summer Gorino showed values of carbohydrates of 5.5 mg g^{-1}, that decreased to 2 mg g^{-1} and to 1 mg g^{-1} in suboxic and anox layers, respectively

(Fig. 7A). Mare station had the lowest values of carbohydrates, 1.8 mg g^{-1} (Fig. 7A).

Giralda during the winter had the highest content of carbohydrates, 11 mg g^{-1} (Fig. 7B). All three layers (oxic, suboxic and anoxic) had similar values of carbohydrates about 3.5 mg g^{-1} (Fig. 7B).

Gorino presented total values of carbohydrates equal to 9.5 mg g^{-1}, with higher values in the suboxic layer, 4.5 mg g^{-1}, and the lowest in the anoxic layer, 1.5 mg g^{-1} (Fig. 7B).

Mare station had the lowest values of carbohydrates, 1.8 mg g^{-1} in total; the oxic layer had the highest content of carbohydrates, 1 mg g^{-1} (Fig. 7B).

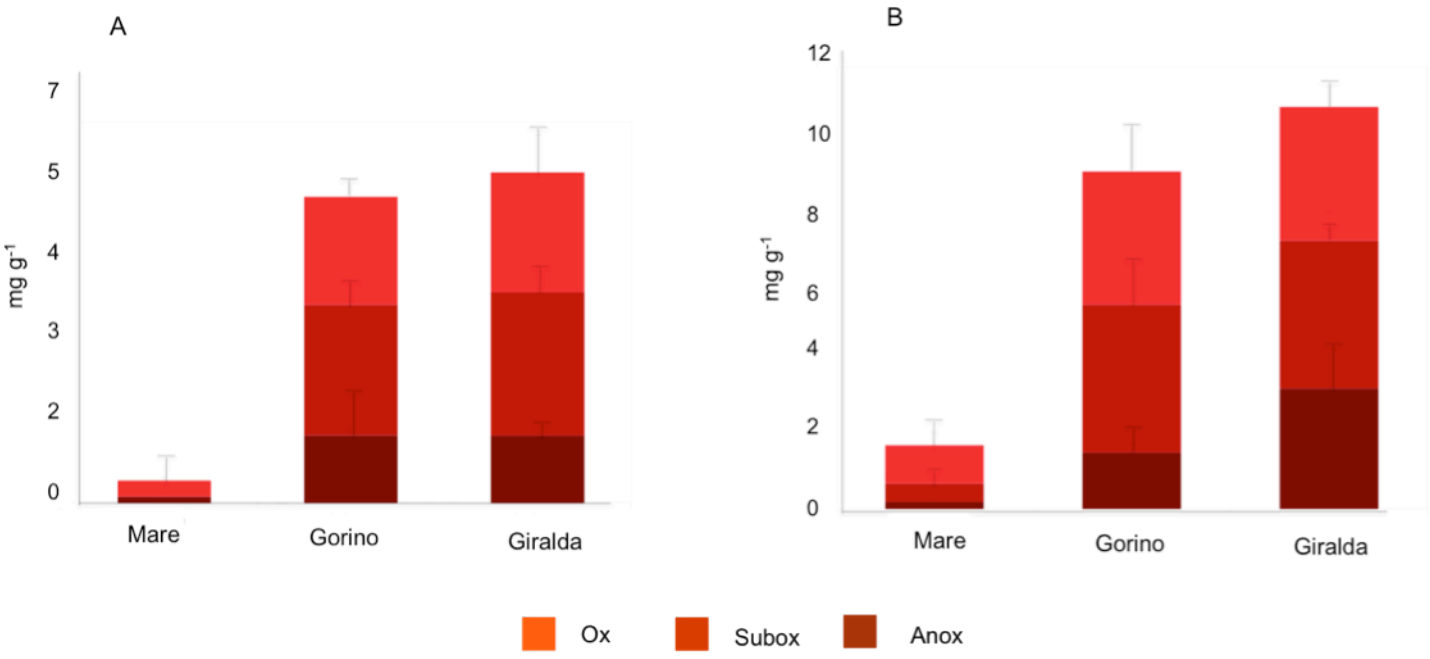

Fig.7 A) Carbohydrates content in the three stations during the summer; **B)** Carboydrates content in winter

III.4.1.5. Biopolymeric Carbon

During the summer Giralda was the station with the highest content of biopolymeric Carbon, 18 mgC g^{-1}. In particular, the oxic layer was characterized by higher concentrations, 9 mgC g^{-1}. The suboxic layer presented lower values, 3 mgC g^{-1} (Fig. 8A).

Gorino had a total content of biopolymeric carbon equal to 16 mgC g^{-1}, with the suboxic layer characterized by a content of biopolymeric carbon of 7 mgC g^{-1}. The oxic and anoxic layers have similar values of biopolymeric carbon, 4 mgC g^{-1} (Fig. 8A).

Mare station has the lowest amount of biopolymeric carbon 0.5 mgC g^{-1} (Fig. 8A).

During the winter Gorino had the highest biopolymeric carbon content with a total value of 24 mgC g^{-1} (Fig. 8B). The anoxic layer had more content of biopolymeric carbon with values equal to 11 mgC g^{-1}. The oxic layer had lower biopolymeric carbon content with values equal to 6 mgC g^{-1} (Fig. 8B). Giralda had a total content of carbon biopolymeric 20 mgC g^{-1}, all three layers had similar amounts, ~ 6-5 mgC g^{-1} (Fig. 8B).

Mare station had the lowest content of biopolymeric carbon with the overall values of 3.5 mgC g^{-1}, the oxic layer presented a greater amount of bioplymeric carbon 2 mgC g^{-1} (Fig. 8B).

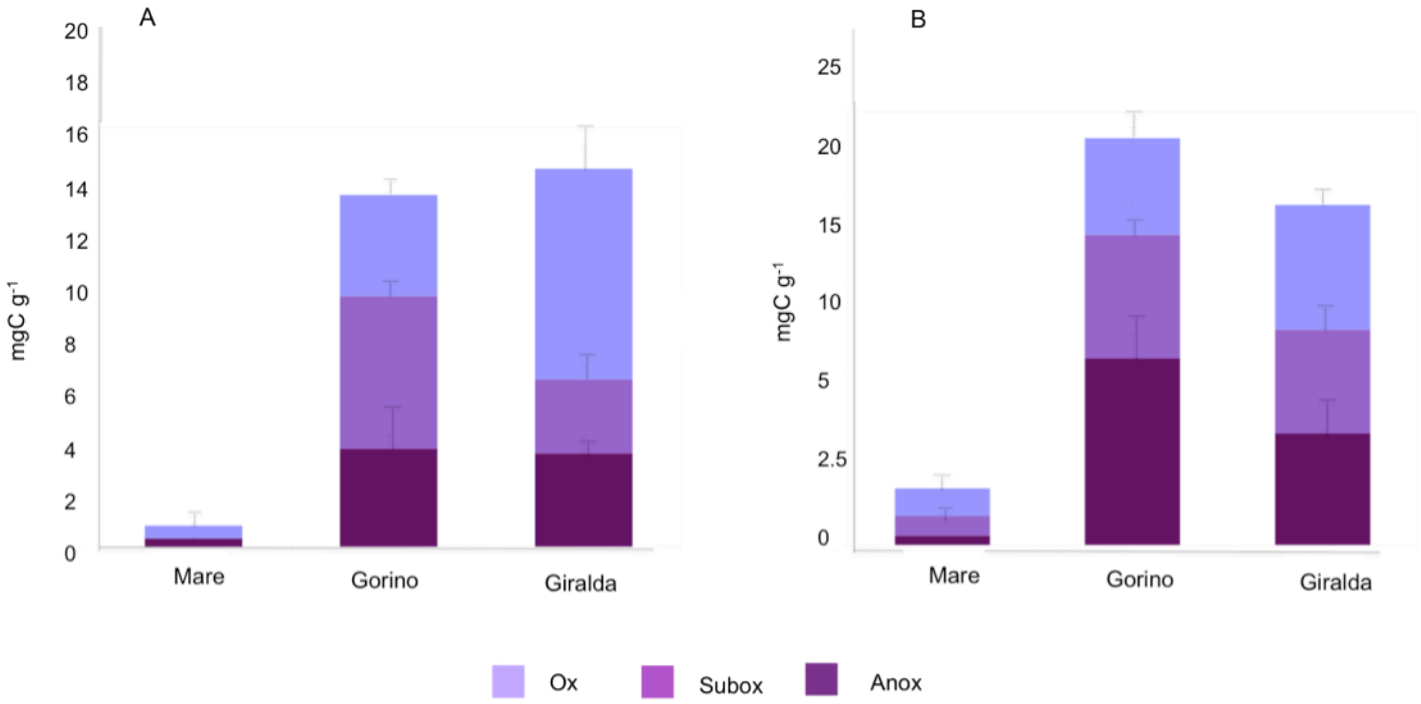

Fig.8 A) Biopolymeric carbon content in the three stations during the summer; **B)** Biopolymeric carbon content in winter

III.4.2. Bacteria and Archaea Abundances

In Giralda during the summer sampling bacterial abundance decreased significantly with the sediment depth (ANOVA, SNK test, $p < 0.01$). The highest value was in the oxic layer, 2.3 x 10^8 cells g^{-1}. The lowest one was in the anoxic layer, 1.2 x 10^8 cells g^{-1} (Fig. 9A). The abundance of Archaea displayed a constant trend along the entire sediment profile, 0.5 x 10^8 cells g^{-1} (Fig. 9A).

Bacterial abundance observed in Giralda sediments during winter also showed significant difference between the layers (ANOVA, $p<0.001$). Bacterial abundance was higher in oxic layer, however there was any clear trend with

sediment depth (Fig. 10A). Archaeal abundances of oxic and anoxic layers was not statistical different (about 0.5 x 10^8 cells g^{-1}), but they were significant lower than the abundance found in suboxic layer, 2.2 x 10^8 cells g^{-1} (ANOVA and SNK, $p<0.01$; Fig. 10A).

In Gorino during the summer the abundances of Bacteria decreased with the sediment depth. The highest values were observed in the oxic layer, 2.1 x 10^8 cells g^{-1} (Fig. 9B), and the lower values were observed in the anoxic layer, 1.5 x 10^8 cells g^{-1} (Fig. 9B). The abundances of Archaea increased slightly with the depth, with highest values in the anoxic layer, cell 0.7 x 10^8 g^{-1} cells (Fig. 9B). Both archaeal and bacterial abundance trends with sediments profile was not significant (SNK-test ns).

Also in Gorino winter sampling the abundances of Bacteria was higher in top layer, 2.2 x 10^8 cells g^{-1}, and it tended to decrease significantly with the sediment depth (ANOVA, $p<0.001$; Fig. 10B). The abundances of Archaea were constant up to the suboxic layer, values of 0.5 x 10^8 cell g^{-1} (Fig. 10B) and they increased significantly in the anoxic layer with values of 1 x 10^8 cell g^{-1} (ANOVA, $p<0.001$; Fig. 10B).

During the summer, in Mare station, the abundances of Bacteria are fairly constant in the three layers of the sediment, values around 2.5 x 10^8 g^{-1} (Fig. 9C). The abundances of Archaea tend to increase with depth. Lower values of 0.5 x 10^8 cell g^{-1} in the oxic layer and higher values, 1 x 10^8 cell g^{-1} in the anoxic layer (Fig. 9C).

ANOVA showed no significant statistically changes in the abundance of

Bacteria and Archaea (SNK-test ns).

During the winter period the abundances of Bacteria tended to slightly decrease with depth, with values ranging from 1.2 x 10^8 cell g^{-1} in the suboxic layer to 0.8 cell x 10^8 g^{-1} in the anoxic layer (Fig. 10C).

The abundances of Archaea were constant along the entire depth of the sediment, values equal to 0.5 x 10^8 cell g^{-1} (Fig. 10C).

ANOVA showed no statistically changes with the abundance of Bacteria and Archaea (SNK-test ns).

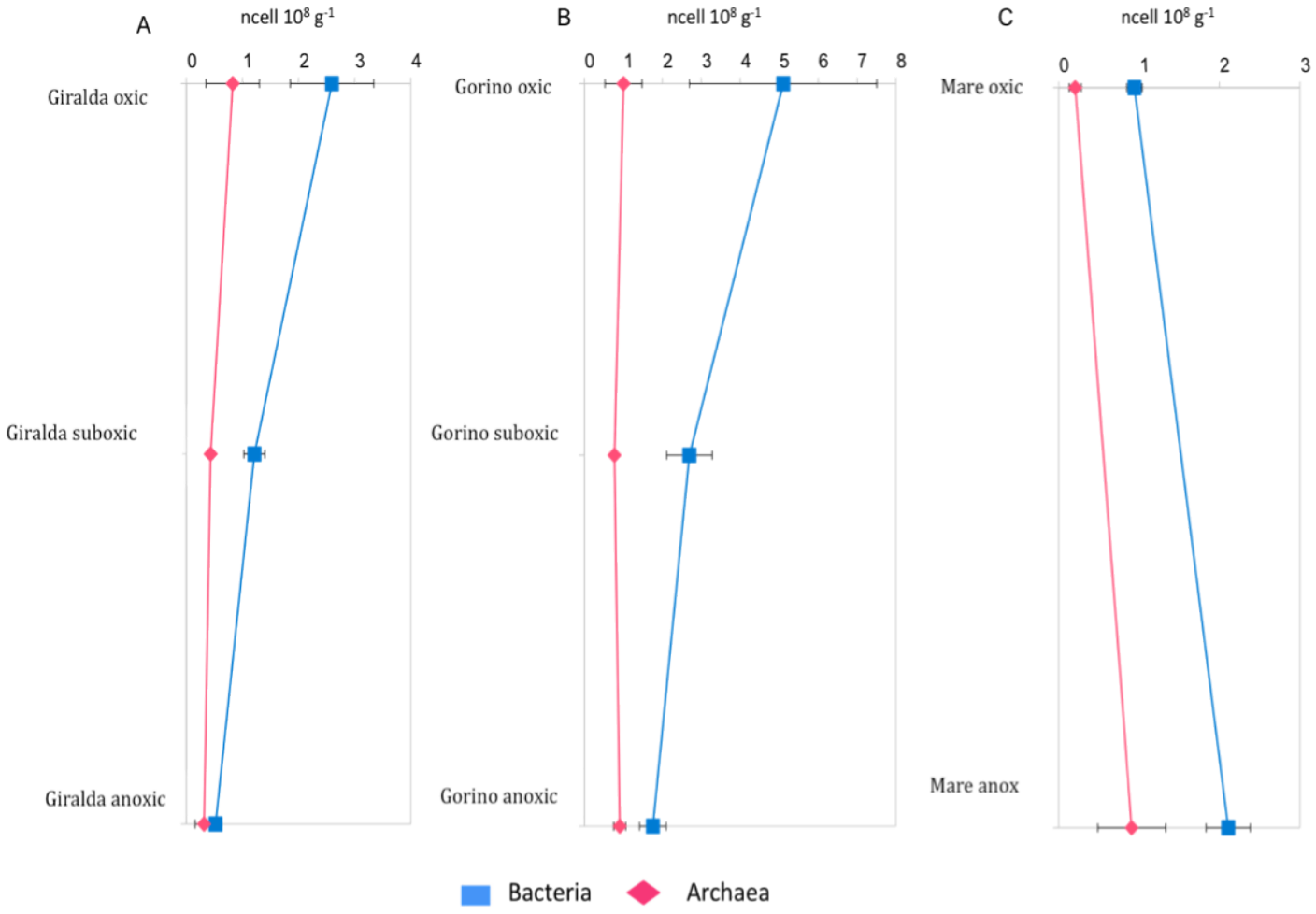

Fig. 9 A) Bacterial and archaeal abundance in Giralda during the summer; **B)** Bacterial and archaeal abundances in Gorino during the summer; C) Bacterial and archaeal abundances in Mare during the summer

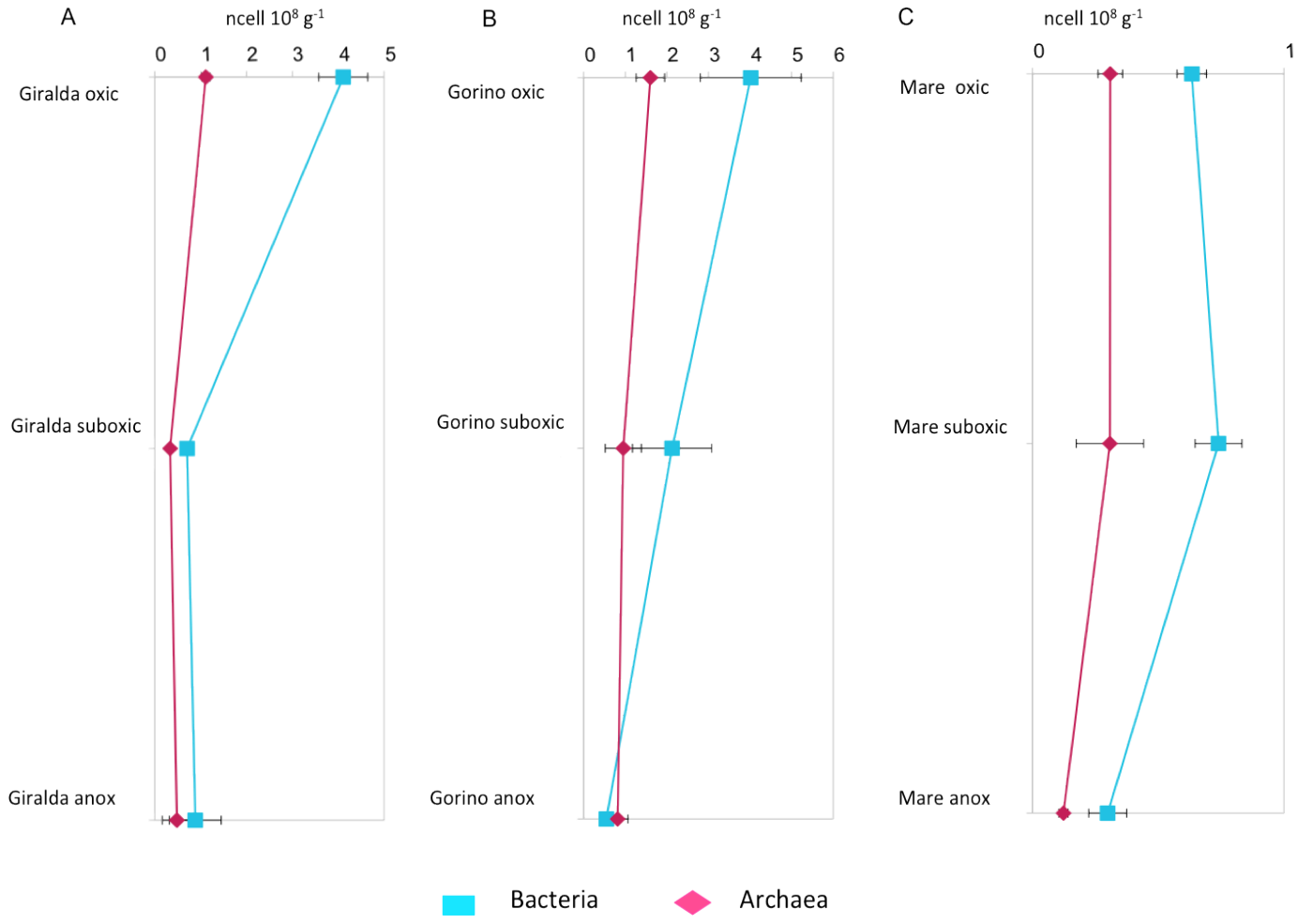

Fig. 10 A) Bacterial and archaeal abundance in Giralda during the winter; **B)** bacterial and archaeal abundance in Giralda during the winter; C) bacterial and archaeal abundances in Mare during the winter

III.4.3. Percentage composition of the prokaryotic community

In Giralda sediment, during the summer sampling, the relative abundance of Bacteria ranged from 25%, in the suboxic and anoxic layer, and in the suboxic layer in winter sampling, to 58% in the anoxic layer during winter (Fig. 11A-11D). The percentage contribution of Archaea to the total prokaryotes abundance ranged from 8%, in the suboxic layer in summer, to 30%, in the anoxic layer in winter (Fig. 11A-11D).

In Gorino sediment the percentage contribution of Bacteria to the total prokaryotic abundance varied from 31% to 47% in the oxic layer and anoxic

layer, respectively (Fig. 11B). The relative abundance of Archaea varied from 10%, in the oxic and suboxic layer of summer sediments, to 44% in the anoxic layer of winter sediments (Fig. 11B-11E).

In Mare bacterial contribution percentage to the total prokaryotes abundance varied from 39%, in the oxic layer of summer sampling, to 55%, in the suboxic and anoxic layers of winter sampling (Fig. 11C-11F). The archaeal contribution percentage varied from 10%, in the oxic layer in summer, to 25%, in the suboxic layer of winter sediments (Fig. 11C-11F).

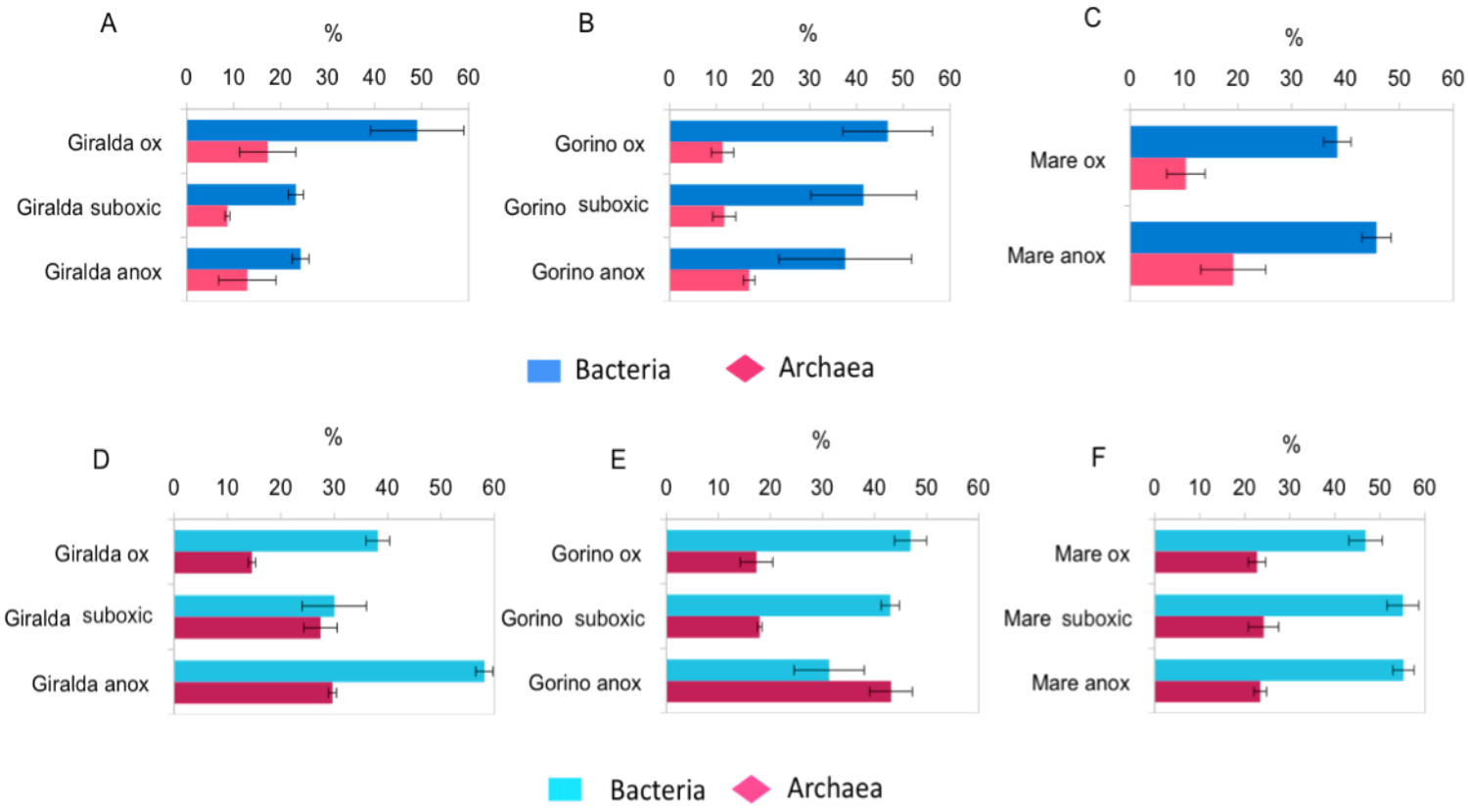

Fig. 11 A) Percentage contribution of Bacteria and Archaea in Giralda during the summer; **B)** percentage contribution of Bacteria and Archaea in Gorino during the summer; **C)** percentage contribution of Bacteria and Archaea in Mare during the summer; **D)** percentage contribution of Bacteria and Archaea in Giralda during the winter; **E)** percentage contribution of Bacteria and Archaea in Gorino during the winter; **F)** percentage contribution of Bacteria and Archaea in Mare during the winter

III.4.4.Statistical Analysis

In Table 2 are reported the results of distance-based permutational multivariate analyses of variance (PERMANOVA). The layer is the principal source of variability in my dataset, explaining more than half of bacterial and archaeal abundance variance.

TABLE 2 Permanova: differences in the composition of the prokaryotic community were tested between the different layers of sediment, different stations and different sampling periods

	Df	MS	Pseudo-F	P	% of variance explained
Sampling	1	1,0695	25,7117	0,0002	20,6
Station (sampl.)	2	0,1266	3,0449	0,0168	4,9
Layer (sampl x stat.)	8	0,359	8,6321	0,0002	55,3
Results	24	0,0416			19,2
Total	35				100

The figure 12 summarized the results achieved with non-parametric multivariate multiple regression analyses. The multiple regression analysis is carried out on bacterial and archaeal abundances in the oxyc layer using multivariate explanatory variables as temperature, salinity, dissolved oxygen, pH, nitrates, nitrites, ammonia, chlorophyll-a, lipids, proteins and carbohydrates. The results highlight that whereas more than 50% variance of archaeal abundance is explained only by pH, almost all of bacterial variance is explained by ammonia and physiological parameters.

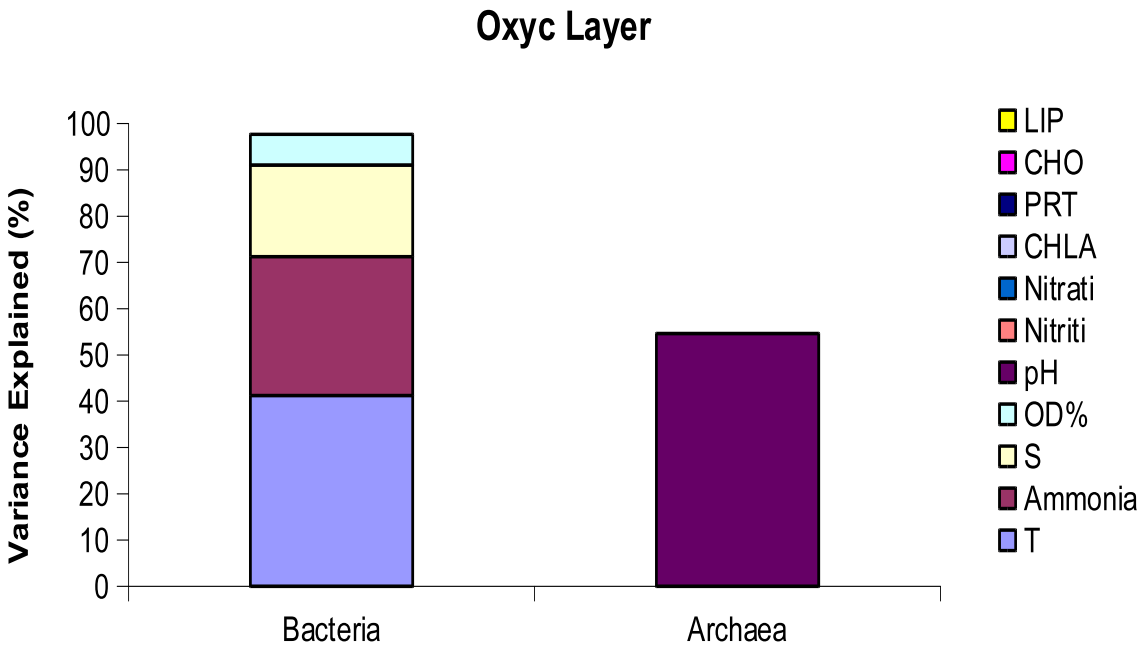

Fig. 12 Multiple Regression Analysis in the oxic layer

III.4. Discussion

Shallow, productive, and sheltered marine coastal systems, such as estuaries and coastal lagoons, are generally characterized by a strong spatial and temporal variability of physicochemical characteristics and productivity patterns (Newell 1982). In these environments prokaryotes are key players, and their role appears to be even more relevant in areas characterised by large organic C accumulation. Benthic prokaryotes in coastal lagoons are indeed key components of the remineralization process allowing the recycling of the nutrients needed to sustain primary production (Alongi, 1994), guaranteeing a buffer system against sulphide accumulation under dystrophic conditions (de Wit et al., 2001) and representing an important trophic source for benthic deposit feeders (Alongi, 1994). Despite their importance, little is known about the factors controlling community structure and abundance of prokaryotes in benthic marine sediments even less in lagoon sediments, making even more difficult to predict the magnitude and direction of the ecological responses to inorganic nutrient increase (i.e., eutrophication). The purpose of this study is to investigate together the variation of environmental parameters and the prokaryotic community structure (in terms of abundance of Bacteria and Archaea) in order to understand how the changes of physicochemical setting influence benthic prokaryotic assemblages of the Italian lagoon Sacca di Goro.

Changes in temperature, salinity, pH, dissolved oxygen and inorganic nutrients (ammonia and nitrates) were registered in the Sacca di Goro during the two sampling periods. These changes showed the presence of gradients, moving from the station closer to Po di Volano (Giralda) to the station at mare (Mare), concerning the decreasing of salinity, pH and ammonia in both sampling periods (Tab. 1). Below the sediments surface the decreasing of pH were observed only at Giralda and Gorino stations. The temperature and dissolved oxygen (at the

sediments surface) were constant between the sampling stations, but they showed higher value in summer and in winter, respectively. In all sites investigate and in each period the oxygen were depleted after few centimetres of sediments. All these results are commune features of the stations investigated as confirmed by previous studies (Viaroli et al., 2005; Viaroli et al 2008; Christian et al., 1996; de Wit et al., 2001).

The spatial and temporal heterogeneity of the investigated area is also evident in the content and composition of organic matter in the sediments. The analysis of the organic matter showed, indeed, the presence of high organic matter content in Giralda and Gorino, whereas lower amount in sediments of Mare station (Fig. 8A-8B). Fewer differences have been recorded in the three sediment layers analysed (oxic, suboxic and anoxic) within the 3 stations, as well as in the two different sampling periods. The elevate concentration of BPC found at Giralda and Gorino are to be linked to high productive zones characterized to eutrophic conditions (Pusceddu et al., 2009). Further typical alluvial mud with high clay and silt contents at Giralda and sandy/mud sediment at Gorino, together to low hydrodynamics contribute to higher accumulation of OM compared to the Mare. These results are in agreement with previous literature (Manini et al., 2001; Manini et al., 2003; Pusceddu et al., 2007; Danovaro and Pusceddu, 2007) reporting for eutrophic systems like Giralda and Gorino a higher content of organic matter in contrast to those oligotrophic one as Mare.

Overall the environmental characterization confirmed that the choice of study sites is consistent with the hypothesis to test: inside Sacca di Goro the spatial and temporal variation of environmental parameters influence abundance of Bacteria and Archaea. Bacterial and archaeal abundance was determined using Fluorescence *In Situ* Hybridization (FISH) with specific probe for the enumeration of the two prokaryotic domain cells in oxic, suboxic and anoxic layer for Giralda, Gorino and Mare during summer 2011 and winter 2012.

The total cells targeted by FISH (sum of Bacteria and Archaea) were on overage 51 ± 8 % and 70 ± 10 % (± standard error) of the total DAPI-stained cells in summer and winter, respectively. This low recovery efficiency is consistent with that reported for other studies carried out on marine sediments (Ishii et al., 2004; Ravenschlag et al., 2001; Llobet-Brossa et al., 1998; Sahm and Berninger, 1998). As previously reported in other studies (Molari et al., 2011; Molari and Manini, 2012; Schauer et al., 2010) Bacteria dominate the prokaryotic assemblages, encountering for ca. 50% of the total prokaryotes. Only in Gorino anoxic-layer (February 2012) Archaea outnumbered Bacteria, accounting on average for 43% of the total prokaryotes (Fig. 11F), however in all other sites their relative abundance were, on overage, 14% and 24% during the summer and winter, respectively. Although lower counts of Archaea were typically reported for marine sediments (Ishii et al., 2004; Ravenschlag et al., 2001; Llobet-Brossa et al., 1998; Sahm and Berninger, 1998), the studies carried out until now are to few, comparing to the heterogeneity and variety of the costal and transition aquatic environments, to can generalize on the pattern of archaeal abundance. Here I demonstrate that Archaea are present in all the investigated sediments of Goro and they are an important component of the microbial community (on overage 20%) up to now neglected in lagoon ecosystems.

My results highlighted that at Giralda and Gorino the abundances of Bacteria tend to decrease with sediment depth, both in summer and in winter (Fig. 9A-9B; 10A-10B). In other shallow marine sediments the bacterial abundances has been also reported to decrease along sediment profile (Ishii et al., 2004; Molari et al., 2012). Just to below the sediment surface the redox condition change dramatically, and the sediment became anoxic, acid and rich in sulfide. Under these conditions the prokaryotic abundance and activity are less. The reduction in the availability of electron acceptor is proposed to be also a factor in controlling prokaryotic abundance and activity in the subsurface sediments (Schmidt et al., 1998). My results suggest that Archaea are affected differently

than Bacteria. Indeed, Archaea tend to be constant along the whole profile of the sediment, or increase with depth, especially during the summer (Fig. 9C). This stability of number of Archaea and the decreasing of Bacteria, bring to change in prokaryotic community structure along sediment profile. Although not significative trend was observed, the relative abundance of Archaea tends to be increase along sediment profile, whereas that of Bacteria remain constant or decrease (Fig. 11A-11B-11C-11D-11F). These results are agree with that reported for shallow marine sediments (Molari et al., 2012) and continental margin subsurface environments (Lipp et al., 2008), where the contribution of Archaea to total prokaryotic assemblages increase along sediment profile up to become dominant domain about below one meter.

The PERMANOVA results confirmed the role of layer as a principal source of variability for bacterial abundance (Tab. 2). Also sampling period affects the abundance of Bacteria and Archaea, whereas the station has a minor role in shaping prokaryotic community structure. Although there are very marked physical-chemical gradients (i.e. salinity, pH, nutrients) between the three sampled stations, the environmental setting occurring under anoxic and acid condition have a major effect in influencing prokaryotic abundance and community structure. For this reason, in order to clarify what are the environmental factors that influence abundance of Bacteria and Archaea the multivariate multiple regression analysis (Anderson, 2001) was conducted separately considering oxic, suboxic and anoxic layers. These results show that the physiologically parameters (temperature, salinity and Dissolved Oxygen), which are most subject to strong variations in the space and time, that explain more than 70% of the variance for Bacteria (Fig. 12). In addition, another 20% of the variance for Bacteria is explained by ammonia, confirming that Bacteria play an important role in the nitrogen cycle: both as consumers (autotrophic metabolism) and as producers (heterotrophic catabolism). Surprisingly the 50% of the variance of Archaea abundance is explained only by pH, conversely to

Bacteria that are not affected by pH (Fig. 12). Further, unlike the bacterial assemblages, this suggests that groups physiologically more homogeneous dominate the Archaea populations.

The realization that Archaea were not strict extremophiles but wide spread in the aquatic and soil environments has became one of the most exciting findings in the recent history of microbial ecology. Since the discovery of a new group of mesophilic Archaea, the unveiling of their biogeochemical role in the environment has remained a challenge (Schleper et al., 2005; DeLong, 2006; Brochier-Armanet et al., 2012). The isolation of ammonia-oxidizing Archaea (*Nitrosopumilus maritimus*) in the water of an aquarium (Konneke et al., 2005) has suggested the possible ecological role of widespread mesophilic Archaea and has inspired a lot of researchers to investigate this new functional group. Today the frequent recovery of genes *amoA* (ammonia monooxygenase, the enzyme catalyzing the initial oxidation of NH_3) attributable to Archaea (Francis et al. 2005; Leininger et al. 2006; Wuchter et al., 2006; Lam et al., 2007) and the numerical dominance of *Crenarchaeota* in the ocean (Karner et al., 2001) and soils (Schleper et al., 2005) indicate that Archaea play an important role in nitrification. The environmental conditions related to the presence of Ammonia Oxidizing Archaea (AOA) are based on pH, sulfide, ammonia, temperature, salinity and dissolved oxygen conditions. Erguder and coworkers (2009) have proposed that the AOA might be important actors within the nitrogen cycle in low-nutrient, low-pH, and sulfide-containing environments. In this regard the dominance of a specific physiological group of archaea sensible to pH in environment like Sacca di Goro characterized by strong variation in ammonia, DO, sulfide and salinity fits very well with the picture that is emerging of mesophilic archaea.

III.5. Conclusion

Here for the first time I provide evidence that Archaea are also present in all sediments investigated of Sacca di Goro. Further they represent an important component of prokaryotic assemblages, which has not been taken into account in the understanding of the biogeochemical cycles of the lagoon so far. My results confirmed also that variations, both in space and in time, of physiological environmental parameters (temperature, salinity, pH, DO) have an important role in shaping the prokaryotic community structure. Bacterial and archaeal abundance are differentially controlled by these factors, suggesting that they could have a different role in the ecosystem functioning of lagoon. In particular the data provide by literature about the physiology of mesophilic Archaea and the importance of pH variation in controlling their abundance, observed in this study, bring me to hypothesise that they could be have an important role in nitrification. This hypothesis will be tested in the next chapter.

IV. IDENTIFICATION OF AMMONIA OXIDIZING KEY PLAYERS BY STABLE ISOTOBE PROBING

IV.1. Abstract

The niche partitioning between aerobic ammonia oxidizing Bacteria (AOB) and Archaea (AOA) is currently an important subject of study, but the factors that regulate and control the distribution and activity of ammonium oxidizing organisms (AOO) is still not clear. Recently it has been described that the availability of ammonium, the trophic status as well as the pH can influence the niche of AOO. Here, I challenge current perspectives by showing that AOA dominate over AOB in estuarine sediments highly loaded with ammonium, organic matter and at elevated pH (~8.2).

I have analysed the abundance and community structure of prokaryotes and nitrifiers, and nitrification in estuarine sediments from three distinct sites, Giralda, Gorino and Mare with specific chemical, physical and biological characteristics. The sampling area was the Sacca di Goro Lagoon of the Po estuary (Italy). Microcosm stable isotope probing (SIP) experiments with $^{13}CO_2$ were carried out to identify dominating populations of ammonia oxidisers, and to clarify whether the contribution of AOA and AOB to gross nitrification is a function of their abundance and of pH in sediments. This study suggests that in Sacca di Goro lagoon at least three groups of ammonia oxidizers were actively involved in nitrification: members of Bacteria domain (potentially *Nitrosospira sp*.) and two taxa belonging to the Archaea (related to *Nitrosopumilus and Nitrososphaera*). Indeed, AOB seemed to dominate the process in Giralda sediments under high rates of nitrification and low salinity, whereas Archaea dominated in Gorino sediments, under low nitrification rates and high salinity. This advances our understanding of the role of Archaea in the nitrogen cycle in coastal transition systems subject to high inputs of nitrogen and under strong

anthropogenic pressure.

IV.2. Introduction

The intertidal areas in coastal zones include some of the most productive marine ecosystems and therefore are vital as breeding and feeding grounds for many species of birds, fishes and crustaceans. These areas are under threat from anthropogenic activities, through land reclamation, fisheries and in particular through eutrophication caused by nutrient input through terrestrial runoff of nitrogen. Nitrification, the oxidation of ammonia to nitrate via nitrite, is central to the global cycling of nitrogen and, when linked to anoxic environments, where NO_3^- can serve as alternative electron acceptor for denitrification, is a major regulating factor alleviating eutrophication processes (Kemp et al., 1990; Rysgaard et al., 1994). However, nitrification processes depend on the availability of dissolved oxygen and may be totally eliminated if hypoxia occurs through eutrophication (Kemp et al., 1990).

The first, usually rate-limiting oxidation step in nitrification, is carried out by ammonia-oxidizing bacteria (AOB) and ammonia-oxidizing archaea (AOA). In particular the putative AOA have been recently discovered (Spang et al., 2010) and proposed to belong to a new archaeal phylum, *Thaumarchaeota*.

Ammonia-oxidizing bacteria consist of three evolutionary distant groups, two of which belong to the class *Proteobacteria* (Head et al., 1993; Koops et al., 2003). One group forms a deep branch within the *Gammaproteobacteria* and comprises only three recognized, closely related marine *Nitrosococcus* species. The second group, which includes the majority of cultured strains, forms a monophyletic group within the *Betaproteobacteria* and consists of two genera, *Nitrosomonas* and *Nitrosospira*. The third group, belonging to the order *Planctomycetales*, is associated with the Anammox process and its importance in marine systems has been suggested, particularly for oxic–anoxic interfaces (Jetten et al., 2003). Molecular studies of AOB communities in freshwater and estuarine systems suggest the dominance of beta-proteobacterial AOB (Caffrey et al., 2003). Laboratory isolates of freshwater and marine betaproteobacterial AOB (Koops

and Pommerening-Roeser, 2001), and AOB 16S rRNA gene sequences from freshwater and estuarine environments (Speksnijder et al., 1998; de Bie et al., 2001; Caffrey et al., 2003) fall predominantly within Nitrosomonas lineages. In marine systems, prevalent sequence types are associated with the *Nitrosomonas eutropha* lineage (Phillips et al., 1999) or belong to the *Nitrosomonas* cluster 5 or *Nitrosospira* cluster 1 clone groups, for which no cultured representative has yet been isolated (McCaig et al., 1999; Hollibaugh et al., 2002; Freitag and Prosser, 2003; 2004).

The isolation of the first ammonia-oxidizing Archaea (AOA), *Nitrosopumilus maritimus* SMC1 of the until then enigmatic group I.1a archaea, was reported (Könneke et al., 2005). Members of this lineage are ubiquitously distributed in open ocean and coastal waters and have been demonstrated to represent 20% to 30% of marine microbes (Herndl et al., 2005; Karner et al., 2001; Massana et al., 2000, Wuchter et al., 2006). Within the past few years, additional *N. maritimus* strains have been obtained in enrichment cultures (Park et al., 2010; Wuchter et al., 2006). Furthermore, the uncultivated marine sponge symbiont *Candidatus Cenarchaeum symbiosum* was shown to encode genes essential for the oxidation of NH_3 and thus became regarded as an AOA (Hallam et al., 2006; Hallam et al., 2006; Preston et al., 1996). However, this organism has not yet been shown to catalyze the oxidation of NH3 and, until further data are available, should be considered an amoA-encoding archaeon (AEA; Dang et al., 2009). Later, the group I.1a AOA Ca. *Nitrosoarchaeum* limnia SFB1 was enriched from a low-salinity sediment and its genome was nearly completely reconstructed via a combination of metagenomics and single-cell sequencing (Blainey et al., 2011). The genomes of Ca. *Nitrosoarchaeum koreensis* and Ca. *Nitrosopumilus salaria* were obtained from enrichment cultures from agricultural soil and estuary sediment, respectively (Jung et al., 2011; Kim et al., 2011; Mosier et al., 2012). Very recently, novel (as-yet-unnamed) AOA species were enriched from freshwater sediment (French et al., 2012), expanding our knowledge about the

environmental distribution of this archaeal lineage. Besides this group I.1a Archaea, two thermophilic AOA species, Ca. *Nitrososphaera gargensis* (Hatzenpichler et al., 2008) and Ca. *Nitrosocaldus yellowstonii* (de la Torre et al., 2008), have been described. While the former was the first characterized member of group I.1b archaea, the latter represents a deep-branching lineage (thermophilic AOA [ThAOA] group; formerly hot water crenarchaeotal group III [HWCG-III]) with wide distribution in high- temperature habitats.

Besides the known lineages of AOA (group I.1a, group I.1a-associated, group I.1b, ThAOA), sequence data suggest that more, as-yet-unidentified amoA-encoding and potentially ammonia-oxidizing groups might exist (Mincer et al., 2007; Pester et al., 2011; Pester et al., 2012; Prosser et al., 2008).

Based on the distribution of Archaea *amo*A (ammonia monooxygenase) and 16S rRNA genes, it seems that Archaea with the potential capacity to oxidize ammonia (AOA) are found in almost every environment on Earth, including ocean waters, estuaries, sediments and soil, hot spring, the guts of animals, plant leaves, and even in the ultra-clean rooms of NASA (Moissl et al., 2008). Astonishingly, estimates based on gene count (quantitative polymerase chain reaction) indicate that AOA, which have been overlooked for so many years, outnumber AOB in most environments, often even by orders of magnitude (Schleper, 2010). Despite this, there are very few environmental studies that provide evidence that the presence and activity of AOA is directly related with ammonia oxidation.

Even more so, this is true for lagoon ecosystems. Therefore, the aim of this study was to test the hypothesis that in lagoon ecosystems, not only Bacteria but also Archaea are involved in nitrogen cycle. In particular the environmental gradients (i.e. nitrogen loads, salinity, pH, DO) typical of lagoon are enable to structure different community of ammonia oxidizers. Further since pH is resulted to be most important factor influencing the abundance of Archaea and contribute to explain also that of Bacteria in Goro sediments (see Chapter III),

here I tested the effect of the pH on nitrification rates and community structure of ammonia oxidizing organisms (AOO).

In my project, ammonia-oxidizing bacterial and archaeal communities were analysed by amplification of 16S rRNA gene fragments from environmental DNA and subsequent analysis by Terminal-Restriction Fragment Length Polymorphism (T-RFLP), sequencing and phylogenetic analysis. These techniques were combined with stable isotope probing (SIP; Radajewski et al., 2000; Lueders et al., 2004) to characterize the active AOB and AOA community. Application of SIP to determine AOB and AOA activity involves incubation of environmental samples with 13C-labelled CO_2 and fractionation of extracted 13C-labelled and unlabelled nucleic acids. Molecular analysis of labelled and unlabelled nucleic acids characterizes active and inactive community members, respectively, and thereby provides a more reliable measure of links between community structure and ecosystem function.

To date only two studies using DNA-SIP have been conducted in order to understand the role of AOB and AOA in aquatic ecosystems (Freitag et al 2006; Yucheng et al 2013). Thus, this is the first time that the DNA-based Stable Isotope Probing (DNA-SIP) is applied in marine sediments in order to clarify the role of AOA in the nitrogen cycle. The sampling area was Sacca di Goro (Fig. 1, Chapter III), a shallow-water embayment of the Po River Delta. The samples were collected from the same stations, Giralda, Gorino and Mare, sampled during summer 2011 and winter 2012 (see Chapter III).

IV.3. Material and Methods

IV.3.1. SIP experiment

SIP is a method used in microbial ecology that provides a means by which specific functional groups of organisms, involved in a given process and that incorporate particular substrates, are identified without the prerequisite of cultivation. Briefly, an isotopically labelled substrate (13C and/or 15N) is added to a natural microbial community, where specifically active microbial populations incorporate the stable isotope into DNA biomarkers. Whole community DNA is then extracted and separated by density gradient ultracentrifugation. The gradient is fractionated, and fractions containing 13C-DNA of active microorganism are identified using molecular tools (Fig. 1).

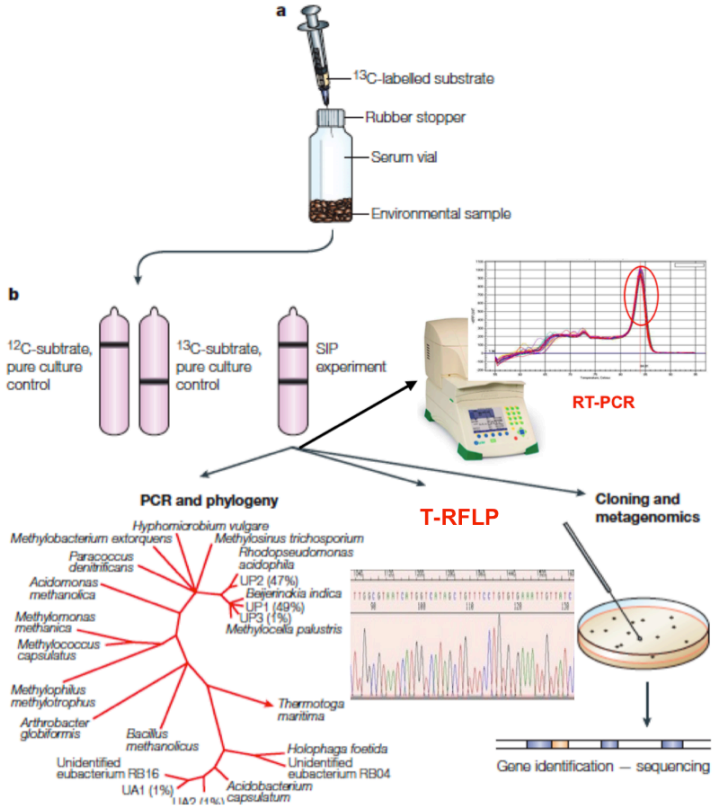

Fig. 1 DNA-based stable isotope probing (SIP); **a)** 13C-labelled substrate is added to an environmental sample. The sample is incubated so that the labelled carbon from the substrate can be incorporated into the biomass of the active microorganisms in the sample; b**)** total DNA that has been purified from the incubated sample should represent those microorganisms that grew using the 13C-labelled substrate. This genomic DNA-enriched with the 13C isotope can be separated from the community DNA (12C-DNA) by CsCl gradient centrifugation. Phylogenetic analyses of sequence data produced by PCR amplification of the isolated 13C-labelled DNA using

selected primers sets can help to identify organisms that are active in the soil sample. (Adapted from Dumont and Murrell, 2005).

IV.3.2.Ex situ microcosms experiment

Before starting with the real ex-situ microcosm experiment, in September 2012 it was conducted a pilot experiment to define the experimental conditions and test the SIP-DNA procedure.

The real experiment started in April 2013, bare sediments were collected from Giralda, Gorino and Mare to set up microcosms. The sampling activities were carried out using a small boat of Ferrara's Province. The sediment was collected using Plexiglas carrots of 8 cm diameter, chemical-physical parameters of water and water/sediments interface (salinity, temperature, pH, dissolved oxygen) were measured *in situ* using a multiparametric probe (ISI Instruments, mod. 556). In total 30 litres of water and 6 kg of sediment were collected. After the sampling the samples were stored at 12°C in the dark, before starting the experiment set up.

After 36 h of sampling the water from Giralda, Gorino and Mare was analyzed using Ion Chromatography (ICS-90, Dionex) for determining ammonia, nitrate and nitrite concentration. Using a simple alkalinity test (Aquamerck®), the dissolved inorganic carbon concentration (DIC) was also measured.

The microcosm consisted of 18 bottles (equipped with O_2 sensor spot, as described below) of 1 liter with 50 ml of sieved sediment from Giralda, Gorino and Mare plus 400 ml of Giralda, Gorino and Mare DIC-Free water (filtered 0.2 μm). As nitrification is sensitive to variation in pH and O_2 (Suzuki et al., 1974; Wrage et al., 2001), different pH (7.4 and 8.2) were recreated in the laboratory using HCl and NaOH in order to understand under what pH values conditions the AOA and AOB contribute most to nitrification. Furthermore to identify the active population of ammonia-oxidizing prokaryotes the microcosms were amended with 13C-bicarbonate. During ammonia oxidation there is not an assimilation of nitrogen, so to mark this process is necessary to use inorganic

sources of carbon labelled with the 13C as the ammonia oxidizing are chemolithoautotrophs. The experimental design (Fig. 2) consisting of eighteen microcosms, sampled at six different times (day 0, day 1, day 2, day 8, day 16, day 21). The experiment consists of a control, of a treated with enriched NH_4Cl and another treated with the addition of 13C-bicarbonate and NH_4Cl [200 μM]. The extraction and fractionation of DNA-SIP will be conducted as described in Lueders, 2010. Bottles were capped with butyl stoppers and incubated in the dark at 12°C (*in situ* temperature) with moderate shaking.

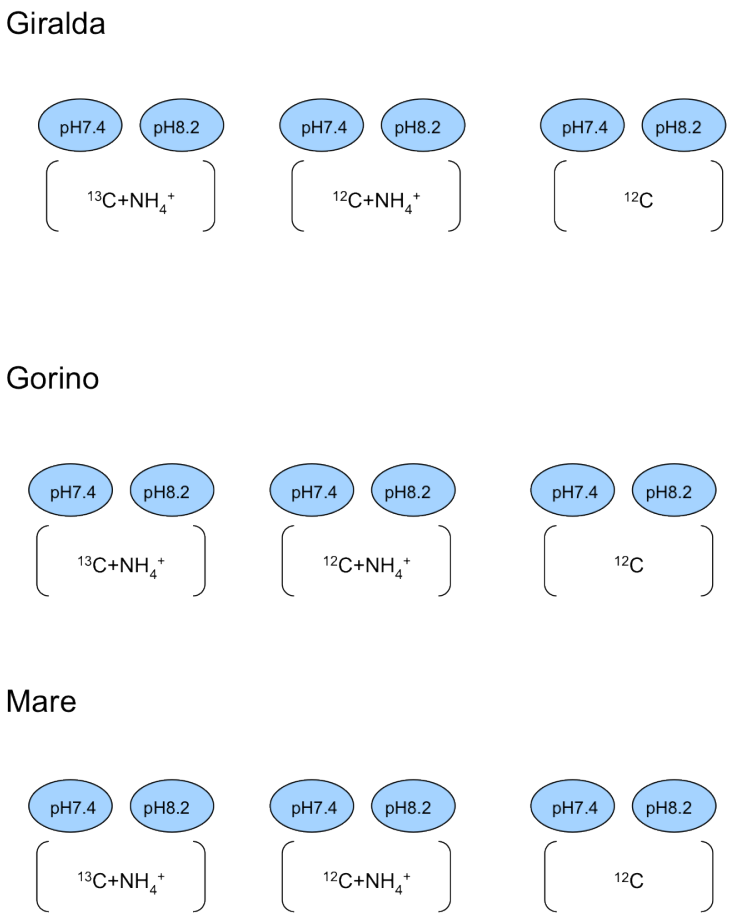

Fig. 2 The microcosms were set up considering 18 bottles of 1L each one, 3 different stations, 2 different pH, the presence/absence of 13C and NH_4^+

IV.3.1.3 Calibration of a PSt3 Sensor Spot

For microcosms 18 bottles of one liter were autoclaved and prepared with the

optical sensor spot (PSt3 PreSens) for monitoring the dissolved oxygen concentration.

1st Calibration Point with oxygen-free water:

to prepare oxygen-free water I dissolved 1 g of sodium sulfite (Na_2SO_3) and 50 µL cobalt nitrate ($Co(NO_3)_2$) standard solution (ρ(Co) = 1000 mg/L; in nitric acid 0.5 mol/L) in 100 mL water. I used a suitable vessel with a tightly fitting screw top and I labelled it cal 0. I checked that there is only little headspace in vessel. Due to a chemical reaction of oxygen with the Na_2SO_3 the water becomes oxygen-free. Additional oxygen, diffusing from air into the water, is removed by surplus of Na_2SO_3. I closed the vessel with the screw top and I shacked it for approximately one minute to dissolve Na_2SO_3 and to ensure that the water is oxygen-free. To prepare oxygen-free water you also can use sodium dithionite ($Na_2S_2O_4$).

I filled the calibration solution cal 0 in the vessel with mounted the sensor spot in. I verified that the sensor spot surface is covered completely with the liquid. To minimize the response time, I slightly stirred the solution. Then I followed the instructions in the respective transmitter manual for calibration. After recording the first calibration point I removed the calibration solution cal 0, I filled the vessel with distilled water and I stirred it for 1 minute. I repeated this procedure at least 5 times in order to clean the sensor spot from sodium sulfite.

2nd Calibration Point with Air-satured water:

I added 100 mL water to a suitable vessel and I labelled it cal 100. To obtain air-saturated water, I blown air into the water using an air-pump with a glass-frit (air stone), creating a multitude of small air bubbles, while stirring the solution. After 20 minutes, I switched of the air-pump and I stirred the solution for another 10 minutes to ensure that the water is not supersaturated.

I filled the calibration solution cal 100 in the vessel with mounted the sensor spot in. I checked that the sensor spot surface is covered completely with the

liquid. To minimize the response time, I slightly stirred the solution. Then I followed the instructions in the respective transmitter manual for calibration.

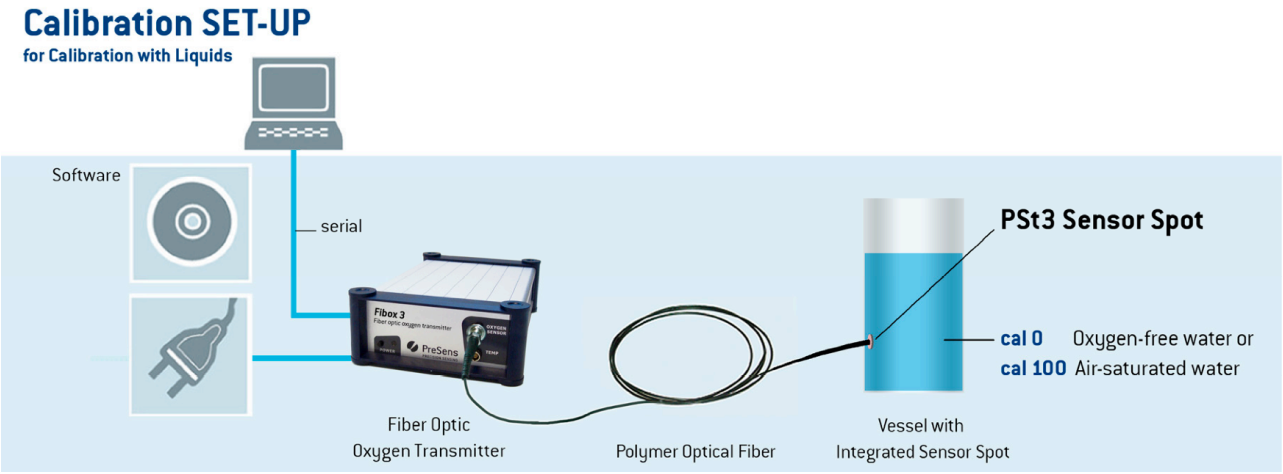

Fig. 3 Calibration set-up: Two-point calibration of a PSt3 sensor spot with liquid calibration standards (© 2011 PreSens Precision Sensing GmbH).

IV.3.1.4.DIC free water treatment

Ammonia-oxidizer organisms (AOO) have slow growth rates, therefore to increase the 13C assimilation the natural 12C-DIC of water was replaced with 13C-DIC. In this way the isotopic dilution (12C:13C ratio) is reduced, resulting in higher labelling of microorganisms.

The DIC free treatment was conducted on Giralda, Gorino and Mare water filtered 0.2 µm. The water pH was reduced to 2 with injection of HCl 10 M, in order to convert all dissolved inorganic C forms in CO_2. Then O_2 and CO_2 were removed by nitrogen (N_2) bubbling for 20 minutes. In 1 litre flask it was prepared the carbonates trap, an aqueous solution of NaOH 5M (500 ml), and connected to air flux and to the big flask containing sampled water (O_2 and CO_2 free). The air CO_2 free, coming from carbonate trap, oxygenate again the experimental water. Then the initial pH was restored with NaOH 10 M. Finally the alkalinity was measured using a alkalinity test (Aquamerck®) and the experimental water was amended with 13C-bicarbonate (and 12C-bicarbonate

the controls) to obtain the natural alkalinity values measured for Giralda, Gorino and Mare.

IV.3.1.5.Sample collection

The microcosm experiment lasted 21 days and it was sampled six different stopping times: 1 hour (T1), 24 hours (T24), 2 days (T2), 4 days (T4), 8 days (T8), 16 days (T16), 21 days (T21).

Before to open the bottles for taking the samples, it was measured the dissolved oxygen concentration (via Oxygen Sensor Spots, Fig. 4) to ensure that they remained oxic during the incubations. For each stopping time it was collected in triplicate 15 ml of slurry, centrifuged at 4000 rpm for 20 minutes. The supernatant was collected, filtered and stored at -20°C for inorganic nutrient analysis. The remaining sediment (~1.5g) was frozen at -20°C for molecular analysis. Further at each stopping the pH was measured.

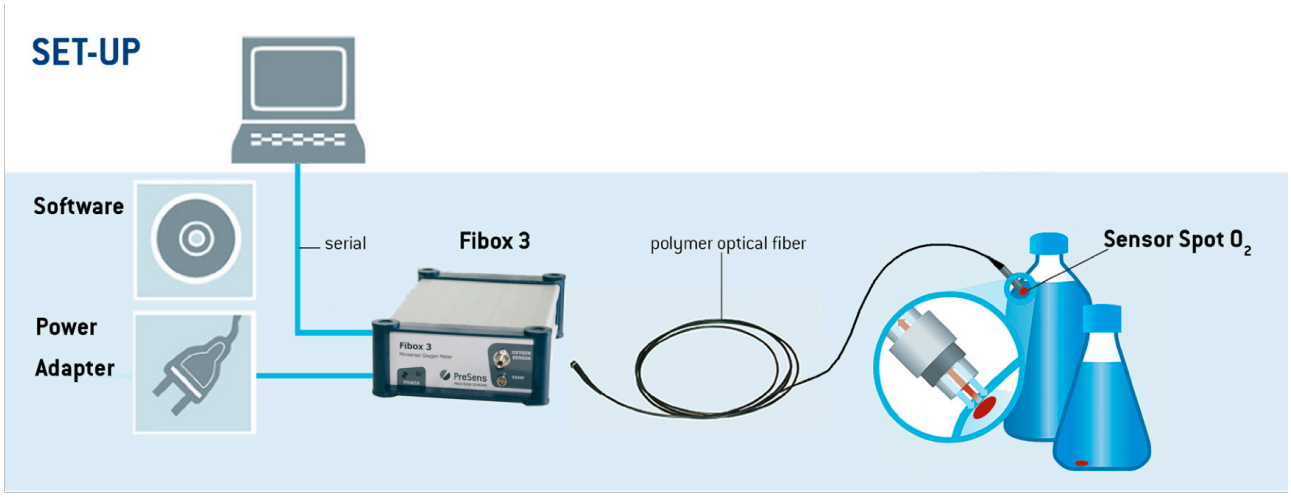

Fig. 4 Set-up for measurement with a sensor spot PSt3 (© 2011 PreSens Precision Sensing GmbH).

IV.3.2. Inorganic Nitrogen measurement

For natural lagoon waters the determination of Ammonia, Nitrate and Nitrite was done through Ion Chromatography (ICS-90, Dionex).

The Dionex ICS-90 Ion Chromatography System (ICS-90) performs isocratic ion analyses using suppressed conductivity detection. An ion chromatography system typically consists of a liquid eluent, a high-pressure pump, a sample injector, a separator column, a chemical suppressor, and a conductivity cell. Before running a sample, the ICS-90 is calibrated using a standard solution. By comparing the data obtained from a sample to that obtained from the standard, sample ions can be identified and quantitated. A computer running chromatography software automatically converts each peak in a chromatogram to a sample concentration and produces a tabulated printout of the results.

The IC analysis consists of four stages (see Fig. 5):

1. Eluent Delivery

- Eluent, a liquid that helps to separate the sample ions, carries the sample through the ion chromatography system. The ICS-90 is an isocratic delivery system. This means that the eluent composition and concentration remain constant throughout the run.
- Liquid sample is injected into the eluent stream either manually or automatically (if an automated sampler is installed).
- The pump forces the eluent and sample through a separator column (a chemically-inert tube packed with a polymeric resin).

2. Separation

- As the eluent and sample are pumped through the separator column, the sample ions are separated. In the ICS-90, the mode of separation is called ion exchange and it is based on the premise that different sample ions migrate through the IC column at different rates, depending upon their interactions with the ion exchange sites.

3. Detection

- After the eluent and sample ions leave the column, they flow through a suppressor that selectively enhances detection of the sample ions while suppressing the conductivity of the eluent.

- A conductivity cell monitors and measures the electrical conductance of the sample ions as they emerge from the suppressor and produces a signal based on a chemical or physical property of the analyte.

  4. Data Analysis

- The conductivity cell transmits the signal to a computer running chromatography software.
- The chromatography software analyzes the data by comparing the sample peaks in a chromatogram to those produced from a standard solution. The software identifies the ions based on retention time, and quantifies each analyte by integrating the peak area or peak height. The results are displayed as a chromatogram, with the concentrations of ionic analytes automatically determined and tabulated.

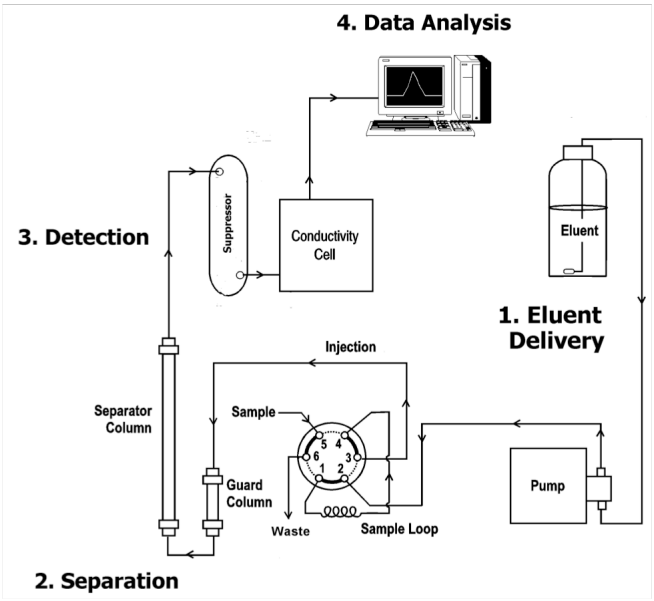

Fig. 5 Ion Analysis Process.

The determination of nitrogen inorganic nutrients in microcosms water was carried out using a colorimetric assay. Ammonium was determined with the blue indophenol method according to Bower and Holm-Hansen (1980). Nitrate was determined after cadmium reduction as nitrite via diazotation (APHA, 1975), for more details see Chapter III.

IV.3.3. DNA extraction

DNA was extracted from ~0.8 g of frozen sediment by bead beating (45 s at 6.5 ms^{-1}) in a FastPrep-24 (MP Biomedicals, Solon, OH) with ~0.2 ml of zirconia-silica beads (1:1 mix of 0.1- and 0.7-mm diameter; Roth, Karlsruhe, Germany) in 2 ml screw-cap vials, in the presence of sodium phosphate, TNS solution and Phenol/Chloroform/Isoamylalchol (25:24:1) (Lueders et al., 2004). After centrifugation, the nucleic acid containing aqueous supernatant was extracted consecutively with equal volumes of phenol-chloroform-isoamyl alcohol [PCI, 25:24:1 (vol/vol/vol)] and chloroform-isoamyl alcohol [CI, 24:1 (vol:vol), Sigma], prior to precipitation with two volumes of polyethylene glycol (Griffiths et al., 2000) and centrifugation at 20 000 x *g* and 4°C for 30 min. Nucleic acid pellets were washed once with 70% ethanol and resuspended in 100 ml elution buffer (EB; Qiagen). Aliquots of DNA extracts were visualized by standard agarose gel electrophoresis to verify the quality of extracted total DNA. DNA was quantified in extracts using the PicoGreen nucleic acid quantification dyes (Molecular Probes), according to the manufacturer's instructions. Measurements (10 ml of unknown sample per 100 ml assay) were carried out in 96-well microtitre plates in a Safire fluorescence microplate reader (Tecan Deutschland GmbH). Nucleic acid standards included in the quantification kits were diluted to concentrations between 1 and 50 ng per 100 ml well.

IV.3.4. Isopycnic ultracentrifugation and fractioning

IV.3.4.1.Centrifugation of DNA-SIP gradients

Density gradient centrifugation was performed in 5.1 ml polyallomer quick-seal tubes to be spin in a VTI 65.2 vertical rotor. For DNA, gradients should be prepared at an average BD of 1.71–1.72 g ml^{-1} CsCl before centrifugation (Lueders et al., 2004b; Neufeld et al., 2007c). This will ensure an optimal resolution of unlabeled and labelled DNA into ''light'' and ''heavy'' gradient

fractions after centrifugation. Below is reported the laboratory procedure applied to samples.

1. Add 5.1 ml of CsCl stock solution (~1.84 g ml^{-1}), up to 1 ml of gradient buffer (GB), and 5 μg of DNA (Pico Green quantified, volume must be subtracted from GB volume) to a sterile 15 ml plastic tube.
2. Mix carefully (do not vortex), measure the refractory index of a 75 ml aliquot of the mixture to control for average BD. For the protocol and solutions described here, the temperature-corrected refractive Index (nD-TC, 20°C) should be at 1.4042 ± 0.0002 (≅1.71 g ml-1 CsCl). Adjust by adding 100 ml aliquots of GB or CsCl and repeated measuring, if BD is too high or low, respectively.
3. Transfer medium to 5.1 ml polyallomer ultracentrifugation tubes using a 6 ml syringe with a 120 mm needle. Be careful not to injure the tube with the needle and to avoid air bubbles. Fill tube up to the bottom of the filling nozzle and do not leave droplets inside the nozzle when removing the needle.
4. Seal tubes by welding with the Tube Topper tool leaving a small air bubble (~5 ml) on top of the medium. Take care not to melt the aluminium-welding cup into the dome of the tube.
5. Sort multiple tubes into opposing pairs of ± 0.02 g on a balance. Place inside VTi rotor and close loaded slots with the appropriate caps and sealing rings. Do not close the empty slots. Spin 60 h at 20°C and 44,500 rpm (180,000 gav). Turn off brakes after the run or use brakes only above ~5,000 rpm. This minimizes mixing when the gradient flips over by 90° inside the tube when the rotor stops.
6. Carefully remove tubes from rotor, minimize any mechanical disruption, and proceed immediately with gradient fractionation.

IV.3.4.2.Gradient Fractionation

1. Fix tube with gentle pressure in a laboratory clamp for fractionation (Fig. 33).

2. Using luer-lock adapters fit a sterile 24 mm needle to flexible but pressure-tight tubing from a syringe pump filled with sterile water. Shortly operate the pump to eliminate air bubbles in tubing or needle.
3. Carefully poke needle into the centrifugation tube at the location of the small air bubble on top of the medium (Fig. 6). Apply only mild pressure, so the needle does not exit the tube on the opposite side. Stab needle minimally into opposing wall for fixation, so that the water will be gently placed on top of the gradient medium with minimal mixing.
4. Using another, sterile 24 mm needle, poke a hole into the bottom of the tube. Avoid disturbance of the gradient by minimizing shaking. After removing the needle, the gradient should not start dripping if all above connections are airtight.
5. Operate the pump at a rate of 1 ml min^{-1}. Using a stopwatch, collect equal volumes of gradient fractions in sterile 2 ml microfuge tubes by shifting cups between drops every 25s (13 fractions of ~416 µl). After fraction 13, stop the pump, immediately close, and label cups.
6. Sacrifice 75 µl of each fraction to measure the refractory index (nD-TC) on the refractometer. Start with lightest (=13^{th} fraction). Calculate BD for each fraction.

Fig. 6 Fractionation of SIP ultracentrifugation gradients via a syringe pump and manual fraction collection.

IV.3.4.3.Nucleic acid precipitation

1. Precipitate DNA from CsCl gradient fractions by adding 2 volumes of PEG precipitation solution.
2. Mix thoroughly (do not vortex) and precipitate by centrifuging for 30 min at full speed (14,000 rpm) and 4°C in a laboratory microfuge. Take care that all 2 ml cups are identically orientated within the rotor (hinges upward), since pellets will not be visible after centrifugation and may be lost during washing if touched with the pipette tip.
3. Remove supernatant with a pipette, do not decant to avoid pellet loss. Add 150 ml of ice cold 70% ethanol, wash gently, spin down again for 5 min at 14,000 rpm and 4°C.
4. Quantitatively remove the ethanol (best done with a 200 µl pipette tip). Place 25µl of RNA-grade elution buffer (EB) on the presumed pellet. Shake cups for 1 min in a Thermomixer at 1,400 rpm and 30°C to dissolve pellets. Spin down 1 min at 14,000 rpm and 4°C.

5. Place re-eluted nucleic acids from gradient fractions in sterile 8-cup PCR strips with single caps for storage (-20°C) and subsequent quantitative and qualitative analysis.

IV.3.5. qPCR

Bacterial and archaeal 16S rRNA genes precipitated from gradient fractions were quantified specifically by real-time PCR in an Mx3000P cycler (Stratagene, La Jolla, CA, USA) using the detection primers Ar109f/Ar912r (Lueders and Friedrich, 2003) and Ba519f/Ba907r (Stubner, 2002). Each 50 µl PCR reaction contained 1x PCR buffer II (Applied Biosystems), 1.5 mM $MgCl_2$, 100 µM each of the four dNTPs (Amersham), 0.2 µg μl^{-1} BSA (Roche), 0.2x SybrGreen (FMC Bioproducts), 0.3 µM of each primer (MWG Biotech), 1.25 U of Ampl-iTaq DNA polymerase (Applied Biosystems), and 2 µl of standard or unknown DNA. Thermal cycling was an initial denaturation step for 3 min at 94°C followed by 40 cycles of amplification (30 s at 94°C, 30 s at 52°C, and 60 s at 72°C), and a terminal extension step (5 min at 72°C). After each run, a melting curve was recorded between 65°C and 98°C to discriminate between specific amplicons and unspecific SybrGreen signals (e.g. primer dimers). Standardization of archaeal templates was done with a dilution series (10^7-10^1 copies µl-1) of almost full-length 16S rRNA gene amplicons from pure culture DNA of M. barkeri generated with the primers Ar7f (TTC YGG TTG ATC CYG CC)/Ar1384r (CGG TGT GTG CAA GGA GCA). Bacterial templates were quantified using almost full-length amplicons of the E. coli 16S rRNA gene, generated with the primers Ba27f/Ba1492r (Weisburg et al., 1991).

IV.3.6. T-RFLP

Amplicons of bacterial and archaeal communities in gradient fractions were generated by PCR with the Ba27f/Ba907r, Ar109f/Ar912rt respectively primer

set, of which the forward-primer was FAM-labelled in a Mastercycler ep gradient (Eppen- dorf, Hamburg, Germany) with the following cycling conditions: initial denaturation (94°C, 5 min), followed by 25 or 30 cycles of denaturation (94°C, 30 s), annealing (52°C, 30 s) and elongation (70°C, 60 s). Each 50 μL PCR reaction contained 1 X PCR buffer, 1.5 mM $MgCl_2$, 0.1 mM dNTPs, 1.25 U recombinant Taq polymerase (all from Fermentas, St. Leon-Rot, Germany), 0.2 μg μL-1 bovine serum albumin (BSA) (Roche, Penzberg, Germany), 0.5 μM of each primer (Biomers, Ulm, Germany) and 1 μL of template DNA. After amplicons purification, amplicons were digested in two separate preparations using MspI for Bacteria and TaqI for Archaea for 2 h in a thermocycler at 37 and 65°C, respectively.

Digested amplicons (~50 ng in 10 μl) were desalted by using DyeEx spin columns (QIAGEN). Desalted digests (1 μl) were mixed with 13 μl of Hi-Di formamide (Applied Biosystems) containing a 400-fold dilution of MapMarker-1000 ROX Size Standard, denatured (3 min at 95°C), cooled on ice.

The T-RFLP run was conducted on an ABI 3730 DNA analyzer (Applied Biosystems, Foster City, CA), the electropherograms were processed with GeneMapper (version 4.0) programs (Applied Biosystems, Foster City, CA).

IV.3.7. Archaeal and bacterial diversity through 454 Pyrosequencing

Amplicon pyrosequencing was performed on unfractionated total DNA extracted from 13C-microcosms, only for Gorino.

Barcoded amplicons for multiplexing were prepared with the primers Ba27f (5'-AGA GTT TGA TCM TGG CTC AG-3') and Ba519r (5'-TAT TAC CGC GGC KGC TG-3') for Bacteria and with the primers Ar344f (5'-ACG GGG YGC AGC AGG CGC GA- 3') and Ar915r (5'-GTG CTC CCC CGC CAA TTC CT-3') (Kittelmann et al., 2013) extended as amplicon fusion primers with respective primer A or B adapters, key sequence and multiplex identifiers (MID)

as recommended by 454/Roche (http://454.com/products-solutions/experimental-design-options/amplicon-sequencing.asp). Amplicons were generated under the same cycling conditions as described above for T-RFLP. Each 50 μL PCR reaction contained 1x PCR buffer, 1.44 mM $MgCl_2$, 0.1 mM dNTPs, 1% dimethyl sulphoxide, 1.25 U Taq polymerase (all from FastStart High Fidelity Taq DNA Polymerase kit, Roche), 0.32 μg μL-1 BSA (Roche), 0.3 μM of each MID-primer (Biomers) and 1μL of template DNA. Amplicons were purified and pooled as specified by the manufacturer. Emulsion PCR, emulsion breaking and sequencing were performed applying the GS FLX Titanium chemistry following protocols and using a 454 GS FLX pyrosequencer (Roche) as recommended by the developer.

Quality filtering of the pyrosequencing reads was performed using the automatic amplicon pipeline of the GS Run Processor (Roche), with a modification of the valley filter (vfScanAllFlows false instead of TiOnly) to extract sequences.

Afterwards, reads were further quality-trimmed using the TRIM function of GREENGENES (DeSantis et al., 2006) with the following settings: good-quality score 20, window size 40 bp and window threshold 90%. Subsequently, reads were batched per sample based on MID-identifiers with BIOEDIT (Hall, 1999) and reads with inferior read length (< 250 bp) were excluded from further analysis. The total community composition was classified via read affiliation using the RDP classifier (Wang et al., 2007) at a confidence threshold of 70%. Read abundance percentage of classified lineages was recorded.

Analysis of 454 pyrosequencing for Archaea data-base was conducted using the Mothur software v1.25.0 (http://www.mothur.org/) (Schloss et al., 2009) combined with RDP II for taxonomic identification. All reads obtained were processed by removing tags and primers, only accepting reads with an average quality score above 25 and read lengths between 300-500 bp. The trimmed sequences were aligned against the SILVA bacterial and archaeal 16S rRNA gene databases using the Needleman algorithm. Chimeric sequences were

identified and removed using the implementation of Chimera-uchime (Edgar et al., 2011). Specific taxonomic groups of high-quality sequences were extracted and extended alignment was carried out with RDP Classifier (http://rdp.cme.msu.edu/classifier/classifier.jsp) (Wang et al., 2007). Only those sequences affiliated to target groups with Mothur and RDP alignments (confidence threshold >80%) were used to generate a distance matrix. The average neighbor algorithm was used to cluster sequences into operational taxonomic units (OTU). Representative sequences from each OTU as defined by 97% sequence identity were obtained for further analysis.

IV.4. Prokaryotic community structure and statistical analyses

Raw profiles were checked for stable baselines and voltage, and peak size and absolute areas were then determined by using GeneMapper software v 4.0 (Applied Biosystems) with minimum peak height of 50 fluorescence units for all dyes.

From GeneMapper output tables, conversions to sample-by-fragments tables and subsequently to sample-by-binned-OUT tables were performed by using custom R (http://cran.r-project.org/) interactive and automatic binning algorithms (interactive binner v 1.3 by A. Ramette, 2008). The algorithm rearranges the data and calculates the relative fluorescence intensity (RFI) of each peak by dividing individual peak area by the total peak area for the respective samples. All peaks with RFI value of <0.09% were not included in further analyses since they consisted of background peaks. To include the maximum number of peak while excluding background fluorescence, only fragment above a threshold of 50 fluorescence units and ranging between 100 and 1,000 bp were taken into consideration.

Binning has a significant effect on the obtained samples similarities and must thus be accounted for avoid falsely describing ecological differences that would be only due to technically variability (Hewson and Fuhrman, 2006). In order to

take into account the technical variability in peak size calling (Hewson and Fuhrman, 2006), dye migration discrepancies (Tu et al., 1998) and run-to run variation (Osborn et al., 2000), all peaks within a range of sizes (a window) can be combined (i.e. binned) into a bin window frames, where the window is as wide as the imprecision of the OUT size calling. Here a shifting window size (WS) binning strategy was used to optimally align electrophoretic profiles and to deal with different window starting positions. The binning frame that offers the highest similarity among samples is identified out of all binning frames starting at a given position. If T-RFLP imprecision is ±1 bp thus we have a WS of 2 and this would mean that the two bin frames would start, for example, at 100 and at 101, respectively. The distance between two consecutive binning frames is defined as the shift (Sh) value. Due to dye migration discrepancies the actual, true (but unknown) size value may be different from integer values (i.e. a decimal value could be also representing a "true" size). This means that for a Sh of 0.1 bp and WS of 2, there would therefore be 20 bin window frames to be calculated and evaluated. The script applied here allows for an automatic calculation of series of WS values (e.g. 0.5, 1, 2, 3, 4, and 5) for a given Sh value (e.g. 0.1 bp). This enabled an optimal determination of the best binning strategy for a data set without a priori knowing the ideal WS value (Ramette, 2009).

The sample-by-binned-OUT tables were used to calculate similarities among gradient fractions and treatments based on Bray-Curtis similarity index. The resulting matrix was examined for pattern of bacterial and archaeal community composition along the ultracentrifugation density gradients, in order to assess the presence of 13C-enriched DNA, by using cluster analyses. SIMPER (Similarity Percentages) analysis was then applied to identify which OTUs contribute to the similarities of prokaryotic communities between density gradients and treatments. All these statistical analyses were performed using computer program PRIMER 6.0.

Once it was highlighted the presence of 13-DNA in “heavy” fractions, Microbial Community Analysis III (Shyu et al., 2007) was carried out on T-RFLP results. The program (PAT+) allows the taxonomic identification of T-RFs comparing the size of forward fragment with the potential size of fragment calculated starting from T-RFLP primes and restriction enzyme (used in this study) and the 16S rRNA sequences deposited on open access Database. Since for the binding it was applied a window size of 2, also the mach for forward fragment was settled to ±2.

IV.5. Results

IV.5.1. Environmental parameters

The water parameters measured *in situ* at Giralda, Gorino and Mare stations measured are reported in Table 1.

Tab. 1 Environmental parameters of Giralda, Gorino and Mare, April 2013.

	Giralda	Gorino	Mare
Temperature	12°C	12°C	11.8°C
Salinity	1.66‰	16.8‰	17.8‰
pH	7.3	8.4	8.2
Dissolved Oxygen	6.27 mg l^{-1}	18 mg l^{-1}	10.46 mg l^{-1}

At the beginning of manipulation experiments the concentration of dissolved oxygen in Giralda, Gorino and Mare microcosms was between 10.5 mg l^{-1} and 11 mg l^{-1}. During the all incubation time (21 days) I observed low variation in dissolved oxygen, providing evidence that no anoxia or hypoxia events occurred into the microcosms (Tab. 2). In Giralda there is lower oxygen concentration, 9.45 mg l^{-1}, compared to the other stations, maybe due to higher respiration of the microbial community.

Tab. 2 Dissolved Oxygen concentration in Giralda, Gorino and Mare microcosms during the 13C bicarbonate experiment.

	T0	T1	T2	T4	T8	T16	T21
	mg/L	mg/L	mg/L	mg/L	mg/L	mg/L	mg/L
Giralda pH 7.4 ^{13}C NH_4^+	10.55	10.77	9.92	9.82	9.87	9.45	10.15
Giralda pH 8.2 ^{13}C NH_4^+	10.67	10.12	9.9	9.77	9.8	9.4	10.02
Giralda pH 7.4 ^{12}C NH_4^+	10.7	9.36	9.95	9.93	10.05	9.94	10.25
Giralda pH 8.2 ^{12}C NH_4^+	10.31	10	9.97	9.75	9.8	9.3	10.12
Giralda pH 7.4 ^{12}C	10.6	9.3	9.9	9.97	9.9	9.4	10.05
Giralda pH 8.2 ^{12}C	10.91	10.3	10.56	10.25	10.27	9.66	10.41
Gorino pH 7.4 ^{13}C NH_4^+	10.64	10.51	10.58	10.35	10.35	10.7	10.57
Gorino pH 8.2 ^{13}C NH_4^+	10.45	10.6	10.54	10.3	10.28	10.14	10.5

Gorino pH 7.4 ^{12}C NH_4^+	10.5	10.45	10.42	10.15	10.19	10.15	10.15
Gorino pH 8.2 ^{12}C NH_4^+	10.81	10.8	10.76	10.4	10.6	10.5	10.57
Gorino pH 7.4 ^{12}C	10.8	10.9	10.84	10.45	10.7	10.6	10.64
Gorino pH 8.2 ^{12}C	10.3	10.5	10.36	10.05	10.2	10.13	10.1
Mare pH 7.4 ^{13}C NH_4^+	11.3	11.1	11.15	10.8	11	10.9	10.8
Mare pH 8.2 ^{13}C NH_4^+	11.02	10.7	10.8	10.55	10.7	10.54	10.4
Mare pH 7.4 ^{12}C NH_4^+	11	10.8	11.03	10.7	10.85	10.76	10.72
Mare pH 8.2 ^{12}C NH_4^+	10.8	10.8	10.77	10.65	10.72	10.72	10.87
Mare pH 7.4 ^{12}C	11.11	11	10.97	10.9	11.08	11.02	10.9
Mare pH 8.2 ^{12}C	10.97	10.9	10.87	10.78	10.85	11.35	10.87

IV.5.2. Inorganic Nitrogen Measurement and pH

Ammonia concentration in lagoon water was 99 μM in Giralda, 39 μM in Gorino and 3 μM in Mare. Inorganic nitrogen species in the overlying water of microcosms were determined with colorimetric assay in order to assess the nitrification activity in sediments of microcosms. In Giralda's microcosms the ammonia finished after two days (Fig. 7), and the nitrification rates were so fast that the ammonia decreasing was visible after few hours from beginning of experiments (T0). With the decreasing of the ammonia the nitrates increasing during the first two and four days at pH 7.4 and pH 8.2, respectively, then they remain relatively constant. In pH 7.4 treatment the pH was stable only after day 2, whereas in pH 8.2 treatment the pH were quite constant for all experiments. Although in pH 8.2 treatment the values of pH were below 7.8, after T0 they are 0.2 unit higher then value of pH 7.4 treatments.

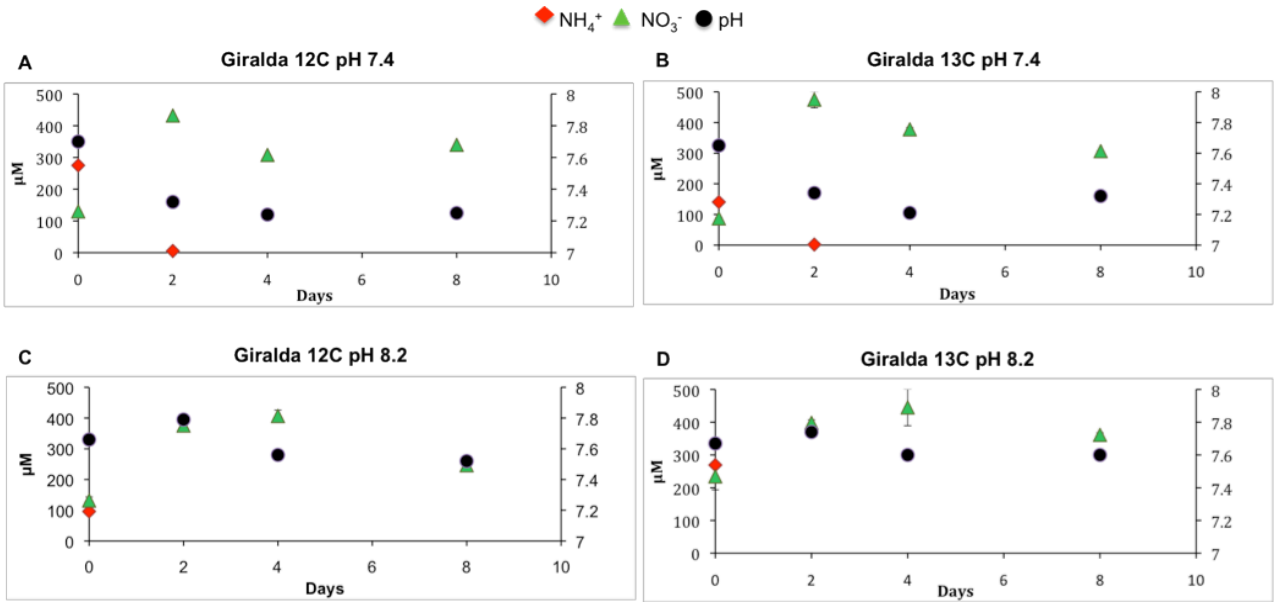

Fig. 7 A) Inorganic Nitrogen measurement and pH in Giralda pH 7.4 12C after 1 week of incubation; **B)** Inorganic Nitrogen measurement and pH in Giralda pH 7.4 13C after 1 week of incubation; **C)** Inorganic Nitrogen measurement and pH in Giralda pH 8.2 12C after 1 week of incubation; **D)** Inorganic Nitrogen measurement and pH in Giralda pH 8.2 13C after 1 week of incubation.

In Gorino the ammonia were oxidized after 8 days from the beginning of experiments (Fig. 8). However the ammonia consumption showed different trend with pH. At pH 8.2 the ammonia concentration was stable until day 4 and then decrease close to 0 at day 8 (fig 8 C and D). At pH 7.4 in 12C treatment the ammonia showed irregular trend: decrease close to 0 after two days, increase at day 4 and then decrease to 0 at day 8 (fig. 8 A). At pH 7.4 in 13C treatment the ammonia was constant until day two, then increase up to 400 µM and at day 8 the ammonia was completed depleted (fig. 8 B). In all microcosms the nitrates were quite constant until day 4 and then increase at day 8. After T0 the values of pH were close to 7.4 and constant in pH 7.4 treatment. Conversely in 8.2 treatment, the values of pH were close to 8 until day 2, then they decrease at 7.6 at day 8.

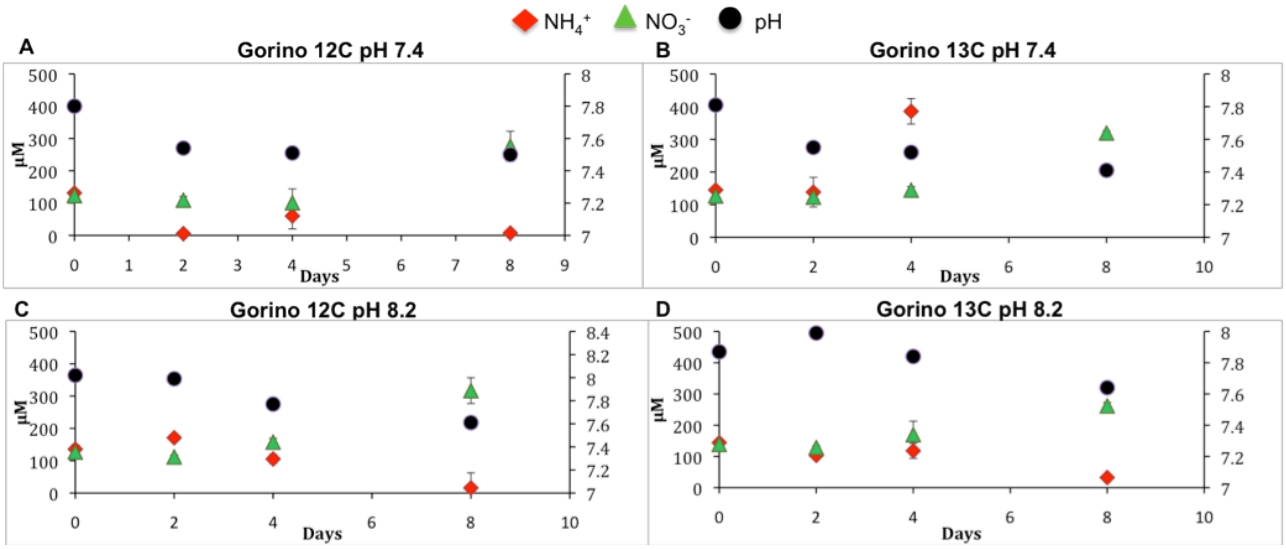

Fig. 8 A) Inorganic Nitrogen measurement and pH in Gorino pH 7.4 12C after 1 week of incubation; **B)** Inorganic Nitrogen measurement and pH in Gorino pH 7.4 13C after 1 week of incubation; **C)** Inorganic Nitrogen measurement and pH in Gorino pH 8.2 12C after 1 week of incubation; **D)** Inorganic Nitrogen measurement and pH in Gorino pH 8.2 13C after 1 week of incubation.

In Mare's microcosms the ammonia and nitrate concentrations were quite constant over 8 days (Fig. 9). The pH is constant around 7.6 and 8-7.8 in treatment pH 7.4 and pH 8.2 treatments, respectively.

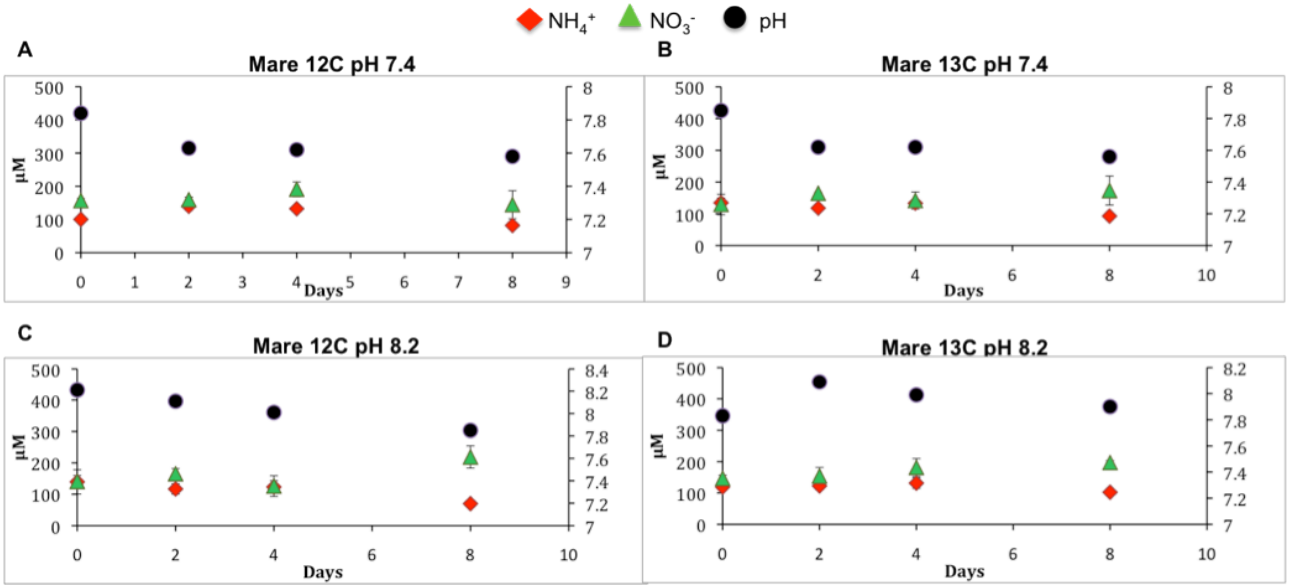

Fig. 9 A) Inorganic Nitrogen measurement and pH in Mare pH 7.4 12C after 1 week of incubation; **B)** Inorganic Nitrogen measurement and pH in Mare pH 7.4 13C after 1 week of incubation; **C)** Inorganic Nitrogen measurement and pH in Mare pH 8.2 12C after 1 week of incubation; **D)** Inorganic Nitrogen measurement and pH in Mare pH 8.2 13C after 1 week of incubation.

IV.5.3. DNA-Stable isotope probing of a different time points

CsCl gradient centrifugation was performed with DNA extracts from 12C and 13C-bicarbonate treatments at different stopping times (T4; T8; T21) and different pH (7.4-8.2). Bacterial and archaeal 16S rRNA genes in all 12 fractions of these gradients were enumerate by qPCR to identify the enrichment of 13C in extracted DNA.

Fig.10 shows the abundance of bacterial (A) and archaeal (B) 16S rRNA genes in the gradient fractions from DNA extracted by T8 (after 8 days of incubation) of Giralda at pH 7.4 and pH 8.2. For Bacteria I observed 13C enrichment only in pH 7.4 treatment, where the higher number of copies of bacterial 16S rRNA genes (here expressed as relative abundance, thus 100%) for 12C-DNA is located in a fraction with lower density (1.68 g ml^{-1}) than the fraction with maximum copies of bacterial 16S rRNA genes for 13C-DNA (1.69 g ml^{-1}). For Archaea in both treatments the qPCR did not highlight any 13C enrichment of DNA.

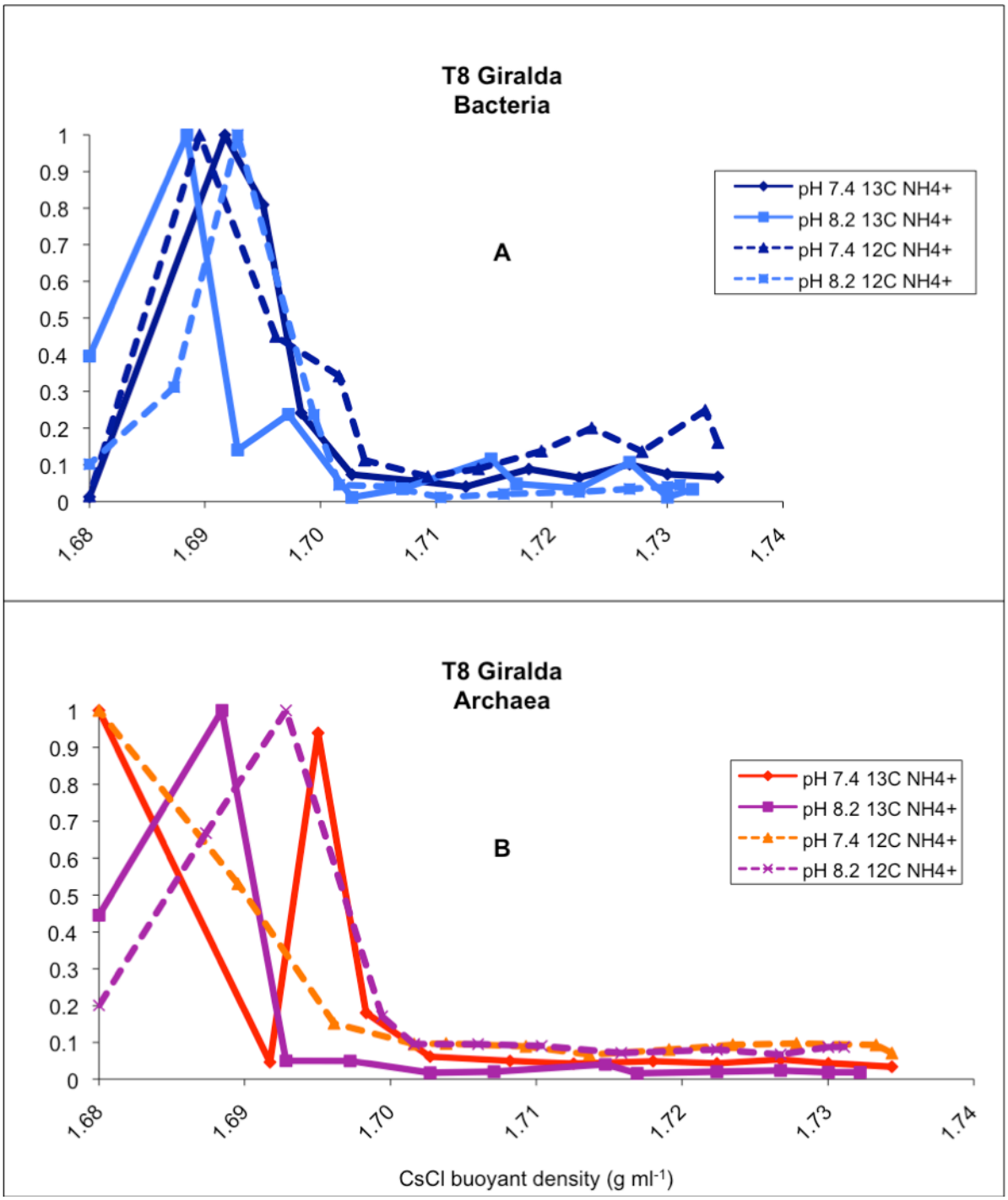

Fig. 10 Distribution of 16S rRNA genes copy numbers from **(A)** Bacteria and **(B)** Archaea across the buoyant density of the DNA isolated from soil incubated with either $^{12}CO_2$ or $^{13}CO_2$ in Giralda after 8 days incubation for both pH 7.4 and 8.2.

Fig. 11 shows the results from the T8 and T4 (after 8 days and 4 days of incubation) of Gorino but considering only pH 7.4. The qPCR showed clear ^{13}C-label incorporation into the DNA of Archaea after 8 days, but not after 4 days. Labelling of bacterial DNA was less significant.

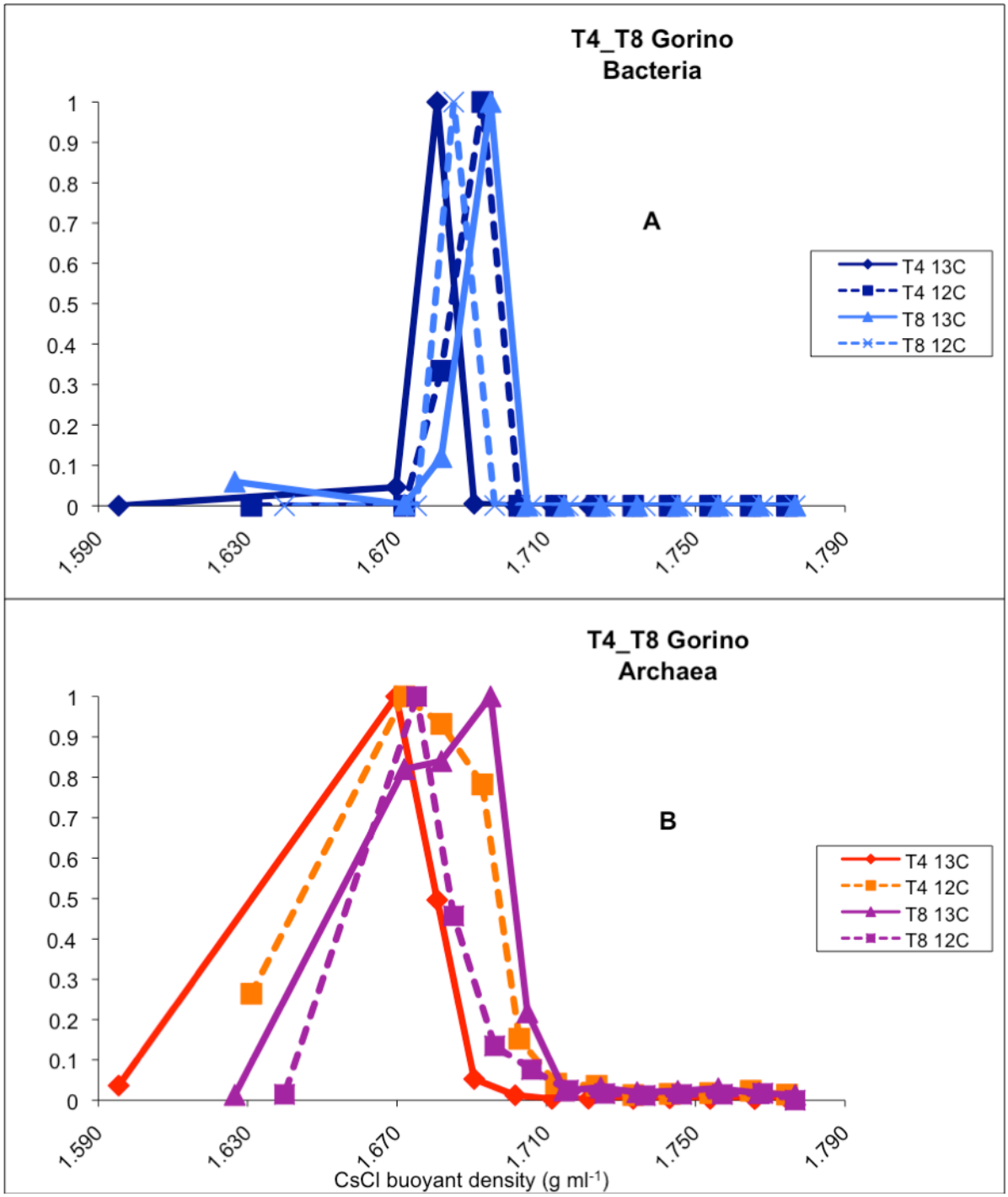

Fig. 11 Distribution of 16S rRNA genes copy numbers from **(A)** Bacteria and **(B)** Archaea across the buoyant density of the DNA isolated from soil incubated with either $^{12}CO_2$ or $^{13}CO_2$ in Gorino after 4 and 8 days incubation for pH 7.4.

Fig. 12 shows the results from the T21 (after 21 days of incubation) of Giralda and Gorino at pH 7.4. Here qPCR hilight that there is a clear 13C-DNA anrichment in Giralda, for Bacteria, and in Gorino, for Archaea.

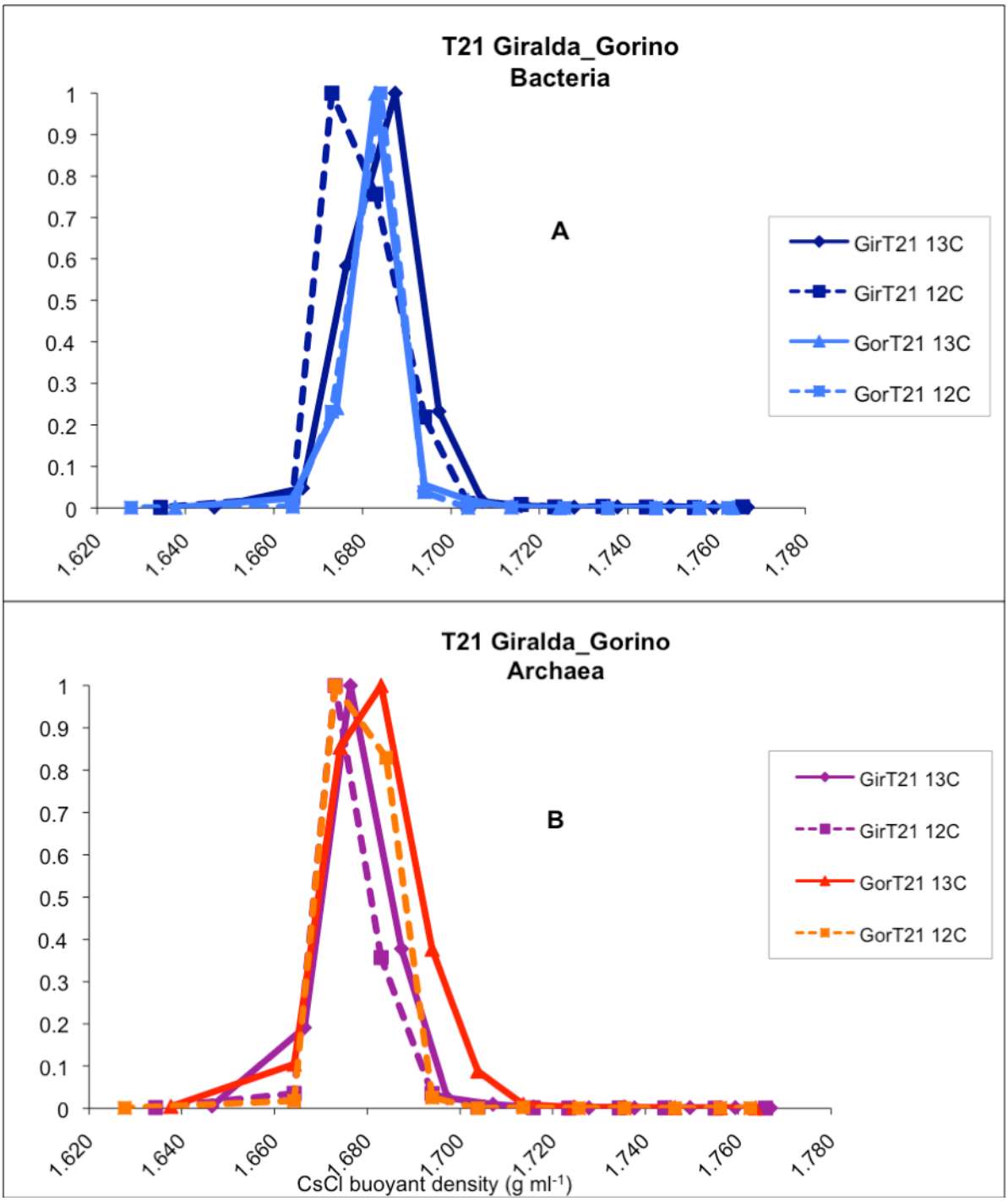

Fig. 12 Distribution of 16S rRNA genes copy numbers from **(A)** Bacteria and **(B)** Archaea across the buoyant density of the DNA isolated from soil incubated with either $^{12}CO_2$ or $^{13}CO_2$ in Giralda and Gorino after 21 days incubation for pH 7.4.

The ultracentrifugation resulted in 12 fractions and the buoyant density ranged from 1.6277 g ml^{-1} to 1.7669 g ml^{-1} from top to bottom of the tube. Bacterial and

archaeal 16S rRNA genes in fractions 6-11 of these gradients were enumerated by qPCR to identify the enrichment of 13C in extracted DNA (Fig. 41 A-B). The abundance of archaeal 16S rRNA genes in all microcosm with 12C-substrate peaked in fractions of buoyant density 1.6731-1.6841 g ml^{-1}. Shift to heavy fractions 1.6939–1.7038 g ml^{-1} were observed in all 13C-spiked microcosms, indicating the assimilation of inorganic carbon by Archaea. The enrichment of 13C in DNA of Archaea was more evident after 21 days as demonstrated by an increased peak at buoyant density of 1.7038 g ml^{-1}, as well as by a decreased peak at lower buoyant density.

Fig. 13 shows the results from the T8 and T21 (after 21 days of incubation) of Gorino at pH 8.2. Seems to be clear from the graphs that there is incorporation of 13C only for Archaea.

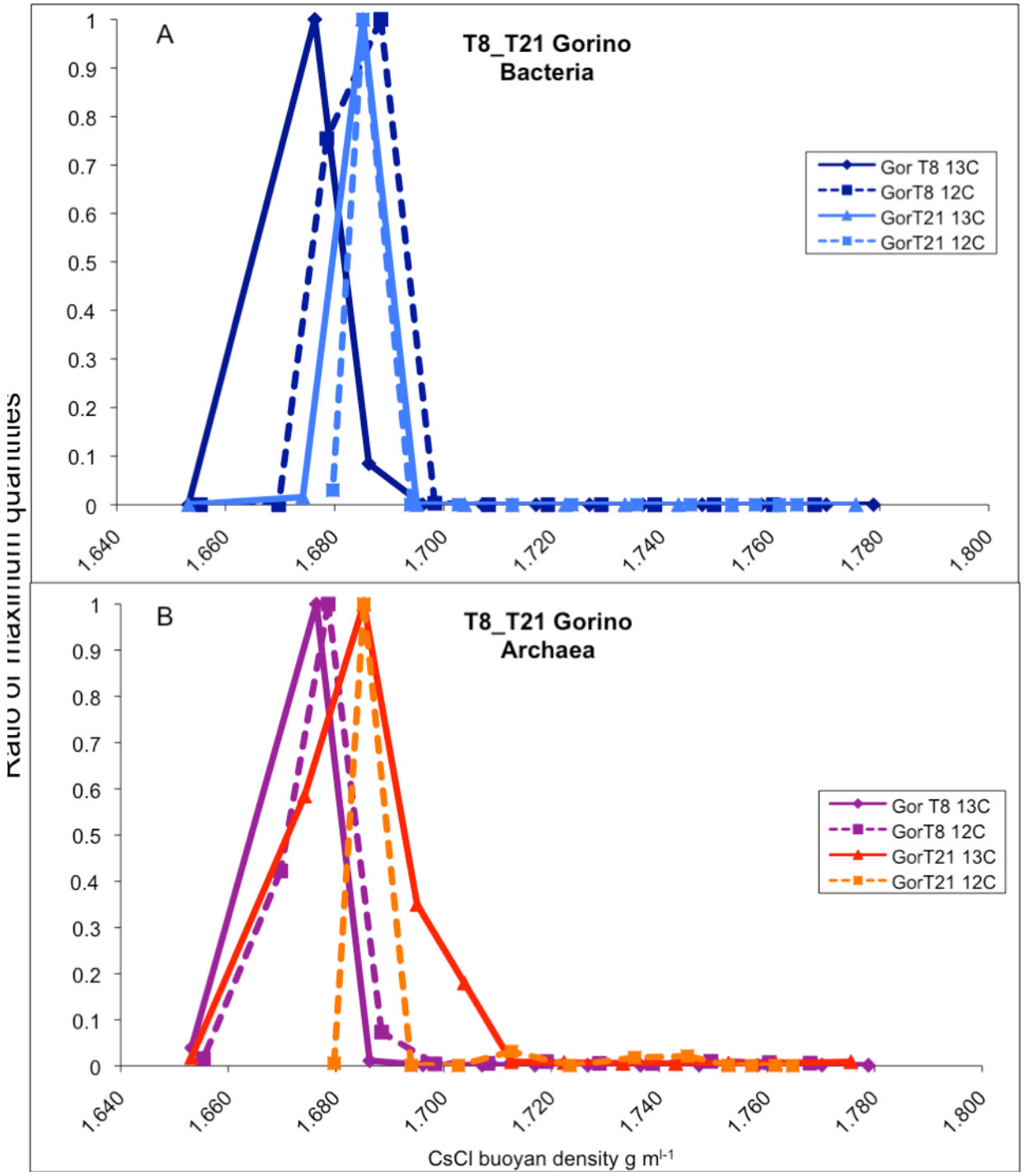

Fig. 13 Distribution of 16S rRNA genes copy numbers from **(A)** Bacteria and **(B)** Archaea across the buoyant density of the DNA isolated from soil incubated with either $^{12}CO_2$ or $^{13}CO_2$ in Gorino after 8 and 21 days incubation for pH 8.2

IV.5.4. T-RFLP fingerprinting of density-resolved bacterial and archaeal communities

T-RFLP of bacterial and archaeal templates was used to specifically trace the populations detectable in distinct gradient fractions at different time points and pH.

The electropherograms, of both light DNA (12C) at different pH (7.4-8.2) for Giralda after 8 days, are highly similar (Figg. 14A-15A). Looking at the heavy DNA (13C) there is almost the same situation: no differences between different pH (Figg. 14B-15B) Comparing the light and the heavy fractions at pH 7.4 seems to be an increase in the peaks in the heavy fractions, certain T-RFs specifically increased in the relative abundance (i.e. T-RFs with 78, 150, 174, 197, 277, 428 and 490 bp) (Figg. 14A-14B). This could explain the possibility that there was incorporation of 13C for bacterial communities at pH 7.4 after 8 days of incubation. Same situation occurs comparing the graphs from the light and heavy DNA at pH 8.2 (Figg. 14B-15B).

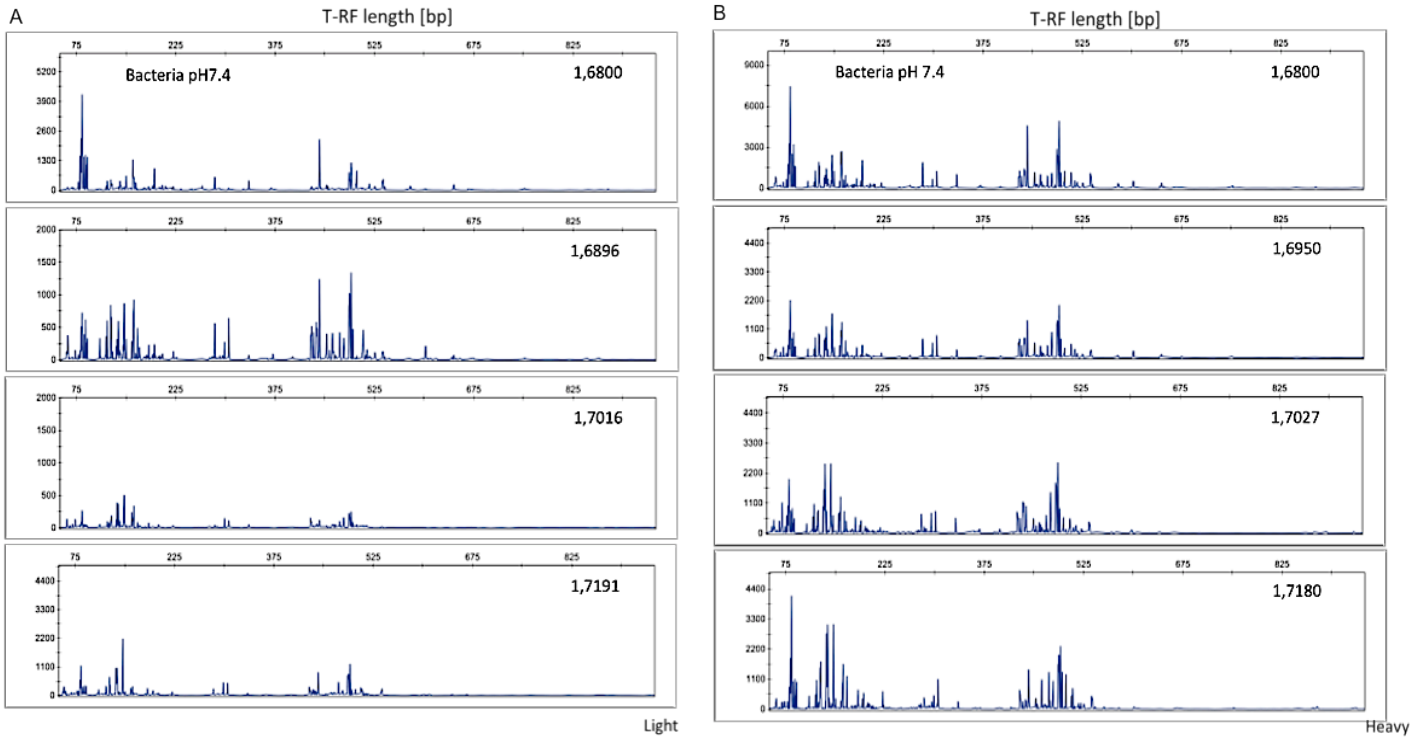

Fig. 14 (A) T-RFLP fingerprints of density-resolved bacterial communities retrieved from 12C-DNA ("light") after 8 days gradient fractions of nucleic acids extracted from Giralda at pH 7.4; **(B)** T-RFLP fingerprints of density-resolved bacterial

communities retrieved from 13C-DNA ("heavy") after 8 days gradient fractions of nucleic acids extracted from Giralda at pH 7.4.

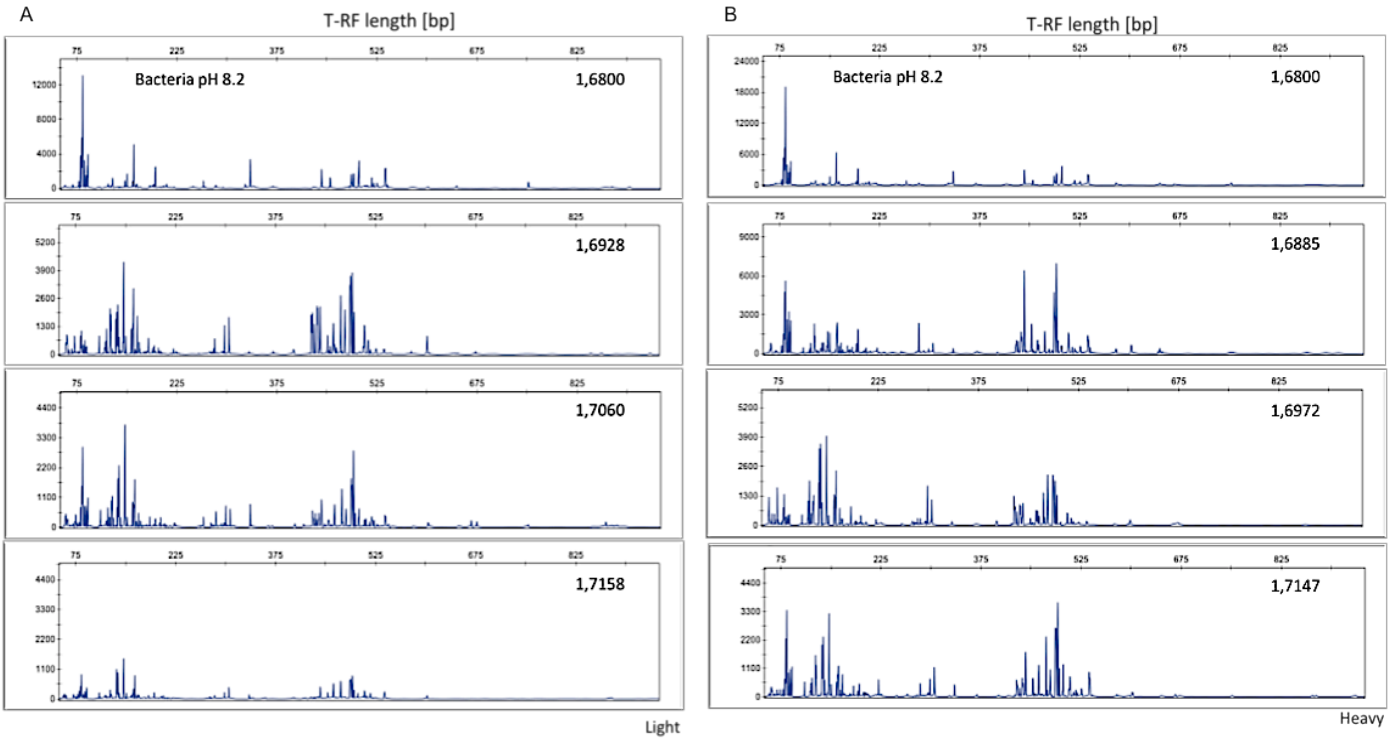

Fig. 15 (A) T-RFLP fingerprints of density-resolved bacterial communities retrieved from 12C-DNA ("light") after 8 days gradient fractions of nucleic acids extracted from Giralda at pH 8.2; **(B)** T-RFLP fingerprints of density-resolved bacterial communities retrieved from 13C-DNA ("heavy") after 8 days gradient fractions of nucleic acids extracted from Giralda at pH 8.2

Fig. 16A and Fig. 17A show the results of the electropherograms of "light" DNA (12C) for archaeal communities at both pH 7.4 and 8.2 in Giralda. There are no differences for the different pH. There is more or less the same situation for the "heavy" DNA (13C) for pH 7.4 and 8.2 (Fig. 16B-17B). The numbers of peaks decrease at pH 8.2 when density is 1.6929 g ml^{-1} and 1.7016 g ml^{-1} (Fig. 16B).

Comparing the light and the heavy fractions at pH 7.4 seems to be a small increase in the peaks in the heavy fractions (i.e. T-RFs with 810 bp) (Figg. 16A-16B). This could explain the possibility that there was little incorporation of 13C for archaeal communities at pH 7.4 after 8 days of incubation. This is also confirmed from the ultracentrifugation gradient graphs (Fig. 13B). This is not possible to see in Fig. 15B for the "heavy" DNA at pH 8.2. The number of peaks decreases or is the same respect to the "light" DNA.

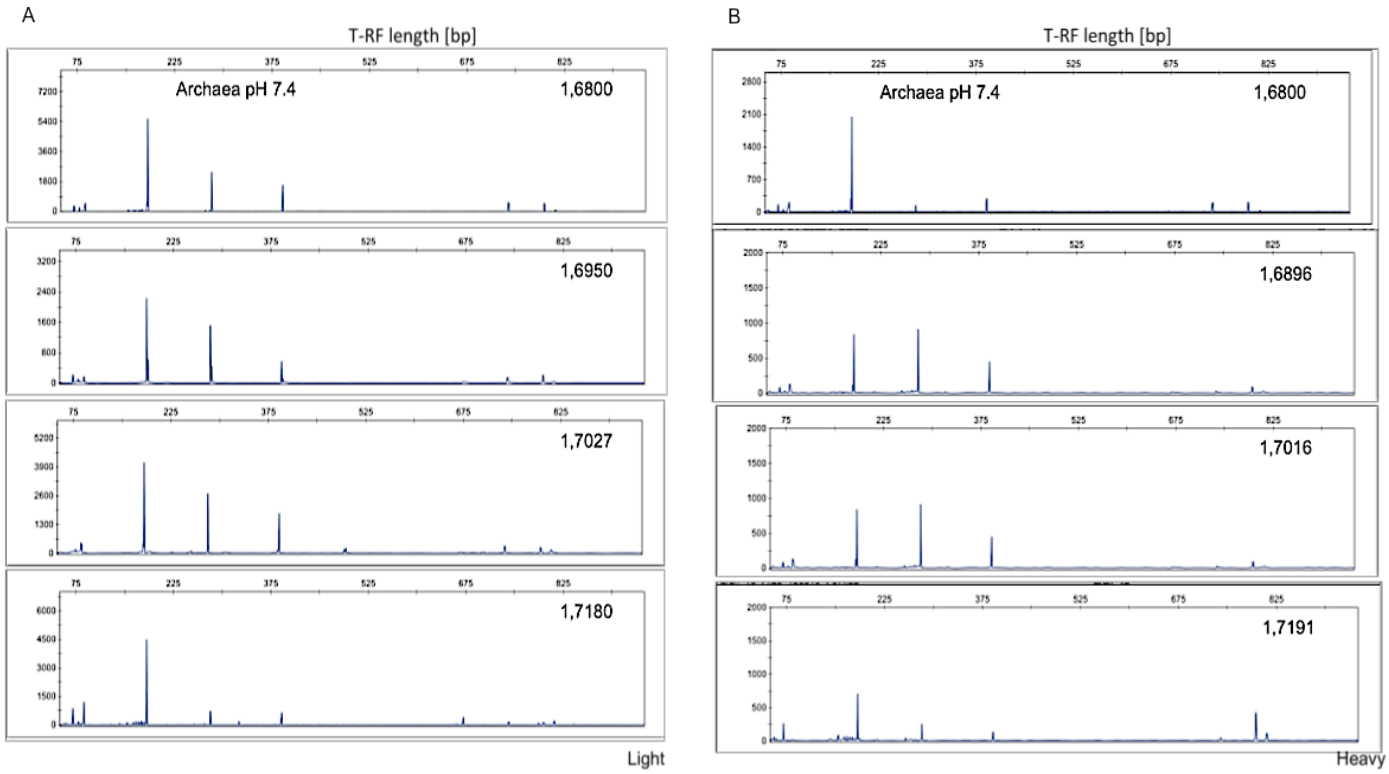

Fig. 16 (A) T-RFLP fingerprints of density-resolved archaeal communities retrieved from 12C-DNA ("light") after 8 days gradient fractions of nucleic acids extracted from Giralda at pH 7.4; **(B)** T-RFLP fingerprints of density-resolved archaeal communities retrieved from 13C-DNA ("heavy") after 8 days gradient fractions of nucleic acids extracted from Giralda at pH 7.4.

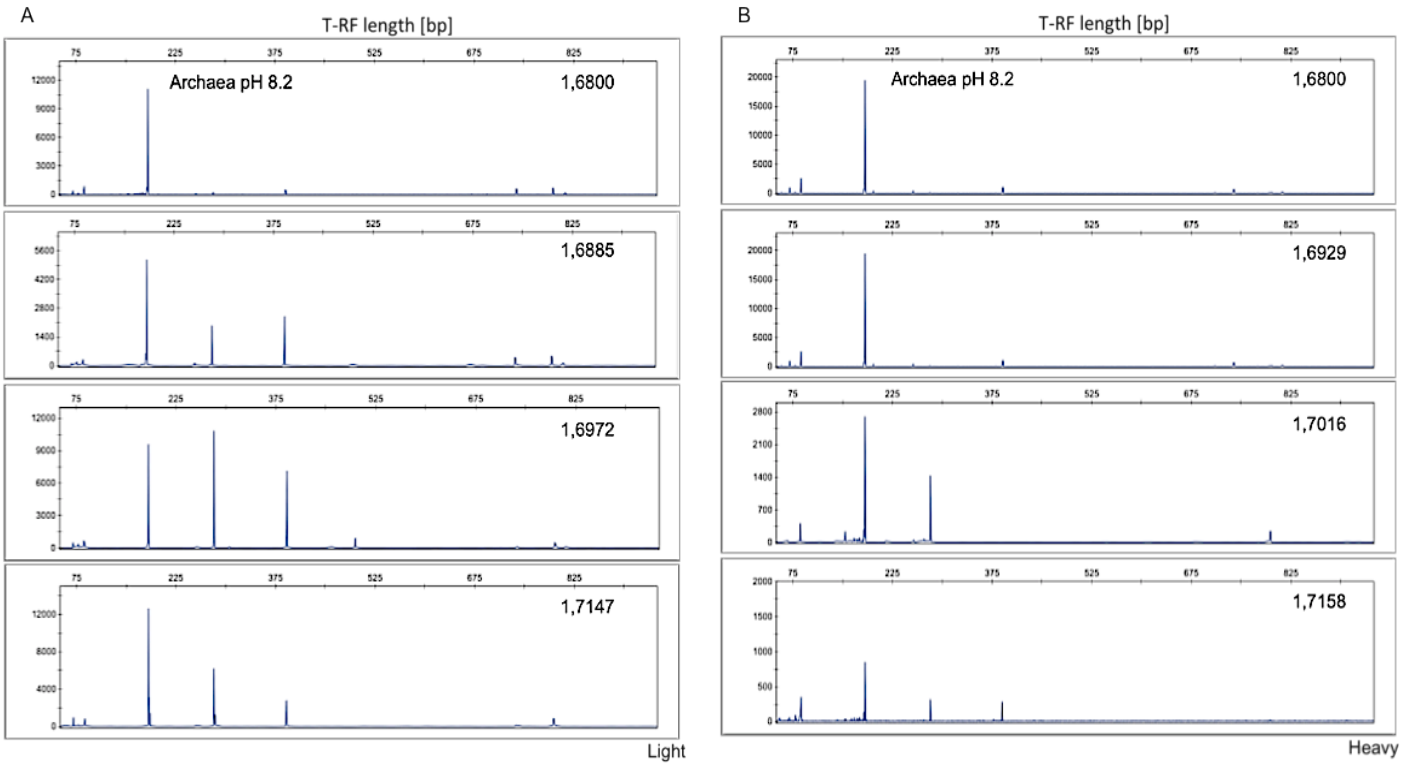

Fig. 17 (A) T-RFLP fingerprints of density-resolved archaeal communities retrieved from 12C-DNA ("light") after 8 days gradient fractions of nucleic acids extracted from Giralda at pH 8.2; **(B)** T-RFLP fingerprints of density-resolved archaeal communities retrieved from 13C-DNA ("heavy") after 8 days gradient fractions of nucleic acids extracted from Giralda at pH 8.2.

In Figg. 18A-18B are reported the results of the light and heavy DNA for archaeal communities at pH 7.4 in Gorino after 8 days of incubation. In this case it is quite clear to see that it is starting the incorporation of 13C in archaeal communities because certain T-RFs specifically increased in relative abundance (i.e. T-RFs with 797 bp). This is also confirmed from the ultracentrifugation gradient graphs (Fig. 14B).

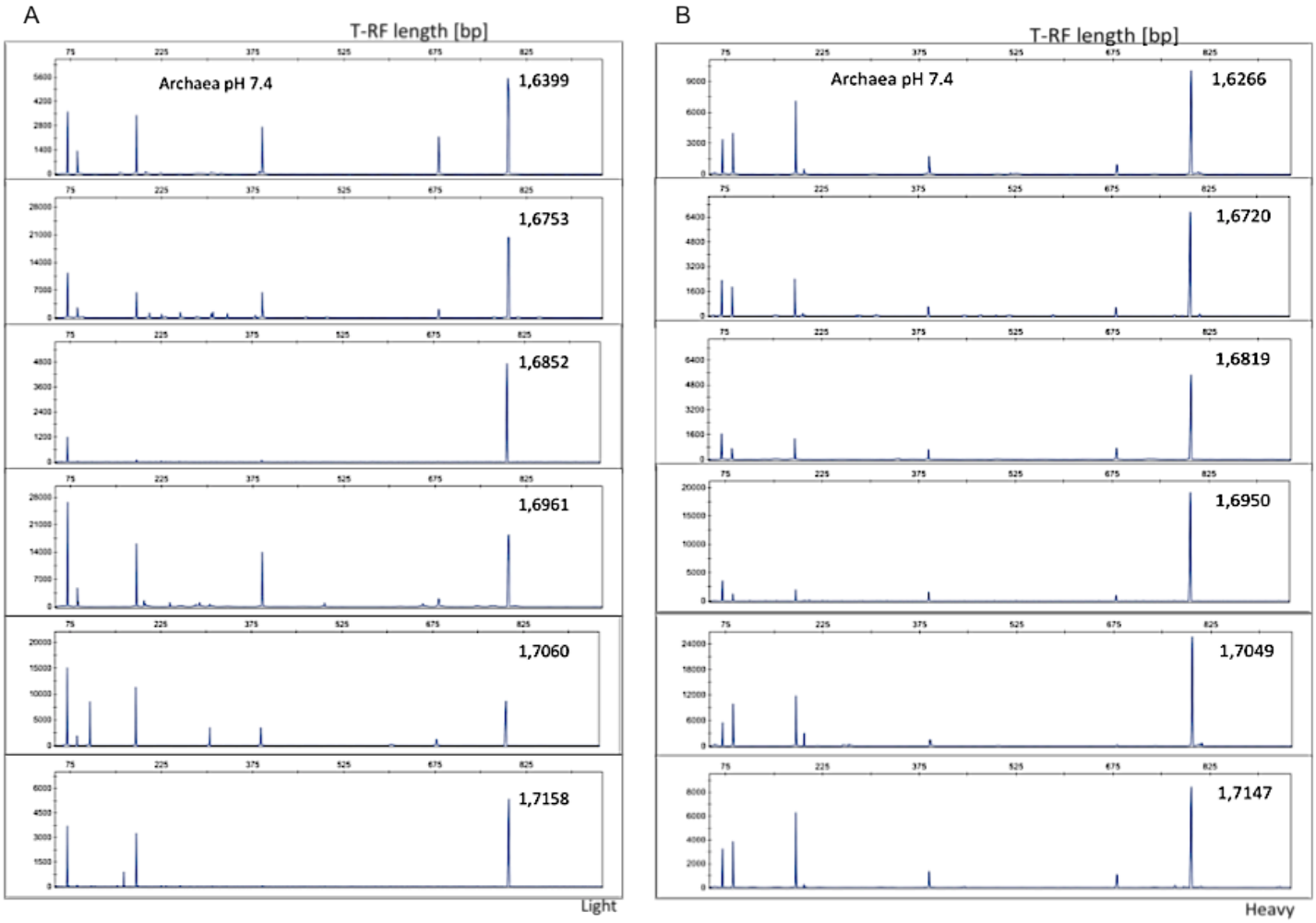

Fig. 18 (A) T-RFLP fingerprints of density-resolved archaeal communities retrieved from 12C-DNA ("light") after 8 days gradient fractions of nucleic acids extracted from Gorino at pH 7.4; **(B)** T-RFLP fingerprints of density-resolved archaeal communities retrieved from 13C-DNA ("heavy") after 8 days gradient fractions of nucleic acids extracted from Gorino at pH 7.4.

In Fig. 19A-19B there are the results of the light and heavy DNA for bacterial communities at pH 7.4 in Giralda after 21 days of incubation. These electropherograms show a little increase for the heavy fractions in certain T-RFs

(i.e. T-RFs with 150, 442 and 517 bp). This little increase is also confirmed from ultracentrifugation gradient graphs, (Fig. 15A).

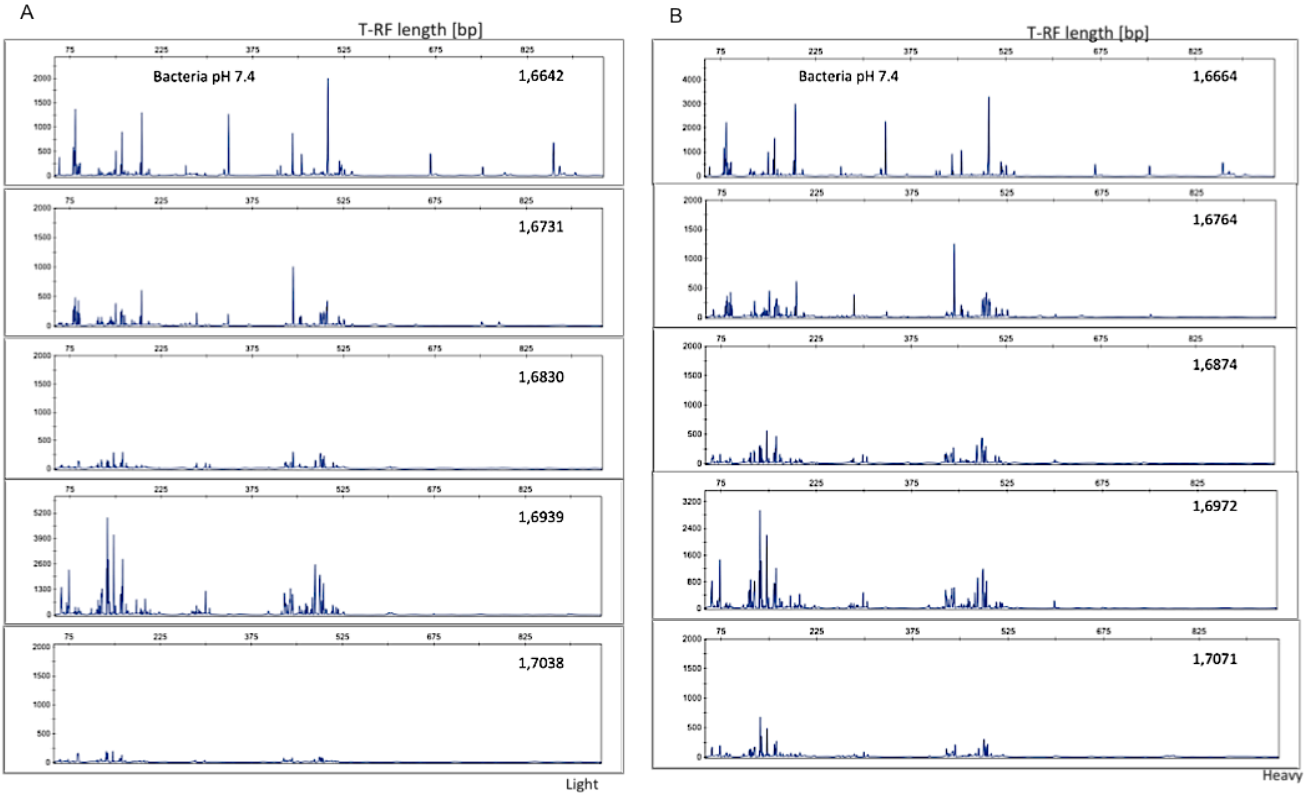

Fig. 19 (A) T-RFLP fingerprints of density-resolved bacterial communities retrieved from 12C-DNA ("light") after 21 days gradient fractions of nucleic acids extracted from Giralda at pH 7.4; **(B)** T-RFLP fingerprints of density-resolved bacterial communities retrieved from 13C-DNA ("heavy") after 21 days gradient fractions of nucleic acids extracted from Giralda at pH 7.4.

Figg. 20A-20B show the results of the light and heavy DNA for archaeal communities at pH 7.4 in Gorino after 21 days of incubation. These electropherograms show an increase in the peaks in the heavy fractions. Certain T-RFs specifically increased in the relative abundance (i.e. T-RFs with 795 bp) (Fig. 49b). This explains the possibility that there was incorporation of 13C for archaeal communities at pH 7.4 after 21 days of incubation. This is also confirmed from the ultracentrifugation gradient graphs (Fig. 15B) in which it is possible to see an increase of the 16S rRNA genes copy numbers for Archaea.

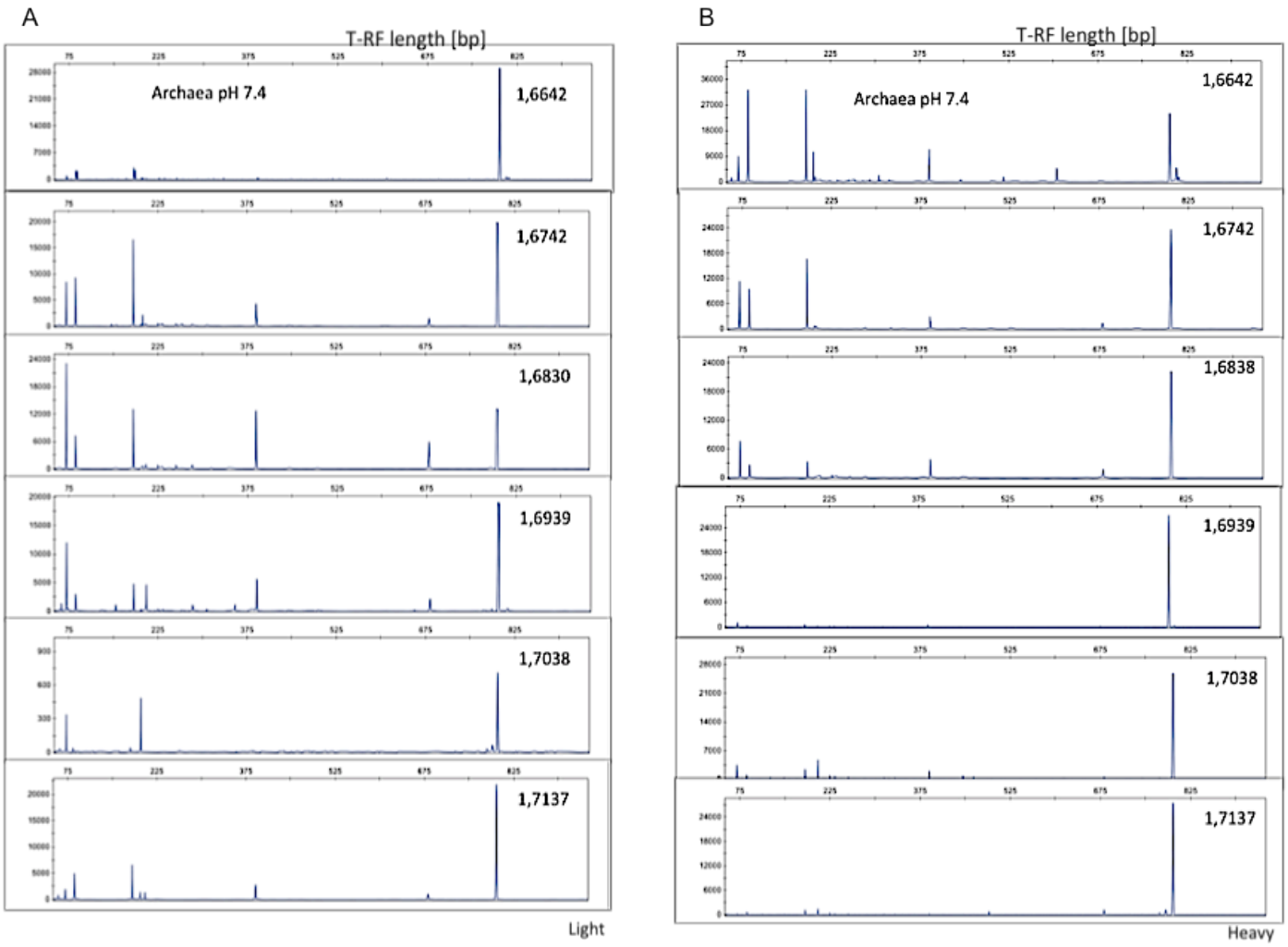

Fig. 20 (A) T-RFLP fingerprints of density-resolved archaeal communities retrieved from 12C-DNA ("light") after 21 days gradient fractions of nucleic acids extracted from Gorino at pH 7.4; **(B)** T-RFLP fingerprints of density-resolved archaeal communities retrieved from 13C-DNA ("heavy") after 21 days gradient fractions of nucleic acids extracted from Gorino at pH 7.4.

Figg. 21A-21B there are the results of the light and heavy fractions for archaeal communities at pH 8.2 in Gorino after 21 days of incubation. Also in this case, there is an increase in the peaks in the heavy fractions (T-RFs with 795 bp). At pH 8.2 the increase of the peak is bigger than pH 7.4. This is confirmed from the ultracentrifugation gradient graphs (Fig. 16B).

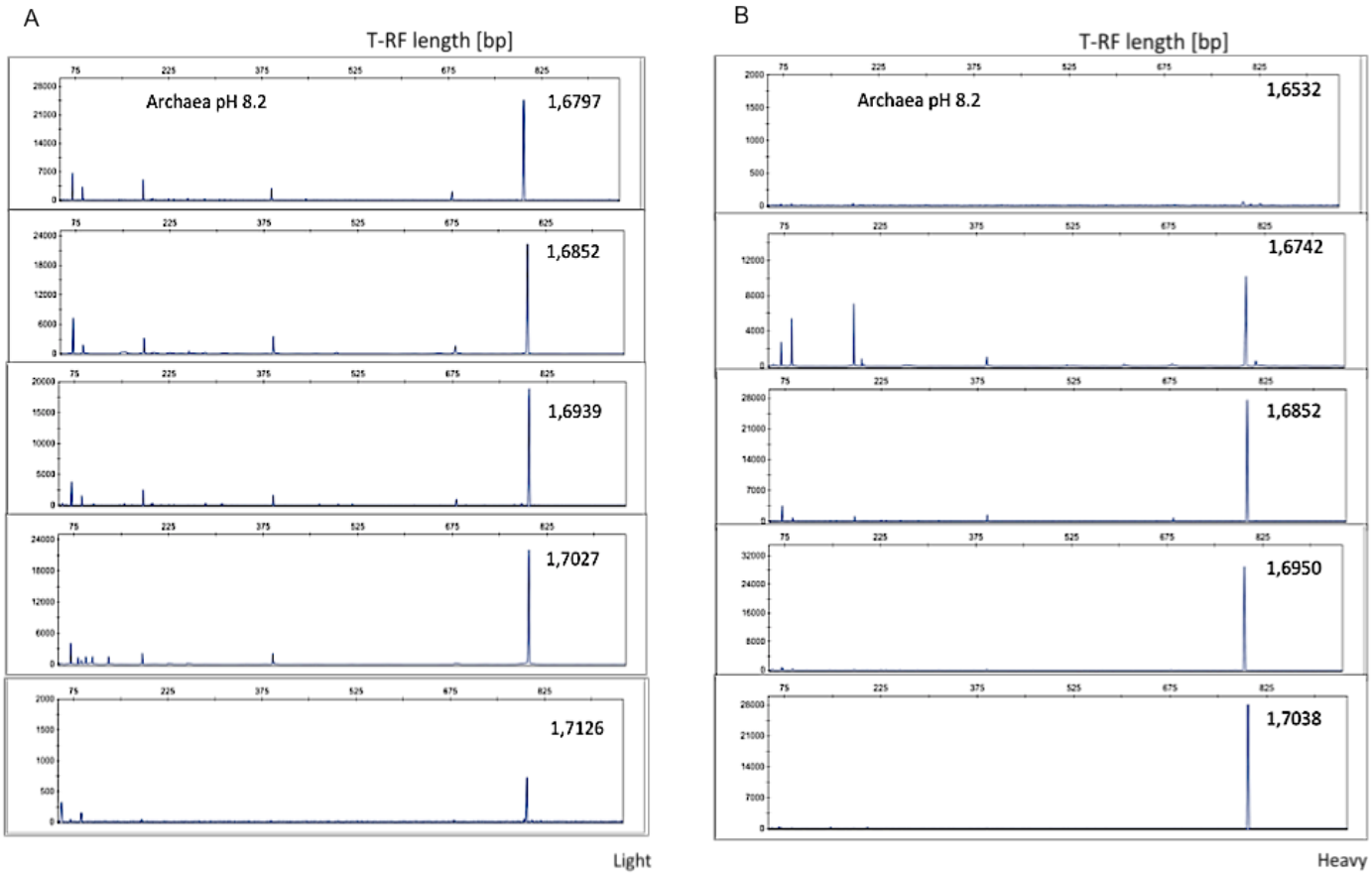

Fig. 21 (A) T-RFLP fingerprints of density-resolved archaeal communities retrieved from 12C-DNA ("light") after 21 days gradient fractions of nucleic acids extracted from Gorino at pH 8.2; **(B)** T-RFLP fingerprints of density-resolved archaeal communities retrieved from 13C-DNA ("heavy") after 21 days gradient fractions of nucleic acids extracted from Gorino at pH 8.2.

IV.5.5. Variation in bacterial and archaeal T-RF number and community structure

In order to carry out a detailed qualitatively analysis of T-RFs detected in boundary density fractions, the electropherograms were converted (by binning) into tables reporting the corresponding forward fragment sizes and relative abundances (Annexes, from Tab.8 to Tab. 1). The need to compare the composition of communities (as reviled by T-RF size and abundance) of different fractions ("light" and "heaver") and different treatments (12-DNA and 13C-DNA) arises since in each fraction on average only between 15 and 50% of the total T-RFs was present (Tab. 3). Indeed the lack of up to 75% of all T-RFs also in the density fractions with higher amount of 16SrRNA gene copies could be limited the capacity to discriminate between labelled and unlabelled DNA only on the base of bacterial and archaeal abundance, in particular when the target organism represent less the 5% of the prokaryotic assemblages. The cluster analysis was then applied to compare the communities showing the similarity between communities found in different fractions and treatments, in order highlighted the "moving" of T-RFs along density gradient and therefore the 13C-enrichment of DNA.

Tab. 3 Here I reported the total number of T-RFs as calculated by binning from different microcosms. Also are reported, both for 12C-DNA and for 13C-DNA, the percentage of total T-RFs found in boundary density fractions and in the fraction with higher number of 16SrRNA gene copies.

Microcosm	Domain	Total T-RFs	12C Mean	13C Mean	12C high abb.	13C high abb.
		n	%	%	%	%
Giralda T8 pH 7.4	Bacteria	69	42	41	48	49
Giralda T8 pH 8.2	Bacteria	69	41	42	41	41
Giralda T8 pH 7.4	Archaea	33	15	33	15	33
Giralda T8 pH 8.2	Archaea	33	18	36	30	36
Giralda T21 pH 7.4	Bacteria	100	33	36	20	59
Gorino T21 pH 7.4	Archaea	118	31	21	50	22
Gorino T21 pH 8.2	Bacteria	82	43	26	78	26
Gorino T21 pH 8.2	Archaea	57	32	16	54	21

The figures from 22 to 25 show the results of cluster analysis based on the similarities between bacterial and archaeal community structure of 12C-treatment and 13C-treatment samples collected from different density fractions. When the 13C-samples of heavy fractions clustered with 12C-samples of light fractions, this provides evidence that there was 13C-DNA enrichment (Fig. 23 and 25). Otherwise the higher similarity between 13C-samples with 12C-samples collected in fractions with same or higher density provides insight that there was no 13C enrichments (Fig. 22 and 24). In T21 Gorino Archaea pH 8.2 microcosms any labelling is highlighted, as the 13C-fractions clustered closely to 12C-frection with similar density (Fig. 22). At T21 Gorino Archaea pH 7.4 the results suggest that there was 13C-enreachment since the community structure of denser 13C-fractions (13C-6 to 13C-9) showed higher similarity with that of lighter 12C-fraction (12C-11) (Fig. 23). In microcosm of T21 Giralda Bacteria pH 7.4 high similarity between 13C-fractions and 12C-fractions with close densities suggests that DNA was not 13C-labelled. At T8 Giralda Bacteria pH 7.4 the high similarity of 13C-8 with both lighter 13C-fractions (13C-10 and 13C-12) and 12C-fraction (12C-11) suggests that limited labelling occurred, and that it has affected only a small portion of bacterial population.

The SIMPER analysis revealed that the similarities in archaeal community composition between 12C and 13C samples are due at the variation of single T-RF (variance explained >80%) (Annexes, Tab. 9a and 9b). The similarities in bacterial community structure are driven by several T-RFs, and the most of variance of 12C- and 13C- samples is explained by the same T-RFs (Annexes, Tab. 10a and 10b).

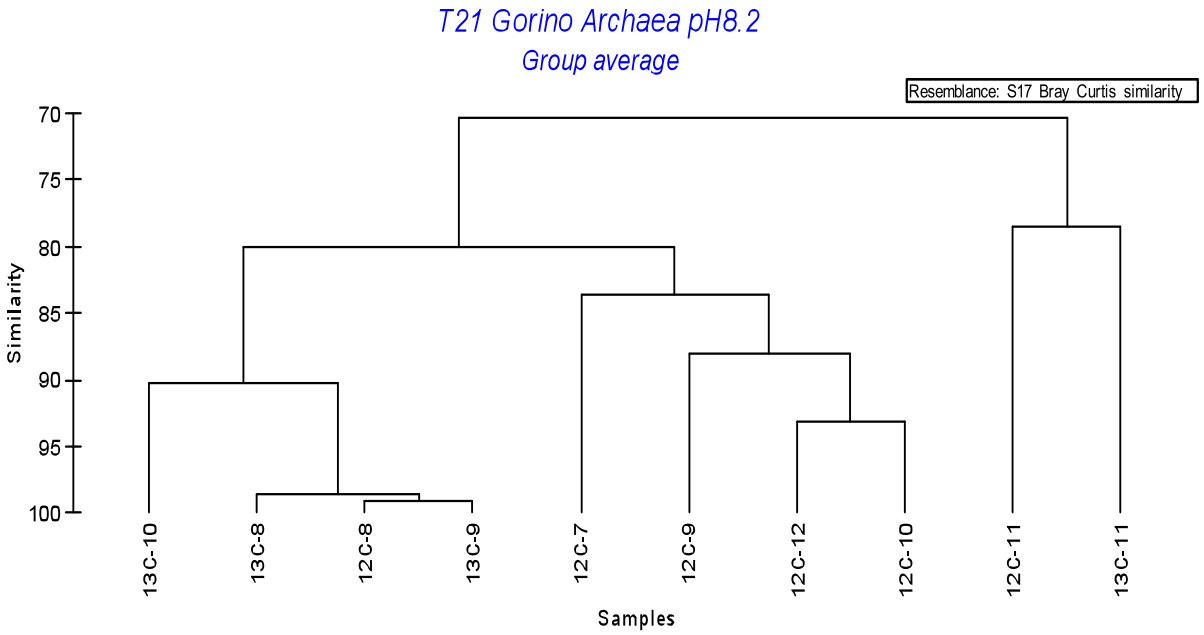

Fig. 22 Cluster analysis based on the similarities between bacterial and archaeal community structure of 12C- and 13C-treatment samples collected from different density fractions for T21 Gorino Archaea pH 8.2. Here any labelling is highlighted, as the 13C-fractions clustered closely to 12C-frection with similar density.

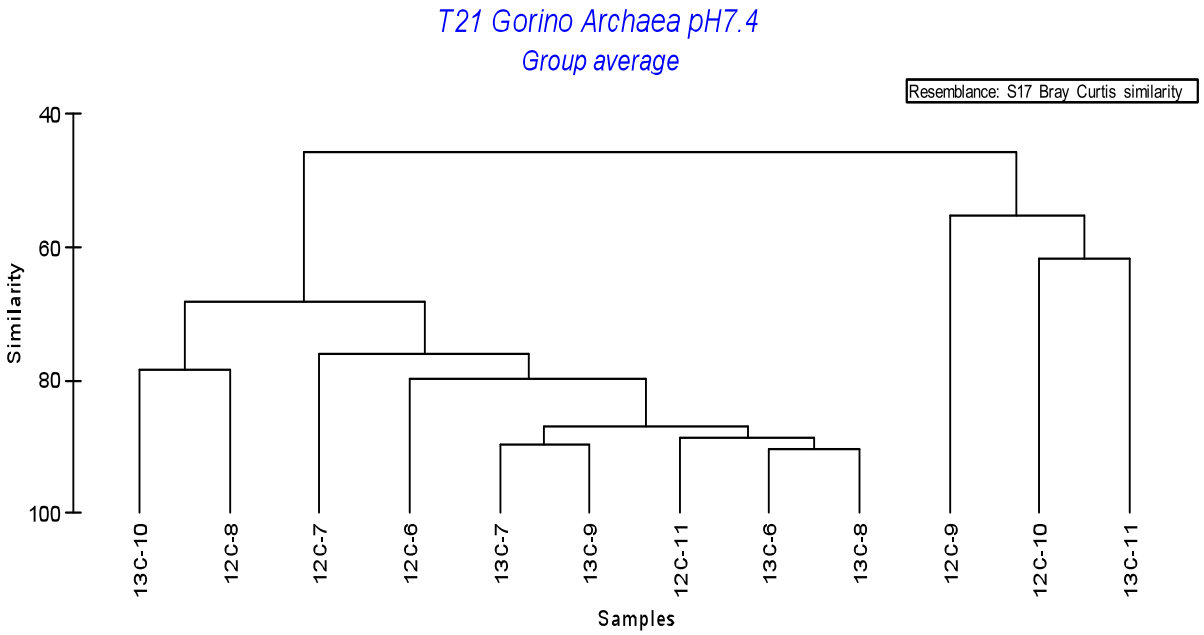

Fig. 23 Cluster analysis based on the similarities between bacterial and archaeal community structure of 12C- and 13C-treatment samples collected from different density fractions for T21 Gorino Archaea pH 7.4. These results suggest that there was 13C-enreachment since the community structure of denser 13C-fractions (13C-6 to 13C-9) showed higher similarity with that of lighter 12C-fraction (12C-11).

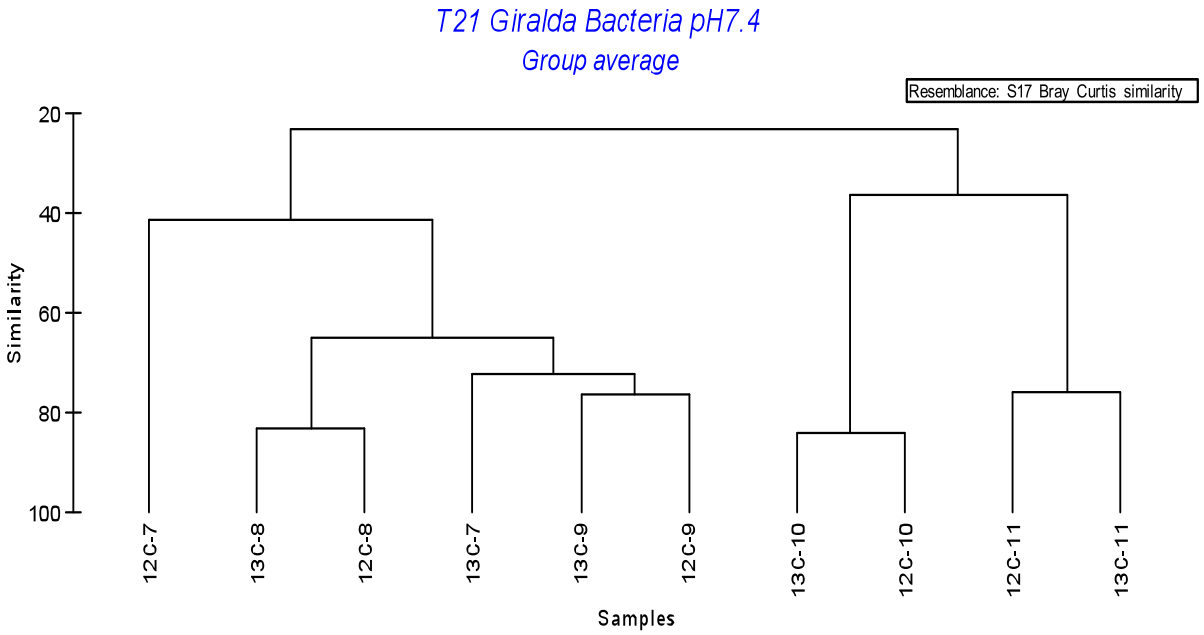

Fig. 24 Cluster analysis based on the similarities between bacterial and archaeal community structure of 12C- and 13C-treatment samples collected from different density fractions for T21 Giralda Bacteria pH 7.4. The high similarity between 13C-fractions and 12C-fractions with close densities suggests that DNA was not 13C-labelled.

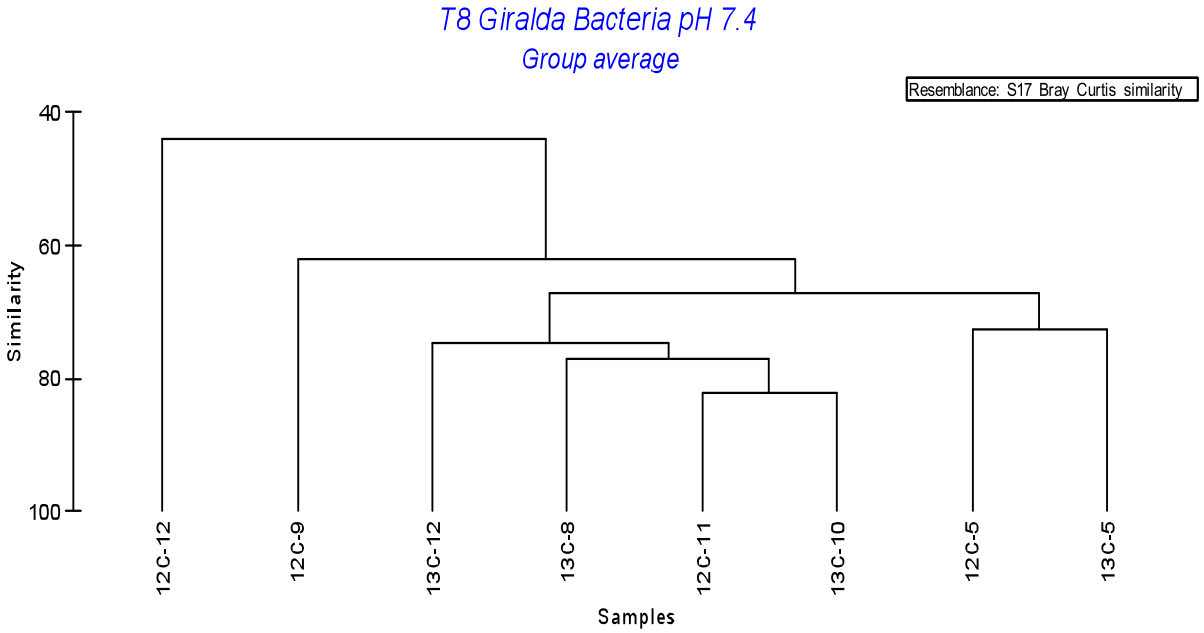

Fig. 25 Cluster analysis based on the similarities between bacterial and archaeal community structure of 12C- and 13C-treatment samples collected from different density fractions for T8 Giralda Bacteria pH 7.4. Here the high similarity of 13C-8 with both lighter 13C-fractions (13C-10 and 13C-12) and 12C-fraction (12C-11) suggests that limited labelling occurred, and that it has affected only a small portion of bacterial population.

IV.5.6. 454-Pyrosequencing of bacterial and archaeal 16S rRNA genes

Specific groups of AOA and AOB have been investigated through the study of prokaryotic diversity in sediments object of this research. I analyzed, by 454-Pyrosequencing of 16S rRNA genes, the diversity of bacterial and archaeal communities in the natural sediment of Gorino as well as in Gorino (pH 7.4 and pH 8.2) and Giralda (pH 7.4) microcosms. Unfortunately here I presented only the results from Gorino natural sediments, since at the time of thesis submission the other results of pyrosequencing are not yet available.

The bacterial composition at the phylum level is given by Actinobacteria 2%, Bacteroidetes 13%, Proteobacteria 41%, Cyanobacteria 13%, Acidobacteria 3%, Verrucomicrobia 2%, Planctomycetes 4%, Chloroflexi 2%, Chlamydiae 1%. The analysis at the species level reveals for Bacteria the presence of ammonia oxidizing *Nitrosospira sp* (Fig. 26).

The archaeal composition at the phylum level showed the presence of Thaumarchaeota (97%) and Euryarchaeota (3%) (Fig. 26). The analysis at the species level reveals the dominance of two species related to archaeal ammonia oxidizer *Nitrosopumilus marittimus* and *Ca. Nitrososphaera gargensis.*

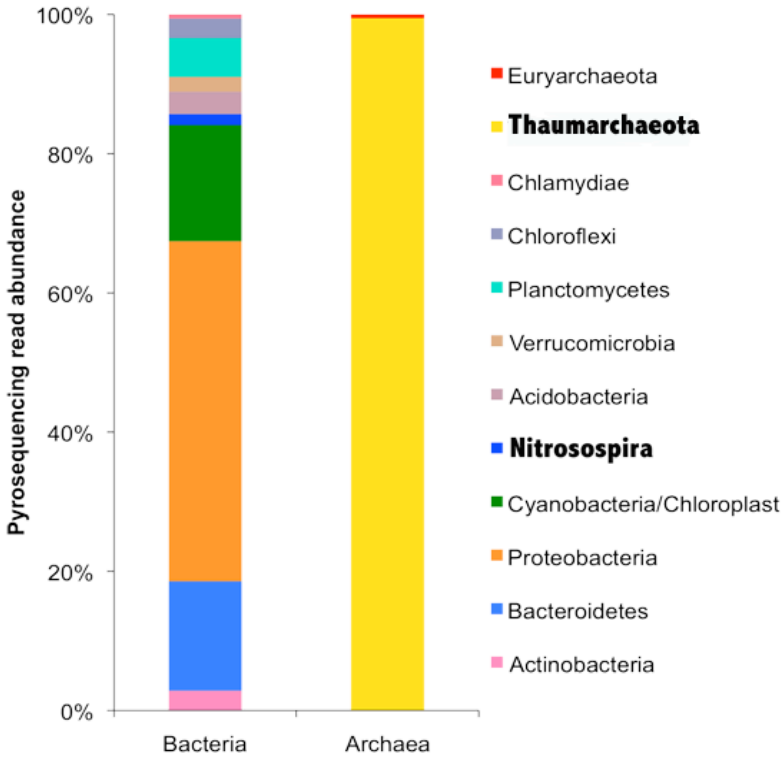

Fig. 26 Community composition of Bacteria and Archaea in the sediments of Gorino, as described by454-Pyrosequencing of 16S rRNA genes.

IV.6. DISCUSSION

The aim of this research was to test the hypothesis that in lagoon ecosystems Archaea are involved in the ammonia oxidation. In this study I also wanted to test the effect due to small changes in pH on nitrification as well as on the community structure of ammonia oxidizer microorganisms.

IV.6.1. Ammonia oxidation

The ammonia oxidation proceeded in different ways in the three-site microcosms, according with the location where the samples were collected. Indeed as reported in literature for Sacca di Goro lagoon (Welsh and Castaldelli, 2004), the oxidation of ammonia to nitrite was faster in the Giralda microcosms, decreased in Gorino microcosm and it was very slow in Mare microcosm (Figg. 7, 8, 9). The effects of changes in physicochemical conditions along estuarine gradient on nitrification rates have been well documented, indicating decreased nitrification with the salinity increases (Rysgaard et al., 1999; Bernhard and Bollmann, 2010). The salinity-induced reduction in NH_4^+ adsorption capacity and stimulation of NH_4^+ afflux has been argued to cause a reduction in nitrification activity since the nitrifying microorganisms become limited by NH_4^+ availability at higher salinities (Rysgaard et al., 1999). Thus my results showed that, despite the nature of microcosms, the nitrification here measured have the same pattern reported for natural sites, supporting the idea that the sediments manipulation and *ex situ* condition did not influence the activity of ammonia oxidizers.

Unclear was the effect of pH variation on nitrification in all microcosms. Giralda nitrification rates seem not to have undergone the effect of pH, however since the ammonia ends up after 2 days there was not time to appreciate a pH effect. Also in Mare microcosms the variation of pH seems not have had any effect on ammonia oxidation, however here it was the extreme low nitrification

making hard to observe a clear response. Only in Gorino's microcosms the oxidation of ammonia showed differences under different pH (Fig. 8), but these difference did not highlight any clear pattern. However after 8 days at pH 7.4 all the ammonia is consumed while at pH 8.2 the ammonia concentration was still ca 30 μM, suggesting higher rate of ammonia oxidation under low pH.

The variation of pH is an important controlling factor of nitrification (Hatzenpichler, 2012; Zhalnina et al., 2012). Reduced pH can inhibit AOB and AOA because uncharged ammonia (NH_3) – rather than NH_4^+ ion – is the substrate used (Suzuki, 1974, Ward, 1987). The NH_3/NH_4^+ equilibrium is pH sensitive ($NH_3 + H^+ \rightleftarrows NH_4^+$; pKa = 9.3) (Zeebe and Wolf-Gladrow, 2001), and use of NH_3 rather than NH_4^+ by AOB is evident from changes in affinity observed with changing pH (Suzuki, 1974). Laboratory- and field-based studies indicate that reduced pH has a nearly universal detrimental effect on nitrification, with lower ammonia oxidation rates and slower AOB growth rates occurring under reduced pH in freshwater (Rudd et al., 1988), soil (Robertsson, 1982; De Boer and Kowalchuk, 2001), activated sludge (Wild et al., 1971; Painter and Loveless, 1983; Quinlan, 1984), and bacterial cultures (Meyerhof, 1917; Hofman and Less; 1953, Suzuki et al., 1974; Ward, 1987; Prosser, 1990; Frijlink et al., 1992; Burton and Prosser, 2001). Although many of these studies are focused on high variation of pH (2 or 3 unit), also small variation of pH has been reported to influence significantly the activities of ammonia oxidiser. Cultures of the widespread marine AOB *Nitrosococcus oceani*, for instance, display maximal oxidation at pH 8, but these rates decline 20-36% as pH is decreased by 0.4-0.5 units (Ward, 1987). Recently, experiments of acidification in open ocean systems pointed out that a pH reduction of 0.05-0.14 unit decreased nitrification rates by 3-44%. Although the difference in pH of my experiments was lower (between 0.1 to 0.4 units) than at the beginning of experiment (0.8), maybe due to buffering effect of the sediments, the difference

in ammonia oxidation observed in Gorino microcosms could be the response of microbial communities to pH variation. However if this is the case we observed an opposite pH effect, since the nitrification rates increased lightly under low pH values. On one hand these results could be due to the presence in sediment of AO-Organisms (AOO) with pH-optimum activity below 8. Indeed if the pH of water-sediments interface at Gorino was 8.2, under the sediments surface (often already below 1 mm) the common value of pH are 7.4-7.6 (see Chapter III). On the other hand the pH variation might have stimulated the activity of different groups of AOO, and this is the hypothesis that I had tested with SIP-DNA experiments.

IV.6.2.DNA-SIP Experiments

Stable isotope probing analysis was carried out to determine if Bacteria or Archaea or both were active at Giralda and Gorino. Due to low nitrification activities observed for Mare microcosms, I decided to not process these sediments. The rationale of experiment is to label the DNA of prokaryotes via ^{13}C-bicarbonate assimilation, since the ammonia oxidizers are chemolithotrophic prokaryotes using the ammonia as a source of energy and the inorganic carbon as source of carbon to produce biomass. To facilitate the AO labelling I have taken into account these devices: (i) the incubation were carried out in dark, in order to avoid the inorganic assimilation by photoautotrophic microorganisms; (ii) the sediment slurries of microcosms were prepared with filtered (0.2 μm) DIC-Free lagoon water amended with 13C-bicarbonate (see IV.3.1.3.); (iii) according with *in situ* ammonia concentration, I injected different ammonia amounts in three-sites microcosms in order to have comparable concentrations. The DNA derived from buoyant density fractions was analysed in two ways to assess active (13C-DNA) prokaryotes: (i) quantitative assessment of increases in relative abundance of 16S rRNA gene copies (qPCR) in 13C fractions in comparison with 12C fractions; (ii) qualitative comparison of prokaryotic

community composition (T-RFs) extracted from 13C and 12C fractions (via cluster analysis).

The qPCR highlighted a shift in density fraction of bacterial DNA for Giralda pH 7.4 (8 days and 21 days) and for Gorino pH 7.4 (8 days). However the cluster analysis supported a shift in density fraction of bacterial community only for Giralda pH 7.4 at 8 days (fig. 25). The labelled bacterial 16SrRNA gene copies were detected in fraction 0.013 g ml^{-1} "heavier" than the unlabelled bacterial DNA. This is a rather weak labelling compared to the maximally 0.04 g ml^{-1} expected for full ^{13}C-labelling (Lueders et al., 2004; Freitag et al., 2006). This suggests that Bacteria have incorporated only few amount of 13C into their genomic DNA. The partial labelling of DNA-pool could be addressed to the dilution of 13C-bicarbonate by sediment DIC, and to the generation time of specific AOB populations. Further the labelled bacterial community most similar to unlabelled bacterial community has been not found in the fraction with higher amount of bacterial DNA of 13 treatments (Fig. 25). These results are in agreement with the presence of heterogenic bacterial communities, with ^{13}C-CO_2 consumers and secondary utilizers (incorporating organic compounds released by autotrophs or biomass following death), where the AOB represent usually less than 5% of total prokaryotic number (see Herbert, 1999 and references therein). The most abundant T-RF (ca 490 bp) found in heavier 13C fraction (i.e. 13C-8) and explaining high 13C-DNA variance has a fragment size similar to predicted fragment for *Nitrosomonas* (Tab. 4). Also interesting is the presence, in the same fraction, of a T-RF with size related to nitrite oxidizers (*Nitrospira*). Thus, according with fast ammonia oxidation observed in microcosms (2 days), the bacterial nitrifiers in Giralda sediments maybe was active in the first days of experiments, then, with the depletion of ammonia, their activity, and therefore 13C-bicarbonate incorporation and DNA duplication, also decreased. The presence of active AOB (maybe *Nitrosomonas*) in sediments

with low salinity and high amount of ammonia is consistent with the ecological niche proposed for AOB (Erguder et al., 2009).

Tab. 4 Results of Microbial Community Analysis III (MiCAIII) performer with program PAT+ on the bacterial forward fragments (13C-8). The program was settled for primers Ba27f (5'-AGAGTTTGATCMTGGCTCAG-3') and Ba907r (5'-CCGTCAATTCMTTTRAGTTT-3'), restriction enzyme MspI (C^CGG). The mach for forward fragment was settled to ±2. (*) The contribution percentage of each T-RF to observed similarity between 13C-fractions.

Fragment length Observed	Fragment length Predicted	Accession n.	Nitrifying related Species	13C-DNA* variance explained
bp	bp			%
490	492	AB000700	Nitrosomonas sp. JL21	14
490	489	AJ431350	uncultured Nitrosomonas sp.	14
138	140	EU780676	uncultured Nitrospirae bacterium 11	5
138	140	EU780679	uncultured Nitrospirae bacterium 28	5
138	140	HM454280	uncultured Nitrospirae bacterium MY2-3C	5
138	140	HQ437531	uncultured Nitrospirae bacterium G38	5
428	430	CP000103	Nitrosospira multiformis ATCC 25196	3
428	430	L35509	Nitrosospira multiformis	3
498	498	AF287298	Nitrosococcus halophilus Nc4	2
498	498	CP002086	Nitrosococcus watsoni C-113	2
498	498	CP000127	Nitrosococcus oceani ATCC 19707	2
284	286	AM110965	Nitrospina sp. 3005	2
166	167	GQ468508	uncultured Nitrospirae bacterium OTU1	2
166	167	HM454279	uncultured Nitrospirae bacterium MY2-1F	2
166	167	EU780678	uncultured Nitrospirae bacterium 20	2
166	167	HM454281	uncultured Nitrospirae bacterium MY3-5B	2
166	167	HM454282	uncultured Nitrospirae bacterium MY3-11A	2
166	167	HM454283	uncultured Nitrospirae bacterium MY4-5C	2
298	297	FN429806	uncultured Nitrospina sp.	<1
150	151	EU266856	uncultured Nitrospiraceae bacterium	<1
141	141	FJ538134	uncultured Nitrosomonadaceae bacterium	<1

Clear shift in buoyant density fraction of archaeal DNA has been observed only for Gorino pH 7.4 microcosms after 21 days (figg. 15 and 23). The higher number of labelled archaeal 16S rRNA gene copies were detected in fraction 0.01 g ml^{-1} "heavier" than the unlabelled bacterial DNA. However more than 80% archaeal community structure variance is explained by only one T-RF (795 bp) and the difference in density between most similar 13-DNA and 12-DNA community structure reach up to 0.05 g ml^{-1}. This suggests that along "heavier" density fractions the archaeal T-RF is increasingly enriched by 13C, up to reach difference in density reported for full 13C labelling of AOA and microbial

genome (Wu et al., 2013; Lueders et al., 2004). The fragment 795 bp has the same size of fragment predicted for many uncultured Thaumarchaeota and for AOA *Cenarchaeum symbiosus* (Annexes, Tab. 11). Thus, the presence of one ribotype actively involved in carbon fixation and potentially related to AOA, strongly support the idea that Archaea have a key role in ammonia oxidation in Gorino sediments.

The lack of labelling of archaeal DNA before to 21 days despite the ammonia was completely consumed after 8 days suggest that, as previously reported (Erguder et al., 2009; Schleper, 2010), the AOA are adapted to low NH_4^+ concentrations. For instance, laboratory studies have showed that affinity of marine archaeon *Nitrosopumilus maritimus* for ammonium/ammonia was 200-fold higher than substrate affinity of AOB (Martens-Habbena et al., 2009; Martens-Habbena and Stahl, 2011). The lack of a clear labelling at pH 8.2 could suggest that AOA also find more suitable grow condition under lower value of pH. In literature Archaea are reported to dominate from in acid soil (i.e. Leininger et al., 2006; Zhang et al., 2011) to open ocean water (i.e. Wuchter et al., 2006; Blaney et al., 2011), therefore covering a wide pH range. Although my results not provide any evidence of a crucial role of pH in structuring ecological niche of AO microorganisms, I can not exclude that lack of labelling could be due to experimental procedure or to biases associated with DNA extraction and PCR amplification, as well as to difficulties in SIP procedure itself.

IV.6.4. 454-Pyrosequencing

The analysis of 454-pyrosequencing showed the presence in Gorino sediments of Nitrosospira such as ammonia oxidizing Bacteria, which represent less than 4% of total diversity (Fig. 26).

The Nitrosospira lineage is often dominant in salty environments such as estuarine or marine systems (Freitag et al. 2006; Ward et al., 2007; Bernhard and Bollmann, 2010). The uncultured *Nitrosospira* cluster 1- and *Nitrosomonas*

cluster 5-like sequences dominate AOB sequences amplified from estuarine and marine sediments (McCaig et al., 1999; Bano and Hollibaugh, 2000; Freitag and Prosser, 2003; 2004; Freitag, et al., 2006). However, pure culture representatives of these groups have not been obtained, and their role in ammonia oxidation is based on clustering of their 16S rRNA genes within a monophyletic group for which all cultivated representatives are autotrophic AOB, and on reports of non-persisting enrichment cultures of *Nitrosomonas* cluster 5 (Stephen et al., 1996). Through SIP-DNA approach, Freitag and colleagues (2006) for the first time confirmed the activity of *Nitrosomonas* sp. Nm143 within an estuarine sediment ecosystem. However they did not find SIP-evidence of *Nitrosomonas* activities in marine station, leaving uncertain the role of these nitrifying Bacteria in ammonia oxidation. Similarly my results suggest that *Nitrosomonas* is present and active in ammonia oxidation in Giralda sediments, whereas *Nitrosospira* replaces them in Gorino sediments. Unfortunately the presence of bacterial nitrifiers in Giralda microcosms is not yet (at time of thesis submission) supporated by 454-pyrosequencing analyses and therefore the possible role of *Nitrosomonas*, *Nitrosospira* and *Nitrospira* in nitrogen cycle remains unresolved.

The analysis of 454-pyrosequencing confirmed that archaeal community in Giralda sediments are dominated by few ribotypes belonging *Thaumarchaeota* phylum (ca. 90%). Further the analysis at the specie level has revealed the presence of *Nitrosopumilus maritimus*, *Candidatus Nitrososphaera gargensis*, and more other species not yet classified (fig. 26). All these species are related to ammonia oxidizing, confirming the results of SIP-experiments. To date, only eight AOA species have been described from marine, soil, sediment, and hot spring environments (Table 5). Two of them were isolated in pure cultures, and five species can grow in enriched cultures but were not isolated in pure cultures. Only six whole genomes of AOA are available in the databases. As the AOA

have been found under a wide variety of conditions including varied temperature, pH, ammonia concentrations, and oxygen supply, designing media for their cultivation has been difficult. The lack of a variety of AOA cultures and genomes has limited the study of their physiology and metabolism. The fact that the single planktonic marine *Thaumarchaeota* cultured to date (*Nitrosopumilus maritimus* SCM1) is a strictly autotrophic ammonia oxidizer (Könneke et al., 2005), and the reports on the abundance of gene encoding archaeal ammonia monooxigenase (*amo*A) in marine environments (Schleper et al., 2005), have led to the belief that marine *Thaumarchaeota* are predominately nitrifiers. However there are any environmental studies that have demonstrate the direct role of Archaea in nitrification. In these regard my results for the first time provide evidence of activity of Archaea, belonged to phylum of *Thaumarchaeota*, in ammonia oxidation within lagoon sediments.

Table 5 Ammonia-Oxidizing Archaea isolated from different environments

#	AOA	Environment	Source of isolation	Classification	Culture	Genome sequence	Reference	Country
1	*Nitrosopumilus maritimus*	Marine	Gravel from a marine tropical fish tank	1.1a	Pure	+	Könneke et al. (2005), Walker et al. (2010)	USA
2	*Cenarchaeum symbiosum*	Marine symbiont	Marine sponge *Axinellamexicana*	1.1a	–	+	Preston et al. (1996), Hallam et al. (2006)	USA
3	*Ca. Nitrososphaera gargensis*	Soil, hot springs	Enrichment cultures from microbial mats of the Siberian Garga hot spring	1.1b	Enriched	+	Hatzenpichler et al. (2008)	Austria
4	*Nitrososphaera viennensis*	Soil	Garden soil in Vienna, Austria	1.1b	Pure	+	Tourna et al. (2011)	Austria
5	*Ca. Nitrosoarchaeum koreensis*	Rhizosphere	Soil sample from the rhizosphere of *Caraganasinica*	1.1a	Enriched	+	Kim et al. (2011), Jung et al. (2011)	Republic of Korea
6	*Ca. Nitrosoarchaeum limina*	Sediments	Sediments in the low-salinity region of San Francisco Bay	1.1a	Enriched	+	Blainey et al. (2011)	USA
7	*Ca. Nitrosocaldus yellowstonii*	Hot springs	Yellowstone National Park, hot springs	ThAOA	Enriched	–	de la Torre et al. (2008)	USA
8	*Ca. Nitrosotalea devanaterra*	Soil	Acidic agricultural soil	1.1a-associated	Enriched	–	Lehtovirta-Morley et al. (2011)	UK

IV.7. Conclusion

This study suggests that in Sacca di Goro lagoon at least three groups of ammonia oxidizers are actively involved in nitrification: members of Bacteria domain (maybe *Nitrosospira sp*.) and two taxa belonging to Archaea domain, *Nitrosopumilus maritimus*, *Ca. Nitrososphaera gargensis*. Bacteria seem to dominate in Giralda sediments under high rates of nitrification and low salinity, whereas Archaea dominated the process in Gorino sediments under low nitrification rates and high salinity.

V. SYNTHESIS AND GENERAL CONSIDERATIONS

The broad distribution and abundance of Archaea in soils and in aquatic ecosystems is one of the most exiting findings in the recent history of microbial ecology. Indeed the presence of a second prokaryotic Domain that contribute to global biogeochemical cycles and to biomass/energy transfer through the food webs has drastically changed the way to think at "microbial loop". Although the application of culture-independent molecular tools (i.e. cloning and pyrosequencing) has considerably enhanced the knowledge about the diversity of Archaea, their abundance and physiology, and therefore their role in biogeochemical cycles, have been little investigate and understood (Karner et al., 2001; Ingalls et al., 2006). Thus questions like "do Bacteria and Archaea occupy different ecological niches?", "are they competitor for the same trophic resources?" or "have Bacteria and Archaea a different role in the ecosystems functioning?" have started to be investigated only recently (e.g. Valentine, 2007; Erguder et al., 2009; Schleper, 2010).

During my PhD project I investigated the ecology of Bacteria and Archaea in the sediments of Italian lagoon Sacca di Goro. The general goal was to investigate the presence of Archaea in this environment and to understand their role in nitrogen cycle. The mesophilic Archaea, classified as phylum *Thaumarchaeota*, which prevails in soils, oceans and freshwater systems (DeLong, 1992, Fuhrman et al., 1992; Francis et al., 2005; Schleper et al., 2005), are believed to be predominantly nitrifiers. However little is known about the environmental factor that effectively affect abundance of Bacteria and Archaea, as well as there are a few evidences that Ammonia Oxidizing Archaea (AOA) are directly involved in ammonia oxidation (Konneke et al., 2005; Hallam et al., 2006; Walker et al., 2010; Blainey et al., 2011; Tourna et al., 2011). Even more so, this is true for aquatic coastal and transition ecosystems.

The Sacca di Goro due to its features is an ideal site to investigate how

environmental factors control the abundance of Bacteria and Archaea, and what is the contribution of Archaea to nitrification. Indeed, the river input and the characteristics of transition environment combined with the intense human activities that affect the lagoon and the adjacent catchment area, leading to both spatial and temporal variations of environmental parameters (i.e. salinity, pH, ammonia, DO, sulfite) that it has been suggested responsible to define the ecological niches of bacterial and archaeal ammonium oxidizers (Enguder et al., 2009). The specific objective of my PhD was to test the following two hypotheses:

1) the spatial and temporal variation of environmental parameters influence prokaryotic community structure, affecting differentially the abundance of Bacteria and Archaea;

2) in lagoon ecosystems, not only Bacteria but also Archaea are involved in nitrogen cycle;

The first hypothesis was addressed into the Chapter III. The bacterial and archaeal cells were enumerated by application of fluorescent *in situ* hybridization (FISH) on sediments collected in three different stations (Giralda, Gorino and Mare), along ammonia and chemicophysical (salinity and pH) gradients typical for Sacca di Goro, in three different sediment layers (oxic, suboxic and anoxic) and in two different periods (summer and winter). During the each sampling in situ measurement were carried out to register difference in temperature, dissolved oxygen (DO), salinity, pH between stations and layer. Further samples were collected for analysis of nitrogen inorganic nutrients and to define the trophic status (as described by analysis of organic matter content and composition). The results for the first time provide evidence that Archaea are present in all stations, layers and periods sampled, and that their abundance was higher, on overage, reach up to 20%. The principal source of variability of procariotic community structure is layer, suggesting that depletion of oxygen

and strong reduction of pH are the most important parameter enables to shape prokaryotic assemblages. This is particular true for Bacteria, which decreases more than Archaea along sediments profile. Multivariata regression analysis highlighted that also surficial bacterial and archaeal populations are affected differentially by environmental parameters taken into account. Indeed, although both seem to be little affected by sedimentary trophic state, up to of 90% of bacterial variance is explained by physiological paramiters (temperature, salinity and DO) and ammonia concentration (20%), whereas archaeal variance is explained only by pH (50%).

These results confirm the hypothesis that bacterial and archaeal abundance are differentially controlled by environmental setting, and suggest that they could have a different role in the ecosystem functioning of lagoon, as result of different physiology. In particular the importance of pH variation in controlling archaeal abundance also support the second hypothesis of my PhD: Archaea have an important role in nitrification as ammonia oxidizing microorganisms.

This hypothesis was tested in the Chapter IV. The study was carried out on sediments collected in the same stations described in Chapter III. However here the sediment was used to carry out microcosms. Indeed in order to investigate the actual contribution of Bacteria and Archaea to nitrification at Giralda, Gorino and Mare DNA-based Stable Isotope Probing (DNA-SIP) experiments were designed and settled. The rationale of experiment is to label the DNA of prokaryotes via ^{13}C-bicarbonate assimilation, since the ammonia oxidizers are chemolithotrophic prokaryotes using the ammonia as a source of energy and the inorganic carbon as source of carbon to produce biomass. To facilitate the AO labelling I have taken into account these devices: (i) the incubation were carried out in dark, in order to avoid the inorganic assimilation by photoautotrophic microorganisms; (ii) the sediment slurries of microcosms were prepared with filtered (0.2 μm) DIC-Free lagoon water amended with 13C-bicarbonate; (iii)

according with *in situ* ammonia concentration, I injected different ammonia amounts in three-sites microcosms in order to have comparable concentrations. The DNA derived from buoyant density fractions was analysed in two ways to assess active (13C-DNA) prokaryotes: (i) quantitative assessment of increases in relative abundance of 16SrRNA gene copies (qPCR) in 13C fractions in comparison with 12C fractions; (ii) qualitative comparison of prokaryotic community composition (T-RFs) extracted from 13C and 12C fractions (via cluster analysis).

The results of this second part of my thesis also confirmed the second hypothesis. Indeed my findings suggest that in Sacca di Goro lagoon at least three groups of ammonia oxidizers are actively involved in nitrification: members of Bacteria domain (maybe *Nitrosospira sp*.) and two taxa belonging to Archaea domain, *Nitrosopumilus maritimus*, *Ca. Nitrososphaera gargensis*. Bacteria seem to dominate in Giralda sediments under high rates of nitrification and low salinity, whereas Archaea dominated the process in Gorino sediments under low nitrification rates and high salinity.

In conclusion my thesis provide evidence that in Sacca di Goro the Domain of Archaea contribute together to Bacteria to influence the lagoon biogeochemical cycles. Although further investigations are need before to elucidate the role of Archaea in ammonia oxidation and what are the environmental factors defining their ecological niche, the results of my PhD advances our understanding of the role of Archaea in the nitrogen cycle in coastal transition systems subject to high inputs of nitrogen and under strong anthropogenic pressure.

References

Adair, K.L., Schwartz, E., 2008. Evidence that ammonia-oxidizing archaea are more abundant than ammonia-oxidizing bacteria in semiarid soils of northern Arizona, USA. Microb. Ecol. 56,420–426.

Beman, J.M., Francis, C.A., 2006. Diversity of ammonia-oxidizing archaea and bacteria in the sediments of a hypernutrified subtropical estuary: Bahia del Tobari, Mexico. Appl. Environ. Microbiol. 72,7767–7777.

Beman, J.M., Popp, B.N., Francis, C.A., 2008. Molecular and biogeochemical evidence for ammonia oxidation by marine Crenarchaeota in the Gulf of California. ISME J. 2,429–441.

Caffrey, J.M., Bano, N., Kalanetra, K. & Hollibaugh, J.T., 2007. Ammonia oxidation and ammonia-oxidizing bacteria and archaea from estuaries with differing histories of hypoxia. ISME J. 1, 660–662.

Chen, X.P., Zhu, Y.G., Xia, Y., Shen, J.P., He, J.Z., 2008. Ammonia-oxidizing archaea: important players in paddy rhizosphere soil? Environ. Microbiol. 10,1978–1987.

Cioffi, F., Di Eugebio, A., Gallerano, F., 1995. A new representation of anoxic crisis in hypertrophic lagoons. Appl. Math. Model. 19, 685–695.

Coolen, M.J.L., Abbas, B., van Bleijswijk, J., Hopmans, E.C., Kuypers, M.M.M., Wakeham, S.G. & Sinninghe, Damste, J.S., 2007. Putative ammonia-oxidizing crenarchaeota in suboxic waters of the Black Sea: a basin-wide ecological study using 16S ribosomal and functional genes and membrane lipids. Environ. Microbiol. 9,1001–1016.

Dalsgaard, T., Nielsen, L.P., Brotas, V., Viaroli, P., Underwood, G.J.C., Nedwell, D.B., Sundbäck, K., Rysgaard, S., Miles, A., Bartoli, M., Dong, L., Thornton, D.C.O., Ottosen, L.D.M., Castaldelli, G. & Risgaard-Petersen, N., 2000. Protocol handbook for NICE-Nitrogen cycling in estuaries: a project under the

EU research programme. Marine Science and Technology (MAST III), 62 pp. National Environmental Research Institute, Silkeborg, Denmark.

Danovaro, R., Pusceddu, A., 2007. Biodiversity and ecosystem functioning in coastal lagoons: does microbial diversity play any role? Estuar. Coast. Shelf Sci. 75, 4-12.

Dodds, W.K. 2006. Eutrophication and trophic state in rivers and streams. Limnol. Oceanogr., 51, 671-680.

Erguder, T.H., Boon, N., Wittebolle, L., Marzorati, M., Verstraete, W., 2009. Environmental factors shaping the ecological niches of ammoniaoxidizing archaea. FEMS Microbiol. Rev. 33,855–869.

Falkowski, P.G., Fenchel, T., and Delong, E.F., 2008. The microbial engines that drive Earth's biogeochemical cycles. Science 320**,** 1034–1039.

Francis, C.A., Beman, J.M, Kuypers, M.M.M., 2007. New processes and players in the nitrogen cycle: the microbial ecology of anaerobic and archaeal oxidations. ISME J. 1, 19-27.

Francis, C.A., Roberts, K.J., Beman, J.M., Santoro, A.E., and Oakley, B.B.,2005. Ubiquity and diversity of ammoniaoxidizing archaea in water columns and sediments of the ocean. Proc. Natl. Acad. Sci. U.S.A. 102**,** 14683–14688.

Freitag, T.E., Chang, L., Prosser, J.I., 2006. Changes in the community structure and activity of betaproteobacterial ammonia-oxidizing sediment bacteria along a freshwater-marine gradient. Environ. Microbiol., 8, 684–696.

Gruber, N., and Galloway, J.N., 2008. An Earth-system perspective of the global nitrogen cycle. Nature 451**,** 293–296.

Hansel, C.M., Fendorf, S., Jardine, P.M., Francis, C.A., 2008. Changes in bacterial and archaeal community structure and functional diversity along a geochemically variable soil profile. Appl. Environ. Microbiol. 74,1620–1633.

Harzallah, A., Chapelle, A., 2002. Contribution of climate variability to occurrences of anoxic crises ''mala.ïgues'' in the Thau lagoon (Southern

France). Oceanologica Acta 25, 79–86.

Herrmann, M., Saunders, A.M., Schramm, A., 2008. Archaea dominate the ammonia-oxidizing community in the rhizosphere of the freshwater macrophyte Littorella uniflora. Appl. Environ. Microbiol. 74,3279–3283.

Herrmann, M., Saunders, A.M., Schramm, A., 2009. Effect of lake trophic status and rooted macrophytes on community composition and abundance of ammonia-oxidizing prokaryotes in freshwater sediments. Appl. Environ. Microbiol. 75,3127–3136.

Ingalls, A.E., Shah, S.R., Hansman, R.L., Aluwihare, L.I., Sanctos, G.M., Druffel, E.R.M., Pearson, A., 2006. Quantifying archaeal community autotrophy in the mesopelagic ocean using natural radiocarbon. Proc. Natl. Acad. Sci. U.S.A. 103, 6442-6447.

Karner, M.B., DeLong, E.F., Karl, D.M., 2001. Archaeal dominance in the mesopelagic zone of the Pacific Ocean. Nature 409, 507-510.

Könneke, M., Bernhard, A., Torre, J.R.D., Walker, C.B., Waterbury, J.B., Stahl, D.A., 2005. Isolation of an autotrophic ammonia-oxidizing marine archaeon. Nature 427, 543-546.

Koops, H.P., Purkhold, U., Pommerening-Roser, A., Timmermann, G., and Wagner, M., 2006. The lithoautotrophic ammonia-oxidizing bacteria. In *The Prokaryotes*. Dworkin, M., Falkow, S., Rosenberg, S., Schleifer, K.H., and Strackebrandt, E. (eds). Heidelberg, Germany: Springer, pp. 778–811.

Kowalchuk, G.A., and Stephen, J.R., 2001. Ammonia-oxidizing bacteria: a model for molecular microbial ecology. Ann. Rev. Microbiol. 55**,** 485–529.

Lam, P., Jensen, M.M., Lavik, G., McGinnis, D.F., Muller, B., Schubert, C.J., et al., 2007. Linking crenarchaeal and bacterial nitrification to anammox in the Black Sea. Proc. Natl. Acad. Sci. U.S.A. 104**,** 7104–7109.

Lam, P., Lavik, G., Jensen, M.M., van de Vossenberg, J., Schmid, M., Woebken, D., Gutierrez, D., Amann, R., Jetten, M.S., Kuypers, M.M., 2009. Revising the

nitrogen cycle in the Peruvian oxygen minimum zone. Proc. Natl. Acad. Sci. U. S. A. 106,4752–4557.

Leininger, S., Urich, T., Schloter, M., Schwark, L., Qi, J., Nicol, G.W., et al., 2006. Archaea predominate among ammonia-oxidizing prokaryotes in soils. Nature 442**,** 806–809.

Li, M., Hong, Y., Klotz, M.G., Gu, J.-D., 2010. A comparison of primer sets for detecting 16S rRNA and hydrazine oxidoreductase genes of anaerobic ammonium-oxidizing bacteria in marine sediments. Appl. Microbiol. Biotechnol. 86,781–790.

Manini, E., Fiordelmondo, C., Gambi, C., Pusceddu, A., Danovaro, R., 2003. Benthic microbial loop functioning in coastal lagoons: a comparative approach. Oceanologica Acta 26, 27-38. Pinardi, M., Bartoli, M., Longhi, D., Marzocchi, U., Laini, A., Ribaudo, C. and Viaroli P., 2009. Benthic metabolism and denitrification in a river reach: a comparison between vegetated and bare sediments. J. Limnol., 68(1), 133-145.

Mincer, T.J., Church, M.J., Taylor, L.T., Preston, C., Karl, D.M., DeLong, E.F., 2007. Quantitative distribution of presumptive archaeal and bacterial nitrifiers in Monterey Bay and the North Pacific Subtropical Gyre. Environ. Microbiol. 9,1162–1175.

Nizzoli, D., Castaldelli, G., Bartoli, M., Welsh, D.T., Arriaga, Gomez, P., Fano, A.E. & Viaroli, P., 2002. Benthic fluxes of dissolved inorganic nitrose in a coastal lagoon of the northern adriatic sea: an interpretation of spatial variabily based on sediment features and infauna activity. Mar. Ecol., 23, 297-306.

Ottosen, L.D.M, Risgaard-Petersen, N. & Nielsen, L.P., 1999. Direct and indirect measurements of nitrification and denitrification in the rhizosphere of aquatic macrophytes. Aquat. Microb. Ecol., 19, 81-91.

Park, H.D., Wells, G.F., Bae, H., Criddle, C.S., Francis, C.A., 2006. Occurrence of ammonia-oxidizing archaea in wastewater treatment plant bioreactors. Appl.

Environ. Microbiol. 72,5643–5647.

Pugnetti, A., Viaroli, P., Ferrari, I., 1992. Process leading to dystrophy in a Po River Delta lagoon (Sacca di Goro): phytoplankton-macroalgae interactions. Sci. Total Env. (Suppl.), 445–456.

Santoro, A.E., Francis, C.A., de Sieyes, N.R., Boehm, A.B., 2008. Shifts in the relative abundance of ammonia-oxidizing bacteria and archaea across physicochemical gradients in a subterranean estuary. Environ. Microbiol. 10,1068–1079.

Schleper, C., Jurgens, G., and Jonuscheit, M., 2005. Genomic studies of uncultivated archaea. Nat. Rev. Microbiol. 3**,** 479–488.

Specchiulli, A., Focardi, S., Renzi, M., Scirocco, T., Cilenti, L., Breber, P., Bastianoni, S., 2008. Environmental heterogeneity patterns and assessment of trophic levels in two Mediterranean lagoons: Orbetello and Varano, Italy. Sci. Total Env., 402, 285-298.

Steger, D., Ettinger-Epstein, P., Whalan, S., Hentschel, U., de Nys, R.,Wagner, M., Taylor, M.W., 2008. Diversity and mode of transmission of ammonia-oxidizing archaea in marine sponges. Environ. Microbiol. 10,1087–1094.

Stein, J.L., Simon, M.I., 1996. Archaeal ubiquity. Proc. Natl. Acad. Sci. U.S.A. 93, 6228-6230.

Urakawa, H., Tajima, Y., Numata, Y., Tsuneda, S., 2008. Low temperature decreases the phylogenetic diversity of ammonia-oxidizing archaea and bacteria in aquarium biofiltration systems. Appl. Environ. Microbiol. 74,894–900.

Viaroli, P., Azzoni, R., Bartoli, M., Giordani, G., Tajè, L., 2001. Evolution of the trophic conditions and dystrophic outbreaks in the Sacca di Goro lagoon (Northern Adriatic Sea). In: Faranda, F.M., Guglielmo, L., Spezie, G.(Eds.), Structure and Processes in the Mediterranean Ecosystems. Springer, Milano, Italia, Chapter 56, 443–451.

Viaroli, P., M. Bartoli, G., Giordani, M., Naldi, S., Orfanidis, & J.M. Zaldivar.,

2008. Community shifts, alternative stable states, biogeochemical controls and feedbacks in eutrophic coastal lagoons: a brief overview. Aquat. Conserv. 10, 956-1002.

Viaroli, P., Naldi, M., Bondavalli, C., Bencivelli, S., 1996. Growth of the seaweed Ulva rigida C. Agardh in relation to biomass densities, internal nutrient pools and external nutrient supply in the Sacca di Goro lagoon (Northern Italy). Hydrobiologia 329, 93–103.

Welsh, D.T., 2000. Nitrogen fixation in seagrass meadows: regulation, plant-bacteria interactions and significance to primary productivity. Ecol. Lett. 3,58–71.

Wuchter, C., Abbas, B., Coolen, M.J.L., Herfort, L., van Bleijswijk, J., Timmers, P., et al., 2006. Archaeal nitrification in the ocean. Proc. Natl. Acad. Sci. U.S.A. 103**,** 12317–12322.

Lueders T, Manefield M, Friedrich MW (2004b) Enhanced sensitivity of DNA- and rRNA-based stable isotope probing by fractionation and quantitative analysis of isopycnic centrifugation gradients. Environ Microbiol 6: 73–78.

Lueders T, Pommerenke B, Friedrich MW (2004a) Stable-isotope probing of microorganisms thriving at thermodynamic limits: syntrophic propionate oxidation in flooded soil. Appl Environ Microbiol 70: 5778–5786.

Lueders T, Wagner B, Claus P, Friedrich MW (2004c) Stable isotope probing of rRNA and DNA reveals a dynamic methylotroph community and trophic interactions with fungi and protozoa in oxic rice field soil. Environ Microbiol 6: 60–72.

Neufeld J, Dumont M, Vohra J, Murrell J (2007a) Meth- odological considerations for the use of stable iso- tope probing in microbial ecology. Microb Ecol 53: 435–442.

Neufeld JD, Vohra J, Dumont MG, Lueders T, Manefield M, Friedrich MW, Murrell JC (2007c) DNA stable- isotope probing. Nat Protocols 2: 860–866.

Neufeld JD, Wagner M, Murrell JC (2007b) Who eats what, where and when? Isotope-labelling experi- ments are coming of age. ISME J 1: 103–110.

Wagner M, Nielsen PH, Loy A, Nielsen JL, Daims H (2006) Linking microbial community structure with function: fluorescence in situ hybridization-microautoradiography and isotope arrays. Curr Opin Biotechnol 17: 83–91.

Manefield M, Griffiths RI, Leigh MB, Fisher R, Whiteley AS (2005) Functional and compositional com- parison of two activated sludge communities reme-diating coking effluent. Environ Microbiol 7: 715–722.

Manefield M, Griffiths R, McNamara NP, Sleep D, Ostle N, Whiteley A (2007) Insights into the fate of a 13C labelled phenol pulse for stable isotope prob- ing (SIP) experiments. J Microbiol Meth 69: 340–344.

Manefield M, Whiteley AS, Bailey MJ (2004) What can stable isotope probing do for bioremediation? Int Biodeterior Biodegradation 54: 163–166.

Manefield M, Whiteley AS, Griffiths RI, Bailey MJ (2002) RNA stable isotope probing, a novel means of link- ing microbial community function to phylogeny. Appl Environ Microbiol 68: 5367–5373.

Kunapuli U, Lueders T, Meckenstock RU (2007) The use of stable isotope probing to identify key iron- reducing microorganisms involved in anaerobic benzene degradation. ISME J 1: 643–653.

Elser JJ, Bracken MES, Cleland EE, Gruner DS, Harpole WS, Hillebrand H, Ngai JT, Seabloom EW, Shurin JB, Smith JE. 2007. Global analysis of nitrogen and phosphorus limitation of primary producers in freshwater, marine and terrestrial

ecosystems. Ecol. Lett. 10:1135-1142.

Vitousek PM, Aber JD, Howarth RW, Likens GE, Matson PA, Schindler DW, Schlesinger WH, Tilman D. 1997. Human alteration of the global nitrogen cycle: Sources and consequences. Ecol. Appl. 7:737-750. Gruber N, Galloway JN. 2008. An Earth-system perspective of the global nitrogen cycle. Nature. 451:293-296.

Spang A, Hatzenpichler R, Brochier-Armanet C, Rattei T, Tischler P, Spieck E, Streit W, Stahl DA, Wagner M, Schleper C. 2010. Distinct gene set in two different lineages of ammonia-oxidizing archaea supports the phylum Thaumarchaeota. Trends Microbiol. 18:331-340.

Herrmann M, Saunders AM, Schramm A. 2008. Archaea dominate the ammonia-oxidizing community in the rhizosphere of the freshwater macrophyte Littorella uniflora. Appl. Environ. Microbiol. 74:3279-3283.

Prosser JI, Nicol GW. 2008. Relative contributions of archaea and bacteria to aerobic ammonia oxidation in the environment. Environ. Microbiol. 10:2931-2941.

Altmann D, Stief P, Amann R, de Beer D. 2004. Distribution and activity of nitrifying bacteria in natural stream sediment versus laboratory sediment microcosms. Aquat. Microb. Ecol. 36:73-81.

Herrmann M, Scheibe A, Avrahami S, Kusel K. 2011. Ammonium availability affects the ratio of ammonia-oxidizing bacteria to ammonia-oxidizing archaea in simulated creek ecosystems. Appl. Environ. Microbiol. 77:1896-1899.

Sauder LA, Engel K, Stearns JC, Masella AP, Pawliszyn R, Neufeld JD. 2011. Aquarium nitrification revisited: Thaumarchaeota are the dominant ammonia oxidizers in freshwater aquarium biofilters. PLoS ONE 6:e23281.

Herrmann M, Saunders AM, Schramm A. 2009. Effect of lake trophic status and rooted macrophytes on community composition and abundance of ammonia-oxidizing prokaryotes in freshwater sediments. Appl. Environ. Microbiol. 75:3127-3136.

Offre P, Prosser JI, Nicol GW. 2009. Growth of ammonia-oxidizing archaea in soil microcosms is inhibited byacetylene. FEMS Microbiol. Ecol. 70:99-108.

Lam P, Jensen MM, Lavik G, McGinnis DF, Mu□ller B, Schubert CJ, Amann R, Thamdrup B, Kuypers MMM. 2007. Linking crenarchaeal and bacterial nitrification to anammox in the Black Sea. Proc. Natl. Acad. Sci. U.S.A. 104:7104-7109.

Freitag TE, Chang L, Prosser JI. 2006. Changes in the community structure and activity of betaproteobacterial ammonia-oxidizing sediment bacteria along a freshwater–marine gradient. Environ. Microbiol. 8:684-696.

Jia Z, Conrad R. 2009. Bacteria rather than Archaea dominate microbial ammonia oxidation in an agricultural soil. Environ. Microbiol. 11:1658-1671.

Zhang L-M, Offre PR, He J-Z, Verhamme DT, Nicol GW, Prosser JI. 2010. Autotrophic ammonia oxidation by soil thaumarchaea. Proc. Natl. Acad. Sci. U.S.A. 107:17240-17245.

XiaW,ZhangC,ZengX,FengY,WengJ,LinX,ZhuJ,XiongZ,XuJ,CaiZ, Jia Z. 2011. Autotrophic growth of nitrifying community in an agricultural soil. ISME J. 5:1226-1236.

Zhang L-M, Hu H-W, Shen J-P, He J-Z. 2012. Ammonia-oxidizing archaea have more important role than ammonia-oxidizing bacteria in ammonia oxidation of strongly acidic soils. ISME J. 6:1032-1045. Pratscher J, Dumont MG, Conrad R. 2011. Ammonia oxidation coupled to

CO2 fixation by archaea and bacteria in an agricultural soil. Proc. Natl. Acad. Sci. U.S.A. 108:4170-4175.

Avrahami S, Jia Z, Neufeld JD, Murrell JC, Conrad R, Kussel K. 2011. Active autotrophic ammonia-oxidizing bacteria in biofilm enrichments from simulated creek ecosystems at two ammonium concentrations respond to temperature manipulation. Appl. Environ. Microbiol. 77:7329-7338.

Stark JM. 1996. Modeling the temperature response of nitrification. Biogeochemistry. 35:433-445.

Thamdrup B, Fleischer S. 1998. Temperature dependence of oxygen respiration, nitrogen mineralization, and nitrification in Arctic sediments. Aquat. Microb. Ecol. 15:191-199.

Koops H-P, Purkhold U, Pommerening-Rosser A, Timmermann G, Wagner M. 2006. The Lithoautotrophic Ammonia-Oxidizing Bacteria, p 778-811. In Dworkin M, Falkow S, Rosenberg E, Schleifer K-H, Stackebrandt E (ed.), The Prokaryotes. Springer, New York.

Koops HP, Bottcher B, Moller UC, Pommerening-Roser A, Stehr G. 1991. Classification of eight new species of ammonia-oxidizing bacteria: Nitrosomonas communis sp. nov., Nitrosomonas ureae sp. nov., Nitrosomonas aestuarii sp. nov., Nitrosomonas marina sp. nov., Nitrosomonas nitrosa sp. nov., Nitrosomonas eutropha sp. nov., Nitrosomonas oligotropha sp. nov. and Nitrosomonas halophila sp. nov. J. Gen. Microbiol. 137:1689-1699.

Avrahami S, Liesack W, Conrad R. 2003. Effects of temperature and fertilizer on activity and community structure of soil ammonia oxidizers. Environ. Microbiol. 5:691-705.

Urakawa H, Tajima Y, Numata Y, Tsuneda S. 2008. Low temperature decreases the phylogenetic diversity of ammonia-oxidizing archaea and

bacteria inaquarium biofiltration systems. Appl. Environ. Microbiol. 74:894-900.

Fierer N, Carney KM, Horner-Devine MC, Megonigal JP. 2009. The biogeography of ammonia-oxidizing bacterial communities in soil. Microb. Ecol. 58:435-445.

Tourna M, Stieglmeier M, Spang A, Konneke M, Schintlmeister A, Urich T, Engel M, Schloter M, Wagner M, Richter A, Schleper C. 2011. Nitrososphaera viennensis, an ammonia oxidizing archaeon from soil. Proc. Natl. Acad. Sci. U.S.A. 108:8420-8425.

de la Torre JR, Walker CB, Ingalls AE, Ko□nneke M, Stahl DA. 2008. Cultivation of a thermophilic ammonia oxidizing archaeon synthesizing crenarchaeol. Environ. Microbiol. 10:810-818.

Tourna M, Freitag TE, Nicol GW, Prosser JI. 2008. Growth, activity and temperature responses of ammonia-oxidizing archaea and bacteria in soil microcosms. Environ. Microbiol. 10:1357-1364.

Liu X, Lu X, Chen Y. 2011. The effects of temperature and nutrient ratios on Microcystis blooms in Lake Taihu, China: An 11-year investigation. Harmful algae. 10:337-343.

James RT, Havens K, Zhu GW, Qin BQ. 2009. Comparative analysis of nutrients, chlorophyll and transparency in two large shallow lakes (Lake Taihu, PR China and Lake Okeechobee, USA). Hydrobiologia. 627:211-231.

Kim J-G, Jung M-Y, Park S-J, Rijpstra WIC, Sinninghe Damsté JS, Madsen EL, Min D, Kim J-S, Kim G-J, Rhee S-K. 2012. Cultivation of a highly enriched

ammonia-oxidizing archaeon of thaumarchaeotal group I.1b from an agricultural soil. Environ. Microbiol. 14:1528-1543.

Wilhelm SW, Farnsley SE, LeCleir GR, Layton AC, Satchwell MF, DeBruyn JM, Boyer GL, Zhu G, Paerl HW. 2011. The relationships between nutrients, cyanobacterial toxins and the microbial community in Taihu (Lake Tai), China. Harmful algae. 10:207-215.

Murase J, Noll M, Frenzel P. 2006. Impact of Protists on the Activity and Structure of the Bacterial Community in a Rice Field Soil. Appl. Environ. Microbiol. 72:5436-5444.

Schloss PD, Westcott SL, Ryabin T, Hall JR, Hartmann M, Hollister EB, Lesniewski RA, Oakley BB, Parks DH, Robinson CJ, Sahl JW, Stres B, Thallinger GG, Van Horn DJ, Weber CF. 2009. Introducing mothur: open-source, platform-independent, community-supported software for describing and comparing microbial communities. Appl. Environ. Microbiol. 75:7537-7541.

Edgar RC, Haas BJ, Clemente JC, Quince C, Knight R. 2011. UCHIME improves sensitivity and speed of chimera detection. Bioinformatics 27:2194-2200.

Wang Q, Garrity GM, Tiedje JM, Cole JR. 2007. Nai□ve Bayesian classifier for rapid assignment of rRNA sequences into the new bacterial taxonomy. Appl. Environ. Microbiol. 73:5261-5267.

Acknowledgements

This PhD thesis has been possible thanks to a funding from the Region of Sardinia through a scholarship called “Master and Back” and an annual funding for spending a period of one year provided abroad (Germany) by the DAAD (Deutscher Akademischer Austausch Dienst).

ANNEXS CHAPTER IV

Table 1. Relative abundance (expressed as percentage) of T-RFs for T8 Giralda Bacteria pH 7.4. On the left side of the table there is the light DNA fractions (12C) ordered from the light to the heavy density fractions. On the right side there is the heavy DNA fractions (13C) ordered from the light to the heavy density fractions.

T8 Giralda Bacteria pH 7.4								
T-RF	12C-12	12C-11	12C-9	12C-5	13C-12	13C-10	13C-8	13C-5
110	0	1.09	0	0.99	0	0	0	0
120	1.99	3.38	2.25	2.02	1.58	1.82	3.01	1.8
122	0	0	0	0	0	0	0	0
125.8	1.56	2.68	2.46	4.76	1.7	2.07	1.34	2.52
127.8	1.2	2.25	5.07	0	1.98	2.11	1.76	3.11
133.8	0	0	1.73	0	0	1.15	1.35	0
135.8	0	1	7.76	7.52	0	1.37	4.61	6.06
137.8	0	2.59	6.27	5.44	2.02	3.36	5.31	5.92
139.8	1.55	0	2.06	0	0	0	1.18	0
141.8	1.15	0	0	0	0	0	0	0
143.8	0	0.91	0	0	0	0	0	0
145.8	0	3.62	12.09	8.81	2.69	4.35	4.85	5.17
149.8	2.69	1.17	0	0	1.36	0	1.04	0
157.8	0	1.23	5.24	1.24	0	1.36	1.27	0
159.8	7.1	6.1	9.31	1.72	6.72	6.51	3.6	4.29
161.8	1.86	0	0	0	0	0	0	0
163.8	1.47	0	0	0	0	0	0	0
165.8	0	1.74	1.87	0	0.9	1.45	1.47	1.89
169.8	0	0	0	0	0	0	0	0

183.8	0	0	0	1.32	0	1.04	1.03	1.16
189.8	1.05	0	0	0	0	0	0	0
191.8	3.49	0	0	1	2.08	1.09	0	0
203.8	1.2	0	0	0	0	0	0	0
207.8	0.94	0	0	0	0	0	0	0
219.8	0	0	0	0	0	0	0	0.99
263.8	0	0	0	0	0	0	0	0
283.8	2.6	2.11	0	1.23	2	1.71	1.46	1
297.8	0	1.14	3.43	2.49	0	1.33	1.32	0.9
303.8	0	2.7	2.98	2.47	1.46	2.17	1.47	1.92
327.8	0	0	0	0	0	0	0	0
333.8	1.98	0	0	0.93	1.26	0	1.13	0
367.8	0	0	0	0	0	0	0	0
427.8	0	3.42	4.78	2.19	1.15	2.76	2.99	2.25
429.8	1.43	2.68	3.02	1.48	1.83	2.5	1.34	0
431.8	0	2	0	1.08	1.13	1.58	1.17	0
433.8	0	0	0	1.34	0	0	0	0
435.8	0.91	3.32	0	1.16	2.3	2.72	3.09	0
437.8	0	2.55	0	0	1.7	2.31	2.49	0
441.8	11.48	6.84	3.79	5.93	6.43	4.43	2.2	3.67
451.8	1.59	2.31	0	0	2.02	2.15	1.69	1.16
453.8	0	0	0	0	0	0	0	0
455.8	0	0.91	0	0	0	0	0	0
459.8	0	0	0	0	0	0	0	0
461.8	0	2.52	0	1.11	1.51	1.5	0.91	2.51
465.8	0	0	0	1.38	0	0	0	0
471.8	0	2.34	2.75	2.99	1.32	1.51	1.69	2.81
477.8	0	2.5	5.85	2.01	2.03	4.09	4.31	2.81
485.8	6.32	9.09	10.68	10.14	7.46	8.62	8.42	7.93
487.8	0	0	0	0	0	0	0	0
489.8	9.39	6.73	6.6	7.09	7.72	6.54	6.22	5.48
491.8	0	2.11	0	1.23	1.24	1.8	1.72	2.53
495.8	1.51	0	0	0	0	0	0	0
497.8	4.45	0	0	1.62	1.73	1.2	1.36	2.46
505.8	0	0	0	1.91	0	0	0	0.91
507.8	0	3.09	0	1.55	2.23	1.88	1.48	1.62
509.8	0	0	0	0	0	0	0	0
511.8	0	0.99	0	0	0	0	0	0
513.8	0	0	0	0	0	1.31	0	0
515.8	1.45	0	0	0	0	0	0.92	0
519.8	0	0	0	0	0	0	0	0

523.8	1.3	0	0	0	0.98	1.04	0	0
525.8	0	0.96	0	0	0	0	0	0
535.8	2.1	0	0	0	3.09	0	1.36	1.28
537.8	3.26	0	0	2.04	0	1.32	0	1.14
539.8	1.06	0	0	0	0	0	0	0
577.8	1.64	0	0	0	1	0	0	0
601.8	0	1.74	0	0	1.31	1.43	0	0
643.8	1.76	0	0	0	0	0	0	0
751.8	0.99	0	0	0	0	0	0	0
877.8	0	0	0	0	0	0	0	0
nT-RFs	31	33	20	31	31	34	34	27

Table 2. Relative abundance (expressed as percentage) of T-RFs for T8 Giralda Bacteria pH 8.2. On the left side of the table there is the light DNA fractions (12C) ordered from the light to the heavy density fractions. On the right side there is the heavy DNA fractions (13C) ordered from the light to the heavy density fractions.

T8 Giralda Bacteria pH 8.2								
T-RF	12C-12	12C-10	12C-7	12C-5	13C-12	13C-11	13C-9	13C-6
109.8	0	0	0.97	1.25	0	0	0	0
119.8	0	1.2	1.52	0	0	1.02	4.42	1.25
121.8	0	0	0	0	1.06	0	0	0
125.8	0	2.24	1.87	1.28	0	1.87	2.28	2.1
127.8	1.76	1.99	2.02	1.86	1.48	1.3	2.55	1.99
133.8	0	1.26	0	0	0	0	1.89	0
135.8	0	1.67	3.22	5.07	0	0	6.04	4.19
137.8	0	2.79	4.12	5.55	0	1.1	5.16	4.19
139.8	0	0	0	0	0	0	1.03	0
141.8	0	0	0	0	0	0	0	0
143.8	0	0	0	0	0	0	0	0
145.8	1.42	5	7.46	7.75	0	1.77	6.73	5.22
149.8	2.51	0	0	1.05	2.7	1.55	0	0
157.8	0.93	1.75	2.32	1.08	0	0	2.74	1.11
159.8	6.4	4.48	5.19	3.35	7.99	5.52	5.03	3.73
161.8	0	0	0	3.87	0	0	0	0
163.8	0.9	0	0	0	1.01	0	0	0
165.8	0	1.8	0.96	1.21	0	0	1.01	1.31
169.8	0	0	0	1.03	0	0	0	0

183.8	0	0	0	0	0	0	1.13	0
189.8	1.04	0	0	0	1.43	0.9	0	0
191.8	3.45	0	0	1.44	4.46	2.03	0	0
203.8	0	0	0	0	1	0	0	0
207.8	0	0	0	0	1.26	0	0	0
219.8	0	0	0	0	0	0	0	1.07
263.8	1.26	0	0	0	1.25	0	0	0
283.8	0	0	0.95	0	0.98	2.25	0	0
297.8	0	1.49	1.49	1.33	0	0	2.6	1.16
303.8	0	2	1.27	2.37	0	0.95	1.8	1.94
327.8	1.16	0	0	0	1.38	0	0	0
333.8	5.72	0	1.69	1.06	4.46	0	0	0
367.8	0	0	0	0	0.96	0	0	0
427.8	0	3.53	2.56	0	0	1.19	2.45	1.86
429.8	0	2.64	0	0	0	1.45	2.33	0.95
431.8	0	1.91	1.28	0	0	1.29	1.11	0
433.8	0	0	0	0	0	0	0	0
435.8	0	3.44	0	0	0	2.52	1.89	1.7
437.8	0	2.95	1.52	0.91	0	1.76	1.62	1.09
441.8	4.25	3.24	2.96	3.4	5.61	8.43	2.14	3.6
451.8	0	1.3	1.15	1.81	0	3.28	0	1.52
453.8	2.3	0	0	0	1.72	0	0	0
455.8	0	0	0	0	0	0	0	0
459.8	0	0	2.38	0	0	0	1.44	2.75
461.8	0	2.24	0	4.18	0	1.65	1.12	0
465.8	0	0	0	0	0	0	1.09	0
471.8	0	3.73	3.57	4.91	0	2.22	2.71	4.21
477.8	0	3.9	2.37	0	0	0	5.25	2.64
485.8	3.9	9.83	8.17	10.67	3.67	9.75	8.14	10.57
487.8	0	0	0	0	1.14	0	0	0
489.8	5.29	4.97	6.94	7.21	5.8	11.01	3.5	7.93
491.8	0	2.57	1.06	2.38	0	1	2.28	1.91
495.8	0	0	0	0	0	0	0	0
497.8	8.5	0	2.28	1.27	8.41	0	0	2.18
505.8	0	0	0	0	0	0	0	0
507.8	0	2.36	0	2.35	0	2.9	1.14	1.72
509.8	1.48	0	0	0	0	0	0	0
511.8	0	1.27	0	0	0	0	0	0
513.8	0	0	0	0	0	0	0	0
515.8	2.15	0	1.74	2.17	1.64	0	0	0
519.8	1.48	0	0	0	0	0	0	0

523.8	1.64	0	0	0	2.15	0	0	0.94
525.8	0	0	0	0	0	1.22	0	0
535.8	4.82	0	1.31	0	5.17	2.5	0	2.46
537.8	5.53	0	1.23	3.01	3.98	1.32	0	1.71
539.8	0.96	0	0	0	0	0	0	0
577.8	0	0	0	0	1.18	0	0	0
601.8	0	1.93	0	1.2	0	1.53	0.94	0
643.8	0	0	0	0	1.21	0	0	0
751.8	1.94	0	0	0	1.3	0	0	0
877.8	1.05	0	0	0	0	0	0	0
nT-RFs	25	28	29	29	27	28	30	29

Table 3. Relative abundance (expressed as percentage) of T-RFs for T8 Giralda Archaea pH 7.4. On the left side of the table there is the light DNA fractions (12C) ordered from the light to the heavy density fractions. On the right side there is the heavy DNA fractions (13C) ordered from the light to the heavy density fractions.

T8 Giralda Archaea pH 7.4								
T-RF	12C-12	12C-11	12C-9	12C-5	13C-12	13C-10	13C-8	13C-5
152.1	0	0	0	0	0	0	0	0.95
154.1	0	0	0	3.7	0	0	0	0
162.1	0	0	0	0	0.86	0	0	1.47
166.1	0	0	0	0	1.13	0	0	2.21
170.1	0	0	0	0	0.89	0	0	1.69
174.1	0	0	0	0	1.18	0	0	2.36
176.1	0	0	0	0	0	0	0	1.33
180.1	0	0	0	0	0.66	0	0	1.76
182.1	57.74	34.71	41.51	29.01	41.81	37.19	36.19	48.29
184.1	0	0	0	0	0	8.29	0	0
186.1	0	0	0	0	0	0	0	0
194.1	0	0	0	0	0	0	0.89	0
196.1	0	0	0	0	0	0	0	0
256.1	0	0	0	0	0	0	1.59	0
280.1	0	0	0	0	0	0	0	0
282.1	4.48	34.18	30.25	11.07	16.19	23.17	20.77	8.39
284.1	0	0	0	0	0	5.91	0	0
304.1	0	0	0	0	0	0	0	0
326.1	0	0	0	0	0	0	0	1.96
388.1	0	0	0	0	0	0	1.32	0
390.1	15.9	24.27	24.05	10.21	18.48	10.67	19.31	12.44
392.1	0	0	0	0	0	1.82	0	0

458.1	0	0	0	0	0	0	0	0
490.1	0	0	0	0	0	0	2.27	0
494.1	0	0	4.18	0	0	0	2.48	0
670.1	0	0	0	0	0	0	0	6.85
710.1	0	0	0	0	0	0	0	0
738.1	12.21	0	0	0	9.34	6.42	6.7	0
740.1	0	0	0	0	0	0	0	3.11
792.1	0	0	0	34.9	6.59	6.53	4.82	0
794.1	9.67	6.84	0	0	0	0	0	2.53
796.1	0	0	0	0	0	0	0	0
810.1	0	0	0	11.11	2.87	0	3.67	4.65
812.1	0	0	0	0	0	0	0	0
nT-RFs	5	4	4	6	11	8	11	15

Table 4. Relative abundance (expressed as percentage) of T-RFs for T8 Giralda Archaea pH 8.2. On the left side of the table there is the light DNA fractions (12C) ordered from the light to the heavy density fractions. On the right side there is the heavy DNA fractions (13C) ordered from the light to the heavy density fractions.

T8 Giralda Archaea pH 8.2								
T-RF	12C-12	12C-10	12C-8	12C-5	13C-12	13C-11	13C-9	13C-6
152.1	0	0	5.61	0	0.51	0	0	0
154.1	0	0	0	0	0	0	0	0
162.1	0	0	0	0	0.7	0	0	0
166.1	0	0	2.44	0	0.71	0.64	0	0
170.1	0	0	0	0	1.22	0.66	0	0
174.1	0	0	2.29	0	1.24	1.05	0	0
176.1	0	0	0	0	0.5	0	0	0
180.1	0	0	0	0	0.57	0	0	0
182.1	76.64	25.84	57.73	58.03	66.56	39.49	29.12	39.59
184.1	0	0	0	0	0	0	0	6.96
186.1	0	0	0	0	0	0	0	3.49
194.1	0	0	0	0	0	0	0	0
196.1	1.36	0	0	0	0	0	0	0
256.1	1.91	0	0	0	0.73	1.27	0.86	0.86
280.1	0.53	0	0	0	0	0	0	0
282.1	0	46.7	23.17	20.66	1.55	13.47	31.23	20.48
284.1	0	0	0	0	0	0	0	3.42
304.1	0	0	0	0	0	0	0.63	0
326.1	0	0	0	0	0	0	0	0
388.1	0	0	0	0	0	0	0	0
390.1	8.72	23.19	0	21.3	6.71	23.8	27.23	13.72

392.1	0	0	0	0	0	0	0	0.61
458.1	0	0	0	0	0	0	0.43	0
490.1	0	0	0	0	0	0	0	0
494.1	0	0	0	0	0	1.13	3.91	0.65
670.1	0	0	0	0	0	1.23	0	0
710.1	0.73	0	0	0	0	0	0	0
738.1	6.36	0	0	0	8.66	7.6	1.35	2.16
740.1	0	0	0	0	0	0	0	0
792.1	0.76	0	0	0	7.64	7.04	3.53	6.92
794.1	0	4.27	8.75	0	0	0	0	0
796.1	0.64	0	0	0	0	0	0	0
810.1	2.35	0	0	0	0	2.63	1.72	1.14
812.1	0	0	0	0	2.7	0	0	0
nT-RFs	10	4	6	3	14	12	10	12

Table 5. Relative abundance (expressed as percentage) of T-RFs for T21 Giralda Bacteria pH 7.4. On the left side of the table there is the light DNA fractions (12C) ordered from the light to the heavy density fractions. On the right side there is the heavy DNA fractions (13C) ordered from the light to the heavy density fractions.

T21 Giralda Bacteria pH 7.4										
T-RF	12C-11	12C-10	12C-9	12C-8	12C-7	13C-11	13C-10	13C-9	13C-8	13C-7
106.3	0	0	0	0.15	0	0	0	0	0	0
110.3	0	0	0	0.41	0	0	0	0.96	0.37	0
116.3	0	0	0	0.43	0	0	0	0	0.46	0
118.3	0	0	0	0.92	0	0	0	1.19	3.1	4
120.3	1.02	2.28	2.63	1.15	0	1.61	1.32	2.4	2.75	3.03
124.3	0.68	0	0	0.56	0	0.58	0	0	0.52	1.68
126.3	0	1.82	5.91	4.76	0	0.48	3.48	5.18	5.53	7.85
128.3	0	0	0	0.15	0	0.74	0	0	0	0
134.3	0	0	1.88	2.52	0	0	0	2.46	2.43	1.47
136.3	0	0	2.76	6.97	21.24	0	0	3.08	7.87	11.4
138.3	0.8	0	3.18	4.38	15.58	0.44	0	3.49	4.06	6.59
140.3	0	1.2	0	0.71	0	0	2.61	0	0.53	0
142.3	0.63	2.33	0	0.14	0	0.82	0	0	0.16	0
144.3	0	1.31	0	0.23	0	0.43	1.52	0	0.27	0
146.3	0.94	0	6.72	7.14	18.21	0.35	1.28	7.51	7.55	10.02
148.3	3.88	4.76	0	0.51	0	3.81	4.2	0.82	0.66	0
150.3	0	1.06	0	0	0	0	1.14	0	0	0
156.3	0	0	0	1.69	0	0	0	3.67	0	0
158.3	6.14	2.4	3.84	1.46	0	6.39	3.37	0	3.88	5.39
160.3	0	7.38	10.21	5.8	12.96	0	5.84	8.84	5.23	7.71
162.3	0	0	0	0	0	0	0	0	0.3	0

164.3	0.91	2.5	0	0	0	1.19	2.25	0	0	0
166.3	0	0	2.17	0.92	0	0	0	2.02	0.96	0
168.3	0.76	0	0	0.17	0	0	0	0	0	0
170.3	0	0	0	0.62	0	0.65	0	1.51	1.58	0
176.3	0	1.32	0	0.22	0	0	1.37	0	0	0
178.3	0	0	0	0	0	0	0	0	0.26	0
182.3	0.91	0	0	0	0	0.72	0	0	0	0
184.3	0	0	0	1.16	0	0	1.04	1.28	1.2	0
188.3	0	2.15	0	0.18	0	2.29	1.91	0	0	0
190.3	1.8	0	0	0.39	0	0	0	0	0.37	0
192.3	7.94	6.96	0	0.36	0	9.73	5.56	0	0.27	0
194.3	0	0	0	0.28	0	0	0	0	0.27	0
196.3	0	0	0	0.81	0	0	0	0	0.7	0
198.3	0	0	0	1.26	0	0	0	0	1.24	0
200.3	0.48	0	0	0.53	0	0	0	0	0.59	0
204.3	1.36	0	0	0	0	1.24	0	0	0	0
206.3	0	0	0	0.38	0	0	0	0	0.48	0
220.3	0	0	0	0.51	0	0	0	0	0	0
222.3	0	0	0	0	0	0	0	0	0.77	0
226.3	0	0	0	0.15	0	0	0	0	0	0
258.3	0	0	0	0.23	0	0	0	0	0	0
264.3	1.37	0	0	0	0	1.3	0	0	0	0
272.3	0	0	0	0	0	0.58	0	0	0	0
276.3	0	0	0	0.59	0	0	0	0	0.39	0
278.3	0	0	0	0.45	0	0	0	0	0.79	0
280.3	0	0	0	0	0	0.41	0	0	0	0
282.3	0	2.89	2.23	1.06	0	0	3.59	1.21	0.51	0
286.3	0	0	0	0.51	0	0	0	0	0.34	0
288.3	0	0	0	0.42	0	0	0	0	0.46	0
290.3	0	0	0	0.17	0	0	0	0	0	0
292.3	0	0	0	0.13	0	0	0	0	0	0
294.3	0	0	0	0.26	0	0	0	0	0	0
296.3	0	0	0	0.12	0	0	0	0	0	0
298.3	0	0	2.14	1.9	0	0	0	2.15	1.52	1.95
304.3	0	0	0	0.63	0	0	0	1.56	0.77	0
326.3	1.83	0	0	0	0	2.27	0	0	0	0
334.3	9.03	2.91	0	0	0	8.83	1.22	0	0	0
368.3	0	0	0	0	0	0.44	0	0	0	0
400.3	0	0	0	0.84	0	0	0	0	0	0
402.3	0	0	0	0	0	0	0	0	0.53	0
414.3	0.99	0	0	0	0	0.93	0	0	0	0
420.3	1.66	0	0	0	0	0.98	0	0	0	0
422.3	0	0	0	0.41	0	0	0	0	0	0

428.3	0	0	6.3	2.38	0	0	0	3.01	4.27	3.97
430.3	0	0	0	1.41	0	0	1.5	2.78	0	0
432.3	0	0	0	1.35	0	0	0	2.66	1.42	0
436.3	0	0	2.78	1.88	0	0	0	2.37	1.73	0
438.3	0	0	3.58	2.58	0	0	0	3.2	2.39	3.1
440.3	6.27	14.45	8.39	2.65	9.61	4.06	15.32	4.37	3.16	6.16
448.3	0	0	0	0.21	0	0	0	0	0	0
452.3	0	3.34	0	0.94	0	0	3.54	0	0.69	0
454.3	3.43	2.6	0	0.16	0	4.77	1.38	0	0	0
456.3	0	0	0	0.66	0	0	0	0	0.58	0
460.3	0	0	0	0.46	0	0	0	0	0.53	0
462.3	0	0	0	1.08	0	0	1.16	0	1.15	0
466.3	0	0	0	1.2	0	0	0	0	1.01	0
468.3	0	0	0	0.29	0	0	0	0	0	0
470.3	0	0	0	0.61	0	0.61	0	0	0.58	0
474.3	1.82	0	0	1.74	0	0.69	0	0	1.65	0
478.3	0	0	6.4	6.42	0	0	0	6.88	4.66	4.77
480.3	0	0	0	0.17	0	0	0	0	0	0
486.3	0	5.93	13.27	6.57	22.4	0	6.3	12.29	7	11.59
488.3	0.78	5.85	4.57	1.21	0	1.21	6	3.63	1.91	4.53
492.3	0	6.6	7.05	3.62	0	0	8.59	4.59	2.89	4.8
494.3	0	0	0	0	0	0.4	0	0	0	0
496.3	0	5.8	0	1.29	0	0	4.78	0	0.56	0
498.3	18.38	6.5	0	0	0	17.32	3.18	0	0	0
502.3	0	0	0	0	0	0.71	0	0	0	0
506.3	0	0	4	0.4	0	0	2.32	0	0.3	0
508.3	0	0	0	1.53	0	0	0	2.53	0.87	0
510.3	0	0	0	0	0	0.63	0	0	0	0
512.3	0	0	0	0.98	0	0	0	2.34	0.96	0
516.3	2.11	2.72	0	0.7	0	2.09	1.58	0	0.96	0
518.3	1.66	0	0	0	0	1.91	0	0	0	0
520.3	2.03	0	0	0	0	1.44	0	0	0	0
524.3	1.38	2.95	0	0.67	0	2.42	2.65	0	0	0
536.3	0	0	0	0	0	0.58	0	0	0	0
538.3	0.94	0	0	0	0	1.23	0	0	0	0
598.3	0	0	0	0.21	0	0	0	0	1.06	0
600.3	0	0	0	0.41	0	0	0	0	0	0
604.3	0	0	0	0.23	0	0	0	0	0	0
666.3	5.1	0	0	0	0	2.9	0	0	0	0
674.3	0	0	0	0.26	0	0	0	0	0	0
750.3	2.23	0	0	0	0	0	0	0	0	0
752.3	0	0	0	0	0	2.87	0	0	0	0
866.3	8.32	0	0	0	0	0	0	0	0	0

868.3	0	0	0	0	0	4	0	0	0	0
878.3	2.43	0	0	0	0	1.46	0	0	0	0
884.3	0	0	0	0	0	0.72	0	0	0	0
902.3	0	0	0	0	0	0.75	0	0	0	0
nT-RFs	33	25	20	79	6	45	29	29	59	18

Table 6. Relative abundance (expressed as percentage) of T-RFs for T21 Gorino Archaea pH 7.4. On the left side of the table there is the light DNA fractions (12C) ordered from the light to the heavy density fractions. On the right side there is the heavy DNA fractions (13C) ordered from the light to the heavy density fractions.

T21 Gorino Archaea pH 7.4												
T-RF	12C-11	12C-10	12C-9	12C-8	12C-7	12C-6	13C-11	13C-10	13C-9	13C-8	13C-7	13C-6
104.7	0	0	0	0.16	0	0	0	0	0	0	0	0
110.7	0	0	0	0	0	0	0	0	0	0	0	0.14
116.7	0	0	0.09	0.1	0	0	0	0	0	0	0	0
124.7	0	0	0	0	0	0	0	0	0	0	0.41	0
128.7	0	0	0	0.28	0	0	0	0	0	0	0	0
134.7	0	0	0.13	0.15	0	0	0	0	0	0	0	0
140.7	0	0.12	0	0	0	0	0	0	0	0	0	0
146.7	0	0.44	0.18	0.17	0	0	0.09	0	0.17	0	0	0
148.7	0	0.1	0.1	0	0	0	0	0	0	0	0.26	0
152.7	0	0	0.24	1.38	0	0	0	0	0.25	0	0	0
154.7	0	0.29	0.17	0.32	0	0	0	0.12	0.09	0	0	0
156.7	0	0	0	0	0	0	0.34	0	0	0	0	0
160.7	0	0	0	0.13	0	0	0	0	0	0	0	0
168.7	0	0	0	0.1	0	0	0	0	0	0	0	0
170.7	0.22	0.14	0.23	0.11	0	0	0.1	0	0.09	0	0	0
182.7	3.8	16.3	13.06	5.32	0	8.86	20.9	19.4	3.79	0.98	2.6	1.42
184.7	2.29	0	0	0	0	0	0	0	0	0	0	0
194.7	0.43	0.65	0.43	0.54	23.49	1.09	4.8	0.94	0	0	0	0
196.7	0.36	0	0	0	0	2.05	0	0	0	0	0	0
198.7	0.24	2.37	0.94	0.34	0	0.14	1.05	1.3	0.4	0	0.18	0
200.7	0	0	0	0	0	0.16	0	0	0	0	0	0
202.7	0.09	0.23	0.26	0.83	0	0.12	0	0	0.09	0	0.5	0.19
204.7	0.22	0.59	0.94	4.05	0	2.07	0	0.2	0.4	0.35	4.32	1.7
208.7	0	0	0	0	0	0	0.44	0	0	0	0	0
212.7	0	0	0	0.25	0	0	0	0	0	0	0	0
214.7	0	0.17	0.11	0	0	0	0	0	0	0	0	0
218.7	0	0.09	0	0	0	0	0	0	0	0	0	0
220.7	0	0	0	0	0	0	0	0.14	0	0	0	0
224.7	0.21	0.7	0.85	0.61	0	0.24	0.22	0.35	0.68	0.35	0.8	0.49
226.7	0.21	0	0	0	0	0	0.11	0	0	0	0	0

228.7	0	0	0	0.19	0	0	0	0	0	0	0	0
232.7	0	0.7	0.63	0.51	0	0.31	0.19	0.32	0.48	0.3	0.6	0.29
234.7	0.26	0.14	0.11	0.19	0	0	0	0	0	0	0	0
236.7	0	0.11	0.09	0	0	0	0.42	0.27	0	0	0	0
238.7	0	0	0	0	0	0	0.24	0	0	0	0	0
242.7	0	0.13	0.16	0.13	0	0	0	0	0	0	0	0
244.7	0	0.13	0.12	0.1	0	0	0.09	0	0	0	0	0
254.7	0.36	0.91	1.13	0.36	0	0.21	0.54	0.27	0.52	0.3	0.51	0.29
262.7	0	0.13	0	0.24	0	0	0.27	0	0	0	0	0
264.7	0	0.73	0.27	0.18	0	0	0.71	0.21	0	0	0	0
272.7	0	0.13	0	0	0	0	0	0	0	0	0	0
274.7	0	0	0.1	0	0	0	0	0	0	0	0	0
278.7	0	0	0	0	0	0	0.33	0	0	0	0	0
282.7	0	0.87	1.44	2.07	0	0	0	0.61	0.77	0	0.16	0
290.7	0	0	0	0	0	0	0.54	0	0	0	0	0
294.7	0	0	0.14	0	0	0	0	0	0	0	0	0
304.7	0	0.4	0.21	0	0	0	1.14	0	0	0	0	0
306.7	0	0	0	0.42	0	0	0	0.19	0.13	0	0	0
308.7	0	0.25	0	0.18	0	0	0.57	0.29	0	0	0	0
310.7	0	0.11	0	0	0	0	0	0	0.09	0	0	0
314.7	0	0.29	0.46	0.23	0	0.17	0.09	0.11	0.23	0.22	0.28	0.24
316.7	0.2	0.11	0	0	0	0	0	0	0	0	0	0
320.7	0	0	0	0	0	0	0	0	0	0	0.17	0
322.7	0	0	0	0.13	0	0	0.69	0	0	0	0	0
324.7	0	0.14	0.4	0.12	0	0	0	0.38	0.14	0	0	0
332.7	0.42	0.09	0.19	0.09	0	0	0	0	0.1	0	0.26	0.2
344.7	0	0	0.31	0.24	0	0	0	0	0	0	0	0
352.7	0	0.12	0.3	1.43	0	0	0	0	0	0	0	0
370.7	0	0	0	0.14	0	0	0.28	0	0	0	0	0
376.7	0	0.12	0.33	0.39	0	0	0	0	0.24	0	0	0
384.7	0	0	0	0.46	0	0	0	0	0	0	0	0
388.7	0.35	6.81	15.3	8.03	0	3.3	3.86	5.93	5.78	1.1	2.32	0.27
390.7	0.22	0	0	0	0	6	6.76	0	0	0	0	0
392.7	0.1	0.09	0	0	0	0	0	0	0	0	0	0
406.7	0	0.13	0.1	0.13	0	0	0	0	0	0	0	0
410.7	0	0.12	0.09	0	0	0	0	0	0	0	0	0
412.7	0	0	0	0.1	0	0	0	0	0	0	0	0
426.7	0	0.1	0.1	0	0	0	0	0	0	0	0	0
428.7	0	0.14	0.12	0.13	0	0	0	0	0	0	0	0
442.7	0	0	0	0.3	0	0	0.75	0	0	0	0	0
444.7	0	0.46	0.44	0	0	0	0	0.62	0.32	0	0.87	0
446.7	0	0.09	0	0	0	0	0	0	0	0	0.13	0
456.7	0	0.1	0.18	0.21	0	0	0	0	0	0	0	0

462.7	0	0.15	0.14	0	0	0	0	0	0.12	0	0.64	0
480.7	0	0	0	0.16	0	0	0	0	0	0	0	0
482.7	0	0	0	0	0	0	0.15	0	0	0	0	0
484.7	0	0.14	0.19	0.2	0	0	0	0	0	0	0	0
488.7	0	0	0	0	0	0	0	0	0	0	0	1.13
492.7	0	0	0.52	0.62	0	0	0	0.38	0	0	0	0
494.7	0	0	0	0	0	0	0.46	0.32	0	0	0	0
508.7	0	0.14	0.1	0.12	0	0	0	0	0	0	0	0
514.7	0.24	0.43	0	0.38	0	0	1.61	0.41	0	0	0	0
516.7	0	0	0.17	0	0	0	0	0	0	0	0	0
524.7	0	0.28	0.11	0	0	0	0	0.49	0	0	0	0
526.7	0.21	0	0	0	0	0	0	0	0	0	0	0
534.7	0	0.28	0.11	0	0	0	0.36	0	0	0	0	0
538.7	0	0.17	0	0	0	0	0.22	0	0	0	0	0
572.7	0	0	0.11	0	0	0	0	0	0	0	0	0
580.7	0	0	0	0	0	0	0.53	0	0	0	0	0
584.7	0	0	0	0	0	0	0.51	0	0	0	0	0
604.7	0.25	0.4	0	0	0	0	5.71	0.37	0	0	0	0
606.7	0.38	0	0	0	0	0	0	0	0	0	0	0
612.7	0	0	0	0.29	0	0	0.33	0	0	0	0.25	0
616.7	0	0.12	0.17	0	0	0	0.16	0	0	0	0	0
620.7	0	0.11	0.11	0	0	0	0	0	0	0	0	0
654.7	0	0	0.38	0.48	0	0	0	0	0.27	0	0	0
678.7	0	0	0	0	0	0	0.42	0	0	0	0	0
680.7	0	3.27	10.63	4.2	0	3.14	0.18	3.45	3.45	0.52	0.85	2.49
688.7	0	0	0	0.27	0	0	0	0	0	0	0	0
692.7	0	0	0	0.16	0	0	0	0	0	0	0	0
706.7	0	0	0.17	0	0	0	0	0	0	0	0	0
716.7	0	0	0.19	0	0	0	0.12	0	0	0	0	0
722.7	0	0.2	0	0	0	0	0.32	0	0	0	0	0
730.7	0	0	0	0	0	0	0.14	0	0	0	0	0
738.7	0	0	0	0	0	0	0.16	0.63	0	0	0	0
742.7	0.24	0	0	0	0	0	0	0	0	0	0	0
744.7	0	0	0	0	0	0	0	0	0	0	0.22	0
768.7	0	0	0	0	0	0	0.15	0	0	0	0	0
770.7	0	0.19	0	0.85	0	0	0	0.47	0	0	0	0
772.7	0	0.17	0.14	0	0	0	0	0	0	0	0.3	1.01
782.7	0	0.23	0.58	0.77	0	0	0	0	0	0	0	2.95
792.7	0	0	16.75	0	0	0	0	0	0	0	0	0
794.7	86.32	36.37	28	58.47	76.51	72.15	34.58	60.21	80.76	94.92	83.36	87.19
796.7	0	20.49	0	0	0	0	0	0	0	0	0	0
802.7	0	0	0	0	0	0	0	0	0.32	0	0	0
804.7	0	0	0	0	0	0	0	0	0	0.97	0	0

806.7	1.34	0	0	0	0	0	5.65	0.44	0	0	0	0
810.7	1.04	0.34	0.21	1.32	0	0	2.08	0.52	0	0	0	0
932.7	0	0	0.33	0	0	0	0	0.67	0.27	0	0	0
nT-RFs	25	59	58	57	2	15	46	30	26	10	22	15

Table 7. Relative abundance (expressed as percentage) of T-RFs for T21 Gorino Bacteria pH 8.2. On the left side of the table there is the light DNA fractions (12C) ordered from the light to the heavy density fractions. On the right side there is the heavy DNA fractions (13C) ordered from the light to the heavy density fractions.

T21 Gorino Bacteria pH 8.2								
T-RF	12C-11	12C-10	12C-9	12C-8	13C-12	13C-11	13C-9	13C-8
109.7	0	0	0	0	0	0	4.64	0
111.7	0	0	0	0	0	0	1.43	0
113.7	0	0	0	0	0	0	1.28	0
115.7	0.28	0	0	0	0	0	0	0
119.7	0.41	0	0	0	0	0	0	0
123.7	0.5	0	0	0	0	0	0	0
125.7	0.16	0	0	0	0	0	0	0
127.7	0.16	1.71	1.01	0	0	0	0	0
129.7	2.35	7.63	3.26	1.71	0	0.56	3.37	0
131.7	0.49	0	0	0	0	0	0.87	1.39
133.7	0.79	1.4	0.99	0	0	0	2.44	3.08
137.7	2.33	8.03	3.6	3.1	0.31	0.6	4.53	0
139.7	1.04	2.02	1.94	2.29	0	0	0	0
141.7	0.72	0	1.3	1.09	2.16	1.31	0	3.09
143.7	0	0	0	0	1.7	0	0	0
145.7	1	2.04	1.84	1.37	0	0.45	1.37	2.45
147.7	1.76	8.29	3.88	2.05	0.8	0.67	5.61	2.5
149.7	0.14	0	0	0	0	0	0	0
151.7	0	0	0	0	0.99	0	0	0
157.7	2.52	3.94	3.41	3.09	0.96	1.21	6.88	5.51
159.7	2.45	2.17	1.01	1.01	0.75	1.72	1.36	1.86
161.7	0.48	0	1.19	3.03	0	0	0	0
163.7	0.17	0	0	1.36	0	0	0	0
165.7	0.13	0	0	3.37	0	0	0	0
167.7	1.3	3.27	2.9	0	0	0	3.57	2.29
171.7	0.19	0	0	0	0	0	0	0
175.7	0.56	0	0	0	0	0	0	0
179.7	0.25	0	0	0	0.76	0	0	0
181.7	0.16	0	0	0	0	0	0	0
189.7	0.87	0	0	0	0	0	0	0
191.7	0	0	0	0	0.52	0	0	0

203.7	1.18	1.21	0	0	0.82	0.62	0	0
209.7	0	0	0	0	1.9	0	0	0
211.7	0.16	0	0	0	0	0	0	0
213.7	0.23	0	0	0	0	0	0	0
219.7	0.4	0	0	0	0	0	0	0
225.7	0.39	0	0	0	0	0	0	0
227.7	0.95	1.74	1.51	1.23	0	0	0	0
229.7	0.22	0	0	0	0	0	0	0
257.7	0	0	0	0	0.32	0	0	0
269.7	0.19	0	0	0	0	0	0	0
281.7	0.15	0	0	0	0	0	0	0
287.7	0.22	0	0	0	0	0	0	0
291.7	0.23	0	0	0	0	0	0	0
293.7	0.68	2.44	1.79	1.34	0	0	1.78	0
295.7	0	0	3.35	0	0	0	0	0
297.7	0	0	2.56	0	0	0	0	0
299.7	0	0	0	0	0	0	0	2.7
305.7	0.5	0	0	0	0	0	0	0
331.7	0	0	0	0	0.38	0	0	0
401.7	0	0	0	0	0.4	0	0	0
435.7	3.82	4.58	4.79	5.69	1.16	3.5	6.19	0
437.7	0.78	2.18	1.67	0	0	0	0	0
447.7	2.9	3.88	2.71	2.23	0	0	7.13	11.45
449.7	1.04	1.15	0.88	1.02	0	0	3.23	2.49
453.7	2.13	1.97	2.35	1.86	0.82	0	7.24	25.79
461.7	2.5	0	2.36	2.17	0	1.34	3.82	4.29
465.7	3.45	4.33	2.97	0	0	0	4.74	3.56
467.7	0	0	0	1.85	0	1.75	0	0
473.7	1.28	0	0	0	1.08	0	0	0
481.7	0.23	0	0	0	0	0	0	0
485.7	0	0	0	0	1.62	0	0	0
487.7	0	0	0	0	0	0	0	2.8
489.7	0	0	0	0	0.65	0	0	0
491.7	24.74	26.45	21.4	13.24	0	10.62	25.73	20.93
495.7	0.51	4.45	15.4	34.1	73.08	4.91	0	0
507.7	2.73	3	4.24	4.88	1.08	3.18	2.79	3.85
509.7	0.48	0	0	0	0	0	0	0
513.7	2.1	2.11	3.18	3.92	1.49	2.32	0	0
519.7	0.96	0	0	0	0	0	0	0
527.7	0.37	0	0	0	0	0	0	0
535.7	0	0	0	0	1.55	0	0	0
537.7	0.36	0	0	0	0.93	0	0	0
543.7	0	0	0	0	0.9	1.14	0	0
603.7	0.74	0	0	0	0	0	0	0

669.7	1.29	0	0	0	0	0	0	0
861.7	3.94	0	0	0	0	12.16	0	0
869.7	0.41	0	2.49	3.01	2.89	14.6	0	0
873.7	0.46	0	0	0	0	0	0	0
881.7	0.57	0	0	0	0	0	0	0
893.7	3.34	0	0	0	0	7.48	0	0
917.7	10.11	0	0	0	0	22.34	0	0
933.7	2.09	0	0	0	0	7.51	0	0
nT-RFs	64	23	28	24	26	21	21	17

Table 8. Relative abundance (expressed as percentage) of T-RFs for T21 Gorino Archaea pH 8.2. On the left side of the table there is the light DNA fractions (12C) ordered from the light to the heavy density fractions. On the right side there is the heavy DNA fractions (13C) ordered from the light to the heavy density fractions.

T21 Gorino Archaea pH 8.2										
T-RF	12C-12	12C-11	12C-10	12C-9	12C-8	12C-7	13C-11	13C-10	13C-9	13C-8
101.6	0	0	0.19	0	0	0	0	0	0	0
103.6	0	0	0	2.42	0	0	0	0	0	0
105.6	0	0	0.42	0	0	0	0	0	0	0
115.6	0	0	0	0	0	10.29	0	0	0	0
129.6	0	0	0	2.31	0	0	0	0	0	0
143.6	0.19	0	0	0	0	0	0	0.22	0	0
145.6	0	0.64	0.21	0	0	0	0	0	0	0.46
147.6	0.18	0	0	0	0	0	0	0	0	0
153.6	0	1	0.48	0	0	0	0	0.14	0	0
165.6	0	0	0.22	0	0	0	0	0	0	0
183.6	7.52	8.15	6.09	3.87	0	3.41	19.28	2.1	0.26	0.14
185.6	0	0	0	0	0	0	0	0	0.17	0
195.6	0.29	0.57	0.39	0	0	0	2.17	0	0	0
197.6	0.72	0.88	0.91	0	0	0	0.73	0	0	0
199.6	0	0.25	0	0	0	0	0	0	0	0
201.6	0	0.2	0	0	0	0	0	0	0	0
203.6	0.15	0.27	0	0.28	0	0	0	0	0	0.64
211.6	0	0	0.24	0	0	0	0	0	0	0
215.6	0	0.24	0	0	0	0	0	0	0	0
223.6	0.36	0.65	0.2	0.56	0	0	0	0.42	0	0
225.6	0	0.37	0	0	0	0	0	0	0	0
231.6	0.32	0.37	0.2	0.35	0	0	0	0.31	0	0
233.6	0	0	0	0	0	0	0	0	0.15	0
243.6	0	0.17	0	0	0	0	0	0	0	0
253.6	0.68	1.32	0	0.52	0	3.42	0	0.37	0	0
255.6	0	0.19	0	0	0	0	0	0	0	0

263.6	0	0	0	0	0	0	0.4	0	0	0
281.6	0.58	1.37	0.86	0	0	1.21	0	0.35	0	0
305.6	0.24	0	0.26	0	0	0	0	0	0	0
309.6	0	0.19	0.65	0	0	0	0	0	0	0
311.6	0	0.41	0	0	0	0	0	0	0	0
313.6	0.19	0.37	0	0.22	0	0	0	0.22	0	0
319.6	0	0	0	0	0	0.6	0	0	0	0
323.6	0.13	0	0	0	0	0	0	0	0	0
331.6	0	0	0	0.19	0	0	0	0	0	0
353.6	0	0.36	0	0	0	0	0	0	0	0
377.6	0	0.26	0	0	0	0	0	0	0	0
385.6	0	0.25	0	0	0	0	0	0	0	0
389.6	5.51	10.18	4.48	4.38	0	2.79	3.93	3.14	0	0.16
391.6	0	0	0	1.31	0	0	0	0	0.32	0
443.6	0	0.32	0	0	0	0	0	0	0	0
445.6	0.48	0	0	0	0	0	0.57	0	0	0
461.6	0	0	0.58	0	0	0	0	0	0	0
491.6	0	0.96	0	0	0	0	0	0	0	0
493.6	0	0	0.62	0	0	0	0	0	0	0
515.6	0	0	0.6	0	0	0	0.78	0	0	0
605.6	0	0	0	0	0	0	1.5	0	0	0
653.6	0	0	0	0.47	0	0	0	0	0	0
679.6	5.14	6.63	3.21	1.29	0	0	2.07	2.13	0	0
695.6	0	0	0.41	0	0	0	0	0	0	0
723.6	0	0.42	0	0	0	0	0	0	0	0
739.6	0	0	0	0	0	0	0.61	0	0	0
771.6	0	0.46	0.48	0	0	0	0.56	0	0	0
783.6	0	0.36	1.14	0.52	0	0	0.54	0	0	0
795.6	77.3	61.72	77.15	80.65	100	76.52	63.2	90.11	99.1	98.6
809.6	0	0.46	0	0	0	0	3.06	0.5	0	0
811.6	0	0	0	0	0	1.76	0	0	0	0
933.6	0	0	0	0.66	0	0	0.6	0	0	0
nT-RFs	17	31	23	16	1	8	15	12	5	5

Table 9. a) Simper analysis result for T21 Gorino Archaea pH 7.4 related to light DNA (12C); b) Simper analysis result for T21 Gorino Archaea pH 7.4 related to heavy DNA (13C). Cut-off 90%.

a)

T-RF	Av.Abund	Av.Sim	Sim/SD	Contrib%	Cum.%
795	59.64	45.52	2.48	80.46	80.46
182.7	7.89	4.14	1.05	7.32	87.78
388.7	5.63	2.2	0.76	3.9	91.68

b)

T-RF	Av.Abund	Av.Sim	Sim/SD	Contrib%	Cum.%
794.7	73.5	60.7	2.86	88.58	88.58

182.7	8.18	3.03	0.65	4.42	93.01

Table 10. a) Simper analysis result for T8 Giralda Bacteria pH 7.4 related to light DNA (12C); b) Simper analysis result for T8 Giralda Bacteria pH 7.4 related to heavy DNA (13C). Cut-off 90%.

a)

T-RF	Av.Abund	Av.Sim	Sim/SD	Contrib%	Cum.%
485.8	9.06	8.71	5.19	16.88	16.88
489.8	7.45	7.48	14.36	14.5	31.38
441.8	7.01	5.62	3.19	10.9	42.28
159.8	6.06	4.51	1.57	8.75	51.03
145.8	6.13	2.87	0.77	5.57	56.6
119.8	2.41	2.27	25.79	4.4	61
125.8	2.87	2.26	4.14	4.38	65.38
137.8	3.58	1.9	0.81	3.69	69.08
429.8	2.15	1.83	3.72	3.54	72.62
135.8	4.07	1.69	0.54	3.29	75.9
427.8	2.6	1.4	0.88	2.71	78.62
303.8	2.04	1.37	0.91	2.66	81.28
471.8	2.02	1.34	0.91	2.59	83.87
477.8	2.59	1.17	0.91	2.27	86.14
283.8	1.49	0.88	0.85	1.7	87.85
297.8	1.77	0.85	0.8	1.66	89.5
127.8	2.13	0.85	0.85	1.64	91.14

b)

T-RF	Av.Abund	Av.Sim	Sim/SD	Contrib%	Cum.%
486	8.11	9.92	32.71	13.49	13.49
489.8	6.49	7.54	13.51	10.24	23.74
159.8	5.28	5.51	3.82	7.5	31.23
145.8	4.27	4.58	3.73	6.23	37.47
441.8	4.18	3.92	3.05	5.33	42.79
137.8	4.15	3.84	2.34	5.22	48.01
477.8	3.31	3.34	3.61	4.54	52.56
127.8	2.24	2.42	11.01	3.29	55.84
427.8	2.29	2.26	2.63	3.08	58.92
119.8	2.05	2.16	17.57	2.94	61.86
507.8	1.8	2.04	9.52	2.77	64.62
125.8	1.91	2.02	5.22	2.75	67.37
303.8	1.76	1.97	8.64	2.67	70.05
491.8	1.82	1.9	5.92	2.59	72.63
451.8	1.76	1.89	4.15	2.56	75.2
471.8	1.83	1.84	10.28	2.51	77.7
497.8	1.69	1.72	5.39	2.34	80.04

283.8	1.54	1.62	4.26	2.2	82.24
135.8	3.01	1.55	0.68	2.11	84.35
461.8	1.61	1.55	3.56	2.1	86.45
435.8	2.03	1.54	0.91	2.09	88.54
165.8	1.43	1.5	4.15	2.04	90.58

Table 11. Results of Microbial Community Analysis III (MiCAIII) performer with program PAT+ on the archaeal forword fragments. The program was settled for primers Ar109f (5'-ACKGCTCAGTAACACGT-3') and Ar912r (5'-GTGCTCCCCCGCCAATTCCT-3'), restriction enzyme TaqI (T^CGA). The mach for forward fragment was settled to ±2.

Fragment length observed	Fragment length predicted	Accesn n. and Name of related archaeal Species
315	313	AY591983; uncultured archaeon Kazan-2A-05/BC19-2A-
315	313	FJ655755; uncultured archaeon SP3G5
315	313	FJ810530; uncultured archaeon JMYA23
315	314	AB329778; uncultured archaeon YS16Ac79
315	314	AB329796; uncultured archaeon YS16As48
315	314	FJ487455; uncultured crenarchaeote SPG12273283A11
315	314	FJ487456; uncultured crenarchaeote SPG12343353A93
315	315	AY592489; uncultured archaeon Napoli-2A-25 BC07-2A
315	316	FJ902296; uncultured archaeon LPROCKA87
315	316	FJ902676; uncultured archaeon LP80MA36
315	316	Y08385; Thermococcus guaymasensis DSM 11113
315	317	EU635910; uncultured archaeon SSWL4F01
315	317	EU924221; uncultured archaeon LHC4L5D07
681	680	AF361211; uncultured crenarchaeote SUBT-14
681	680	DQ490011; uncultured archaeon GBSL2E07
681	**680**	**EU239960; Candidatus Nitrosocaldus yellowstonii HL**
681	680	EU635917; uncultured archaeon SSEL4B03
681	680	HM448057; uncultured crenarchaeote YNPSBCMS2A8
681	680	HM448106; uncultured crenarchaeote YNPSBCBP4A15
681	680	HM448103; uncultured crenarchaeote YNPSBCBP4A4
681	680	HM448108; uncultured crenarchaeote YNPSBCBP4A25
681	680	HM448128; uncultured crenarchaeote YNPSBCMLS2A1
681	680	HM448140; uncultured crenarchaeote YNPSBCQL1A4
681	680	HM448142; uncultured crenarchaeote YNPSBCQL1A11
681	680	HQ395706; uncultured archaeon VG1-1d
681	681	HM448107; uncultured crenarchaeote YNPSBCBP4A20
681	682	HM448097; uncultured crenarchaeote YNPSBCBP3A1
795	793	AB461943; uncultured archaeon Fapm1aA49
795	793	FJ790592; uncultured archaeon QA22
795	793	GU137356; uncultured archaeon PNGTB4B7 5H1A091
795	793	GU137357; uncultured archaeon PNGTB4B7 5H1A026
795	793	GU137369; uncultured archaeon PNGTB4B30H1A003
795	793	GU137383; uncultured archaeon PNGTB4B140H1A033

795	793	AF419628; uncultured archaeon GBa1r015
795	793	AF068815; uncultured archaeon VC2 1 Arc4
795	793	AB019735; unidentified archaeon pMC2A228
795	793	DQ228617; uncultured archaeon CH2a27
795	793	DQ228627; uncultured archaeon OUTa35
795	793	AB260052; Archaeoglobus sp PM70-1
795	793	FJ810190; Archaeoglobus sp PM70-1
795	793	DQ925865; uncultured archaeon 182A11
795	793	AB288281; Methanobacterium sp T11
795	793	AB368917; Methanobacterium sp 169
795	793	AB034183; uncultured rumen methanogen 956
795	793	AB034188; uncultured rumen methanogen 15
795	793	AF356636; uncultured archaeon G26C63
795	793	AF356638; uncultured archaeon G26C82
795	793	L77117; Methanocaldococcus jannaschii (T) DSM 26
795	793	AB235312; Methanocaldococcus sp 70-8-3
795	793	AJ969469; uncultured Methanocaldococcus sp PICO p
795	793	EF079968; hyperthermophilic methanogen FS406-22
795	793	CP001696; Methanocaldococcus fervens AG86
795	793	CP001696; Methanocaldococcus fervens AG86
795	793	CP001901; Methanocaldococcus sp FS406-22
795	793	CP001901; Methanocaldococcus sp FS406-22
795	793	AB603516; Methanocaldococcus jannaschii JCM 10045
795	793	EU585970; uncultured Methanococcoides sp ET51H2
795	793	FN820424; uncultured archaeon GoCArc96D1C0M0
795	793	AM268271; uncultured Methanosarcinales archaeon UB
795	793	AM268272; uncultured Methanosarcinales archaeon UB
795	793	EU731574; uncultured Methanohalophilus sp GNA09G0
795	793	EF031086; uncultured archaeon SalA34
795	793	EF190085; uncultured marine crenarchaeote QGQG2
795	793	EU731575; uncultured Methanohalophilus sp GNA03H0
795	793	EU731582; uncultured Methanohalophilus sp GNA03C0
795	793	EU731584; uncultured Methanohalophilus sp GNA03D0
795	793	EU731586; uncultured Methanohalophilus sp GN210D1
795	793	CP001994; Methanohalophilus mahii DSM 5219
795	793	CP001994; Methanohalophilus mahii DSM 5219
795	793	FN870068; Methanohalophilus halophilus type strain
795	793	CP001994; Methanohalophilus mahii DSM 5219
795	793	HM480173; uncultured euryarchaeote Kir51gry 22-070
795	793	FR733671; Methanohalophilus halophilus type strain
795	793	M59135; Methanolobus tindarius
795	793	U20154; Methanolobus taylorii (T) GS-16
795	793	AY570664; uncultured archaeon PL-9A3
795	793	U20155; Methanolobus vulcani (T) PL-12/M
795	793	EF190079; uncultured archaeon YSSG1
795	793	EF376986; uncultured Methanolobus sp II-B3
795	793	EF376990; uncultured Methanolobus sp VII-D6

795	793	EF376989; uncultured Methanolobus sp VII-D2
795	793	EU546840; uncultured Methanolobus sp IV-A3
795	793	EU546842; uncultured Methanolobus sp IV-B5
795	793	EU546841; uncultured Methanolobus sp IV-A6
795	793	EU546844; uncultured Methanolobus sp IV-E1
795	793	EU546845; uncultured Methanolobus sp IV-E8
795	793	AF354132; uncultured archaeon SB-24a1C2 1441
795	793	AB370245; Methanolobus profundi (T) MobM
795	793	AJ312013; uncultured archaeon SHB-143
795	793	DQ631886; uncultured Methanomethylovorans sp MhI-
795	793	DQ631885; uncultured Methanomethylovorans sp MhI-
795	793	DQ631887; uncultured Methanomethylovorans sp MhI-
795	793	HQ592621; uncultured archaeon Aug05-pVIII-B02
795	793	AJ578088; uncultured archaeon HydCal59
795	793	AF354128; uncultured archaeon Eel-36a2A4 1436
795	793	AF354138; uncultured archaeon SB-24a1C12 1435
795	793	CR937012; uncultured archaeon fos0642g6
795	793	DQ522907; uncultured archaeon SBAK-deep-13
795	793	AM745250; uncultured euryarchaeote GoMGC2324463Arc
795	793	AM745257; uncultured euryarchaeote GoMGC2324463Arc
795	793	AM746094; uncultured euryarchaeote GoM140Arch41
795	793	EF687605; uncultured archaeon 113A26
795	793	EF687535; uncultured archaeon 104A25
795	793	AB461390; uncultured archaeon ANME2aPC
795	793	FJ555676; archaeon enrichment culture clone AOM-Cl
795	793	FJ555677; archaeon enrichment culture clone AOM-Cl
795	793	FJ656258; uncultured archaeon SSWC06
795	793	FJ712364; uncultured archaeon KZNMV-0-A40
795	793	FJ712367; uncultured archaeon KZNMV-5-A4
795	793	FJ712389; uncultured archaeon KZNMV-25-A36
795	793	FJ712375; uncultured archaeon KZNMV-10-A1
795	793	GU190981; uncultured archaeon MatB12arc56
795	793	GU190986; uncultured archaeon Edge0arc44
795	793	FN820437; uncultured archaeon GoCArc119D1C0M0
795	793	HQ588649; uncultured archaeon AMSMV-5-A7
795	793	HQ588648; uncultured archaeon AMSMV-5-A3
795	793	HQ588668; uncultured archaeon AMSMV-20-A2
795	793	HQ588656; uncultured archaeon AMSMV-10-A31
795	793	HQ588662; uncultured archaeon AMSMV-15-A1
795	793	HQ588685; uncultured archaeon AMSMV-30-A24
795	793	HQ588672; uncultured archaeon AMSMV-20-A32
795	793	AJ578116; uncultured archaeon HydBeg134
795	793	AF419644; uncultured archaeon C1R048
795	793	AJ578128; uncultured archaeon BS-K-H6
795	793	AY592811; uncultured archaeon Milano-WF1A-15
795	793	DQ004662; uncultured archaeon CAVMV300A948
795	793	DQ640143; uncultured archaeon SBAK-deep-14

795	793	AM745238; uncultured euryarchaeote GoMGC2324463Arc
795	793	AM745253; uncultured euryarchaeote GoMGC2324463Arc
795	793	EF687607; uncultured archaeon 113A28
795	793	EF687613; uncultured archaeon 113A34
795	793	FM179917; uncultured archaeon a34
795	793	FJ555674; archaeon enrichment culture clone AOM-Cl
795	793	FJ555675; archaeon enrichment culture clone AOM-Cl
795	793	FJ555678; archaeon enrichment culture clone AOM-Cl
795	793	FJ555679; archaeon enrichment culture clone AOM-Cl
795	793	FJ555681; archaeon enrichment culture clone AOM-Cl
795	793	FJ555683; archaeon enrichment culture clone AOM-Cl
795	793	FJ555684; archaeon enrichment culture clone AOM-Cl
795	793	FJ555686; archaeon enrichment culture clone AOM-Cl
795	793	FJ555687; archaeon enrichment culture clone AOM-Cl
795	793	FJ712363; uncultured archaeon KZNMV-0-A25
795	793	AM229230; uncultured euryarchaeote HydGH40-Arch201
795	793	AM229240; uncultured euryarchaeote HydGC-83-548A
795	793	AM229242; uncultured euryarchaeote HydGC-84-251A
795	793	AM229254; uncultured euryarchaeote HydGC-84-213A
795	793	GU190983; uncultured archaeon Edge0arc11
795	793	GU190995; uncultured archaeon Edge12arc26
795	793	EU420680; uncultured archaeon KM07-Ba-3
795	793	FN820392; uncultured archaeon GoCArc65D4C6M0
795	793	FN820427; uncultured archaeon GoCArc110D1C0M0
795	793	FN820429; uncultured archaeon GoCArc111D1C0M0
795	793	FN820431; uncultured archaeon GoCArc116D1C0M0
795	793	FN820432; uncultured archaeon GoCArc113D1C0M0
795	793	FN820434; uncultured archaeon GoCArc117D1C0M0
795	793	GU553626; uncultured archaeon ORI-860-27-PS101-103
795	793	HQ588634; uncultured archaeon AMSMV-0-A1
795	793	HQ588644; uncultured archaeon AMSMV-0-A45
795	793	HQ588658; uncultured archaeon AMSMV-10-A35
795	793	HQ588686; uncultured archaeon AMSMV-30-A27
795	793	AJ012644; Thermococcus sp P6 P6 (4/2000)
795	793	DQ082977; uncultured archaeon FOS0
795	793	AF119123; uncultured archaeon CRA12-27cm
795	793	AY592551; Unknown
795	793	AJ576239; uncultured archaeon GZK72
795	793	AB213097; uncultured archaeon Papm3A41
795	793	AB237748; uncultured archaeon HDBW-WA15
795	793	AB252425; uncultured archaeon OT-A17 18
795	793	EU731630; uncultured Thermoplasmatales archaeon GN
795	793	EU585960; uncultured Thermoplasmatales archaeon ET
795	793	EU585967; uncultured Thermoplasmatales archaeon ET
795	793	AY592451; uncultured archaeon Napoli-1A-18 BC07-1A
795	793	FJ477307; uncultured archaeon MMS111
795	793	FJ655721; uncultured archaeon SP3A4

795	793	FJ655728; uncultured archaeon SP3C3
795	793	FJ902704; uncultured archaeon LPBBA70
795	793	AM229233; uncultured euryarchaeote HydGC-83-542A
795	793	GU363081; uncultured archaeon BD72AR29
795	793	EU420693; uncultured archaeon KM07-Da-2
795	793	GU553473; uncultured archaeon ORI-860-18-PS281-283
795	793	GU553491; uncultured archaeon ORI-860-18-PS401-403
795	793	GU553509; uncultured archaeon ORI-860-25-PS008-010
795	793	GU553557; uncultured archaeon ORI-860-26-PS068-070
795	793	HM187505; uncultured archaeon HDBASISY395
795	793	HQ588688; uncultured archaeon AMSMV-30-A53
795	793	FJ571788; uncultured archaeon R15-73a
795	793	GU137367; uncultured archaeon PNGTB4B30H1A103
795	**794**	**AF083072; Cenarchaeum symbiosum B 60A5**
795	794	AB461942; uncultured archaeon Fapm1aA17
795	794	DQ228616; uncultured archaeon CH2a48
795	794	DQ228620; uncultured archaeon CH3a5
795	794	AE000782; Archaeoglobus fulgidus DSM 4304
795	794	AB293236; uncultured archaeon Pcsc2A09
795	794	AB293237; uncultured archaeon Pcsc2A25
795	794	AB293242; uncultured archaeon Pcsc3A26
795	794	EF644840; uncultured archaeon ROA3
795	794	EU635901; uncultured archaeon SSEL4E01
795	794	FJ638518; uncultured archaeon KCL60a0202
795	794	FJ638519; uncultured archaeon KCL60a0437
795	794	FJ638520; uncultured archaeon KCL70a0104
795	794	FJ638521; uncultured archaeon KCL70a0202
795	794	FN356383; uncultured archaeon DanArch56
795	794	FN356387; uncultured archaeon DanArch46
795	794	FN356421; uncultured archaeon HdaArch9
795	794	FN356422; uncultured archaeon HdaArch32
795	794	AF220165; Geoglobus ahangari (T) 234
795	794	AB111029; uncultured archaeon SH05-CAT-A05
795	794	AB111488; uncultured archaeon NT305-CAT-A04
795	794	AB293245; uncultured archaeon Phtm1A47
795	794	AF169245; Methanobacterium formicicum (T) DSMZ1535
795	794	AF028689; Methanobacterium formicicum FCam
795	794	AJ550159; Methanobacterium sp C5/51
795	794	AJ550160; Methanobacterium sp OM15
795	794	M36508; Methanobacterium formicicum
795	794	DQ649331; Methanobacterium sp Ch
795	794	DQ649309; Methanobacterium formicicum S1
795	794	AB288265; Methanobacterium sp HD-1
795	794	AB288272; Methanoculleus sp M06
795	794	AB288275; Methanobacterium sp T01
795	794	AB294251; uncultured archaeon YWA03
795	794	AB302952; Methanobacterium sp F

795	794	DQ649330; Methanobacterium subterraneum 9-7
795	794	AB479402; uncultured Methanobacterium sp SMS-slud
795	794	AB598270; Methanobacterium sp MO-MB1
795	794	AB542742; Methanobacterium petrolearium Mic5c12
795	794	AB118591; endosymbiont TS1 of Trimyema compressum
795	794	AJ009958; Methanobrevibacter sp SM9
795	794	HQ591420; Methanobacterium formicicum MG-134
795	794	AJ009959; Methanobrevibacter sp NT7
795	794	AJ550156; Methanobrevibacter sp AbM4
795	794	U55233; Methanobrevibacter smithii (T) PS
795	794	U55234; Methanobrevibacter smithii ALI
795	794	U55235; Methanobrevibacter smithii B181 DSM 1197
795	794	U55236; Methanobrevibacter thaueri (T) CW
795	794	U55239; Methanobrevibacter gottschalkii PG
795	794	AB181816; Methanobrevibacter sp Mc30
795	794	AB034185; uncultured rumen methanogen M6
795	794	DQ372974; uncultured methanogenic archaeon 5
795	794	DQ372973; uncultured methanogenic archaeon 4
795	794	CP000678; Methanobrevibacter smithii ATCC 35061 AT
795	794	CP001719; Methanobrevibacter ruminantium M1
795	794	CP001719; Methanobrevibacter ruminantium M1
795	794	HQ677982; uncultured archaeon 3B11
795	794	HQ678037; uncultured archaeon 2E10
795	794	HQ678047; uncultured archaeon 2G12
795	794	AF547621; Methanocaldococcus indicus (T) SL43
795	794	AJ969473; uncultured Methanocaldococcus sp PICO p
795	794	AY941801; Methanococcoides alaskense (T) AK-5
795	794	AY941802; Methanococcoides alaskense AK-9
795	794	CP000300; Methanococcoides burtonii (T) DSM 6242
795	794	CP000300; Methanococcoides burtonii (T) DSM 6242
795	794	DQ280485; Methanomicrobiales archaeon SBAK-CO2-red
795	794	CP000300; Methanococcoides burtonii (T) DSM 6242
795	794	FN820389; uncultured archaeon GoCArc60D1C0M0
795	794	GU553549; uncultured archaeon ORI-860-26-PS008-010
795	794	AB598271; Methanococcoides sp MO-MCD
795	794	EU731576; uncultured Methanohalophilus sp GNA02G0
795	794	GU553621; uncultured archaeon ORI-860-27-PS041-043
795	794	AJ578119; uncultured archaeon HydBeg92
795	794	AF354140; uncultured archaeon Eel-36a2B9 1436
795	794	DQ084450; uncultured Methanosarcinales archaeon AN
795	794	U20149; Methanohalobium evestigatum Z-7303
795	794	DQ084452; uncultured Methanosarcinales archaeon AN
795	794	AY592029; uncultured archaeon Kazan-3A-05/BC19-3A-
795	794	AB461391; uncultured archaeon ANME2bPC
795	794	FJ791566; uncultured archaeon SGXU732
795	794	FJ791589; uncultured archaeon SGXU722
795	794	CP002069; Methanohalobium evestigatum Z-7303

795	794	CP002069; Methanohalobium evestigatum Z-7303
795	794	FR733675; Methanohalobium evestigatum type strain:
795	794	AF354129; uncultured archaeon Eel-36a2A1 1447
795	794	AJ578122; uncultured archaeon BS-K-410
795	794	AM745178; uncultured euryarchaeote GoM161Arch53
795	794	AM745229; uncultured euryarchaeote GoMGC2324463Arc
795	794	FM179895; uncultured archaeon Gullfaksa32
795	794	GU190972; uncultured archaeon MatB0arc24
795	794	GU553530; uncultured archaeon ORI-860-25-PS101-103
795	794	GU553536; uncultured archaeon ORI-860-25-PS101-103
795	794	HQ588667; uncultured archaeon AMSMV-15-A25
795	794	AJ347787; uncultured SA1 group euryarchaeote ST-12
795	794	AJ347788; uncultured SA1 group euryarchaeote ST-3K
795	794	AB050224; uncultured archaeon SAGMA-S
795	794	AB050225; uncultured archaeon SAGMA-T
795	794	AB329797; uncultured archaeon YS16As51
795	794	EU731608; uncultured Thermoplasmatales archaeon GN
795	794	FJ902708; uncultured archaeon LPBBA86
795	794	GU553476; uncultured archaeon ORI-860-18-PS281-283
795	794	GU553493; uncultured archaeon ORI-860-18-PS401-403
795	794	GU553538; uncultured archaeon ORI-860-25-PS128-130
795	794	GU553563; uncultured archaeon ORI-860-26-PS068-070
795	795	FJ638508; uncultured archaeon KCL40a0523
795	795	FJ638514; uncultured archaeon KCL50a0558
795	795	FJ638522; uncultured archaeon KCL80a0101
795	795	FJ638523; uncultured archaeon KCL80a0202
795	795	AB288271; Methanobacterium sp M03
795	795	AB542743; Methanobacterium ferruginis Mic6c05
795	795	U41095; Methanobrevibacter cuticularis (T) RFM-1
795	795	AM269413; Methanobrevibacter sp 87 7
795	795	CP000678; Methanobrevibacter smithii ATCC 35061 AT
795	795	AB598273; Methanobrevibacter sp MO-MVB
795	795	HQ678045; uncultured archaeon 2E9
795	795	DQ402016; uncultured Methanosphaera sp 8
795	795	DQ402032; uncultured Methanosphaera sp 24
795	795	DQ402026; uncultured methanogenic archaeon 18
795	795	AF025822; Methanocaldococcus infernus (T)
795	795	AJ969471; uncultured Methanocaldococcus sp PICO p
795	795	CP002009; Methanocaldococcus infernus ME
795	795	CP002009; Methanocaldococcus infernus ME
795	795	AJ578125; uncultured archaeon BS-K-E9
795	795	X65537; Methanococcoides burtonii DSM 6242
795	795	M59127; Methanococcoides methylutens
795	795	EU585965; uncultured euryarchaeote ET51D11
795	795	EU585968; uncultured Methanococcoides sp ET51G9
795	795	FJ477324; Methanococcoides methylutens MM1
795	795	FM179838; uncultured archaeon Tomm0512743Arch90

795	795	FN820416; uncultured archaeon GoCArc99D1C0M0
795	795	FN820405; uncultured archaeon GoCArc81D0C0M1
795	795	HQ588654; uncultured archaeon AMSMV-5-A48
795	795	FR733669; Methanococcoides methylutens type strain
795	795	AJ579327; uncultured archaeon HMMVBeg-34
795	795	AJ704631; uncultured archaeon HMMVBeg-36
795	795	GU190976; uncultured archaeon MatB12arc16
795	795	GU553619; uncultured archaeon ORI-860-27-PS041-043
795	795	GU553618; uncultured archaeon ORI-860-27-PS041-043
795	795	GU553624; uncultured archaeon ORI-860-27-PS041-043
795	795	HM053965; Methanosalsum sp AME2
795	795	AJ579328; uncultured archaeon HMMVBeg-29
795	795	AJ579330; uncultured archaeon HMMVBeg-32
795	795	AF354130; uncultured archaeon SB-24a1B11 1437
795	795	AF354136; uncultured archaeon Eel-36a2H11 1449
795	795	CR937011; uncultured archaeon fos0625e3
795	795	EF687590; uncultured archaeon 104A9
795	795	AB461393; uncultured archaeon ANME3PC
795	795	AM229241; uncultured euryarchaeote HydGC-83-600A
795	795	AM229243; uncultured euryarchaeote HydGC-84-212A
795	795	Z70250; Thermococcus fumicolans ST557
795	795	DQ303250; uncultured archaeon ant c7
795	795	EU585937; uncultured Thermoplasmatales archaeon EH
795	795	GQ284551; uncultured archaeon ACSAS2P1H3
795	795	FN820414; uncultured archaeon GoCArc98D1C0M0
795	795	GU553560; uncultured archaeon ORI-860-26-PS068-070
795	795	HQ530526; uncultured euryarchaeote Discoveryb
795	796	Y10011; Archaeoglobus veneficus SNP6
795	796	AF418181; Archaeoglobus veneficus (T) DSM 11195
795	796	AJ969472; uncultured Archaeoglobales arcaheon PICO
795	796	FN356382; uncultured archaeon DanArch53
795	796	AF093061; Methanobacterium palustre (T) DSM 3108 F
795	796	DQ447182; uncultured bacterium 4F11
795	796	HM041912; uncultured Methanobacterium sp NRA11
795	796	AB065294; Methanobrevibacter arboriphilus SA
795	796	AF242652; Methanobrevibacter acididurans (T) ATM
795	796	U55237; Methanobrevibacter woesei (T) GS
795	796	AB244742; uncultured euryarchaeote GLY1A02
795	796	EF376991; uncultured Methanobrevibacter sp VII-D1
795	796	HQ678042; uncultured archaeon 2D12
795	796	AB213079; uncultured archaeon FnvA79
795	796	EU731583; uncultured Methanohalophilus sp GNA03C0
795	796	GU553552; uncultured archaeon ORI-860-26-PS008-010
795	796	FJ712381; uncultured archaeon KZNMV-10-A51
795	796	FJ712361; uncultured archaeon KZNMV-0-A11
795	796	FJ712392; uncultured archaeon KZNMV-30-A1
795	796	FN820363; uncultured archaeon GoCArc18D0C1M0

795	796	FN820365; uncultured archaeon GoCArc20D0C3M0
795	796	FN820364; uncultured archaeon GoCArc19D0C1M0
795	796	FN820391; uncultured archaeon GoCArc62D0C1M0
795	796	GU553615; uncultured archaeon ORI-860-27-PS041-043
795	796	FN820419; uncultured archaeon GoCArc101D0C1M0
795	796	GU553622; uncultured archaeon ORI-860-27-PS041-043
795	796	HQ588659; uncultured archaeon AMSMV-10-A44
795	796	HQ588641; uncultured archaeon AMSMV-0-A33
795	796	HQ588683; uncultured archaeon AMSMV-30-A2
795	796	HQ588678; uncultured archaeon AMSMV-25-A12
795	796	FJ224366; Methanosalsum zhilinae (T) DSM 4017
795	796	FJ712365; uncultured archaeon KZNMV-0-A42
795	796	FJ712366; uncultured archaeon KZNMV-5-A1
795	796	AB252424; uncultured archaeon OT-A17 11
795	796	AB107768; Thermococcus celericrescens (T) TS2
795	796	AF017455; Thermococcus sp Rt3
795	796	AY099180; Thermococcus litoralis DSM 5474
795	796	AY099182; Thermococcus pacificus (T) DSM 10394
795	796	AY099187; Thermococcus waiotapuensis (T) DSM 12768
795	796	AY559131; Thermococcus sp Ax00-45
795	796	AY559132; Thermococcus sp Ax99-47
795	796	AY559133; Thermococcus sp Ax01-65
795	796	Y16227; Thermococcus pacificus P-4
795	796	AF098975; Thermococcus waimanguensis Wai21 S1
795	796	AJ291811; Thermococcus pacificus DSM 10394 Type
795	796	AJ310754; Thermococcus atlanticus (T) MA898
795	796	AJ419871; Thermococcus sp MV1092
795	796	AJ419872; Thermococcus sp MV1083
795	796	U76534; Thermococcus zilligii (T) AN1
795	796	AJ874326; Thermococcus sp AT1273
795	796	AB055124; Thermococcus pacificus JCM 10553
795	796	AB055127; Thermococcus waiotapuensis JCM 10985
795	796	AJ969470; uncultured Thermococcus sp PICO pp37 Ra
795	796	FJ638515; uncultured archaeon KCL50a0615
795	796	FJ862789; Thermococcus sp 11N A5
795	796	FJ862791; Thermococcus sp B1
795	796	AB603515; Thermococcus litoralis JCM 8560
795	796	FR749899; Thermococcus litoralis type strain: DSM
795	796	EU731603; uncultured Thermoplasmatales archaeon GN
795	796	FJ655764; uncultured archaeon SP03A3
795	796	FJ705127; uncultured archaeon ACWCSP1D6
795	797	GU553812; uncultured archaeon ORI-860-27-PW27WA04
795	797	DQ649332; Methanobacterium palustre Z2
795	797	DQ649333; Methanobacterium palustre 21
795	797	FJ766848; Methanocaldococcus sp KIN24-T80
795	797	FN429778; uncultured euryarchaeote ANTXXIII706-4Ar
795	797	AY592031; uncultured archaeon Kazan-3A-07/BC19-3A-

795	797	FN820396; uncultured archaeon GoCArc69D0C1M0
795	797	AY099172; Thermococcus barophilus (T) DSM 11836
795	797	AJ874318; uncultured Thermococcales archaeon A800
795	797	FJ477315; uncultured archaeon MMS105
805	804	FJ485532; uncultured crenarchaeote Z273FA95
805	804	AB329806; uncultured archaeon YS18As05
805	805	GU553436; uncultured archaeon ORI-860-18-PS041-043
805	805	GU137351; uncultured archaeon PNGTB4B7 5H1A148
805	805	EU732002; uncultured crenarchaeote GNA04B03
805	806	EU732001; uncultured crenarchaeote GNA05A07
805	806	EU732010; uncultured crenarchaeote GNA06B01
805	806	EU732011; uncultured crenarchaeote GNA05F05
805	807	FJ901878; uncultured crenarchaeote LPBBA50
805	807	EU732006; uncultured crenarchaeote GNA06H03
805	807	EU732007; uncultured crenarchaeote GNA04A07
805	807	EU732013; uncultured crenarchaeote GNA03E05
805	807	EU732014; uncultured crenarchaeote GNA07G05